# 7 LITTLE HIGGS MODELS

## 7.1 Introduction

*Thomas Grégoire, Heather E. Logan, and Bob McElrath*

### *7.1.1 The little Higgs mechanism and collective symmetry breaking*

We should learn soon from the LHC how electroweak symmetry is broken. Electroweak precision tests suggest that the physics responsible for this phenomenon is weakly coupled, or in other words, it is expected that a Higgs particle will be discovered. To have a *natural* theory of electroweak symmetry breaking, the Higgs mass needs to be protected from radiative corrections that would drive it toward the ultraviolet (UV) cutoff of the theory, presumably with the help of a symmetry. Two possible symmetries exist. The first one is supersymmetry, and the well studied MSSM relies on this symmetry to protect the Higgs mass. The other possible symmetry is a shift symmetry, and in fact the only light scalar particles that we know in nature, the pions, are light thanks to this kind of symmetry: they are pseudo-Goldstone bosons.

Goldstone bosons arise whenever a global symmetry is spontaneously broken. Due to the shift symmetry they have derivative couplings, but no potential: they are massless. The strength of their derivative interactions is set by an energy scale $f$, the decay constant. At energies larger than $\Lambda \sim 4\pi f$, the Goldstone bosons become strongly coupled and some new physics is needed to regulate this behavior. The regulating physics can be strongly coupled at scale $\Lambda$, like in QCD, or it can be weakly coupled if the global symmetry is spontaneously broken by an elementary scalar (for example in the SM, the Higgs field regulates $WW$ scattering). Small explicit breaking of the global symmetry can generate a potential for the pseudo-Goldstone bosons. For example, in QCD, the quark masses explicitly break the flavor symmetry and as a result, the pions are not exactly massless. The gauging of electromagnetism also breaks the global symmetry and a quadratically divergent photon loop is responsible for the $\pi^+ - \pi^0$ mass difference:

$$m^2_{\pi^+} - m^2_{\pi^0} \sim \frac{\alpha_{\rm em}}{4\pi}\Lambda^2_{\rm QCD}, \tag{7.1}$$

which is parametrically of order $gf_\pi$ ($f_\pi$ is the pion decay constant). Early attempts to write down a theory of a Higgs as a pseudo-Goldstone boson by Georgi and Kaplan [1–4] faced the following problem. The typical potential generated for a pseudo-Goldstone boson $\phi$ is of the form

$$V(\phi) = f^4(c_1\phi^2/f^2 + c_2\phi^4/f^4)\,, \tag{7.2}$$

with $c_1, c_2$ of order one, which leads to a minimum (if $c_1 < 0$) at $\phi \sim f$. If $\phi$ is the Higgs, $f \sim 100$ GeV, and strong physics at 1 TeV (or a linear sigma model field at $\sim 100$ GeV, which is not any better than having a fundamental Higgs in the first place) is needed. The philosophy of little Higgs models is to avoid having to deal with potentially dangerous contributions to electroweak precision observables coming from strongly-coupled physics by pushing the strong coupling scale up to 10 TeV.

The idea of little Higgs models [5, 6] is to break the global symmetry in such a way that the mass of the Higgs is parametrically *two* loop factors smaller than $\Lambda$ instead of one. We could then have $f \sim 1$ TeV and $\Lambda \sim 10$ TeV. This is achieved through collective breaking of the symmetry. The idea is that any one global symmetry breaking coupling by itself leaves enough of the global symmetry intact so that the Higgs is still an exact Goldstone. However, once all couplings are turned on, the Higgs gets a mass parametrically of order:

$$m_h^2 \sim \left(\frac{g^2}{16\pi^2}\right)^2 \Lambda^2 \tag{7.3}$$

so that the strong coupling scale $\Lambda$ could be as high as 10 TeV, a scale that is out of reach of forthcoming experiments and safe with respect to electroweak precision measurements. In order for this mechanism

to work, the global symmetry group needs to be quite large, which implies the presence of extra particles typically at scale $f \sim 1$ TeV. Those particles are responsible for canceling the one loop quadratic divergences to the Higgs mass. The following ingredients are needed to build a little Higgs model:

- The spontaneous breaking of a global symmetry. The mechanism by which the symmetry breaking happens is not specified. It could be strongly coupled physics at 10 TeV, or weakly coupled physics at 1 TeV. The breaking produces a set of Goldstone bosons, among which is the Higgs, and at low energies these 'pions' are described by a non-linear sigma model field which is written as an exponential of the broken generators $T^a$ of the global symmetry: $\Sigma(x) = \exp\left(i\pi^a(x)T^a\right)$.
- Gauge couplings for the Higgs that implement the collective symmetry breaking principle. To achieve this, one needs to gauge a group larger than the Standard Model gauge group, which breaks to the Standard Model at the scale $f$. There will then be extra gauge bosons at the scale $f$ that cancel the quadratically divergent contributions of the Standard Model gauge bosons to the Higgs mass.
- Yukawa couplings that implement the collective symmetry breaking principle. This leads to extra heavy fermions that cancel the quadratically divergent contribution of the Standard Model top quark loop to the Higgs mass. Note that the size of the quadratic divergence from light fermions is small up to the cutoff at 10 TeV; the contributions of the light fermions to the Higgs mass quadratic divergence need not be canceled and we can couple the light fermions to the Higgs in the usual way.
- Higgs quartic couplings that implement the collective symmetry breaking principle. Once again, this leads to additional scalars and higher-dimensional Higgs self-interactions that cancel the SM Higgs self coupling quadratic divergence at $f \sim 1$ TeV. Some little Higgs models however do not have these features and need some fine tuning to get the light Higgs vacuum expectation value (vev).

As an example of a coupling that respects the collective breaking principle, we write down a typical top Yukawa coupling of a little Higgs model. Consider a 3×3 nonlinear sigmal model field describing the breaking of a SU(3)$_L$×SU(3)$_R$ global symmetry to the diagonal SU(3)$_D$:

$$\Sigma(x) = \exp(i\pi^a(x)T^a) \qquad \Sigma \to \exp(i\alpha_L^a T^a)\Sigma(x)\exp(-i\alpha_R^a T^a) \tag{7.4}$$

$$\Pi = \pi^a T^a = \begin{pmatrix} \phi + \eta & h \\ h^\dagger & -2\eta \end{pmatrix} \qquad \pi^a \to \pi^a + \alpha_L^a - \alpha_R^a + \cdots \tag{7.5}$$

where $T^a$ are the SU(3) generators; $\alpha_L^a$ and $\alpha_R^a$ are infinitesimal vectors in $SU(3)_L$ and $SU(3)_R$ respectively; $\phi$ is an SU(2)$_D$ triplet; $h$ is an SU(2)$_D$ doublet; and $\eta$ is an SU(2)$_D$ singlet. This symmetry shifts the $\pi^a$ by a constant. We consider the coupling of this nonlinear sigma model to a fundamental of SU(3)$_L$, $Q = \begin{pmatrix} u & d & T \end{pmatrix}$, and to one singlet fermion $t^c$. We add a second singlet fermion $T^c$ to give mass to the extra fermion:

$$\lambda Q \Sigma \begin{pmatrix} 0 \\ 0 \\ t^c \end{pmatrix} + M T T^c. \tag{7.6}$$

If $M = 0$, the coupling $\lambda$ respects the SU(3)$_L$ global symmetry and the Higgs is still protected, while with $\lambda = 0$ and $M \neq 0$ the SU(3)$_R$ symmetry under which the $\pi^a$ also shift remains. Therefore both couplings are needed to give masses to the $\pi^a$. The cancellation of one loop quadratic divergences is discussed in more detail in Sections 7.1.7 and 7.1.8.

In the next subsections we will examine some specific models. They all have sligthly different properties, but they all have a set of TeV-scale gauge bosons, colored fermions and scalars that cancel the quadratic divergences due to the ususal SM gauge bosons, Yukawa and Higgs quartic couplings, respectively. The models are summarized in Table 7.1.

Table 7.1: Various little Higgs models classified by their type: theory space (t.s.), product gauge group (p.g.g.), or simple gauge group (s.g.g).

| Model | Global group | Gauge group | Type | Comments |
|---|---|---|---|---|
| Minimal moose [7] | $SU(3)^8/SU(3)^4$ | $SU(3)\times SU(2)\times U(1)$ | t.s. | can contain extra light triplet and singlet scalars |
| Minimal moose with $SU(2)_C$ [8] | $SO(5)^8/SO(5)^4$ | $SO(5)\times SU(2)\times U(1)$ | t.s. | less constrained from electroweak precision tests (EWPT) |
| Moose with T-parity [9] | $SO(5)^{10}/SO(5)^5$ | $(SU(2)\times U(1))^3$ | t.s. | very few constraints from EWPT, larg spectrum, complicated plaquettes |
| Littlest Higgs [6] | SU(5)/SO(5) | $(SU(2)\times U(1))^2$ | p.g.g | Minimal field content |
| SU(6)/Sp(6) model [10] | SU(6)/Sp(6) | $(SU(2)\times U(1))^2$ | p.g.g | Small field content, contains a heavy vector-like quark doublet |
| Littlest Higgs with $SU(2)_C$ [11] | SO(9)/ $(SO(5)\times SO(4))$ | $SU(2)^3\times U(1)$ | p.g.g. | less constraints from EWPT |
| Littlest Higgs with T-parity [12] | SU(5)/SO(5) | $(SU(2)\times U(1))^2$ | p.g.g | Minimal field content, very few constraints from EWPT |
| SU(3) simple group [13, 14] | $(SU(3)\times U(1))^2/$ $(SU(2)\times U(1))^2$ | $SU(3)\times U(1)$ | s.g.g. | no large quartic |
| SU(4) simple group [13] | $(SU(4)\times U(1))^4/$ $(SU(3)\times U(1))^4$ | $SU(4)\times U(1)$ | s.g.g. | Two Higgs doublets, large quartic |
| SU(9)/SU(8) simple group [15] | SU(9)/SU(8) | $SU(3)\times U(1)$ | s.g.g. | Two Higgs doublets, large quartic |

### *7.1.2 Theory space models*

Theory space models [5, 7–9, 16] were the first little Higgs models and were inspired by the deconstruction [17–19] of extra dimensional models where the Higgs is the fifth component of a gauge field. Theory spaces are sets of sites and links, also called moose diagrams. Sites represent gauge groups, and links are $N \times N$ nonlinear sigma model fields transforming as bifundamentals under the gauge groups associated with the sites they touch (see Fig. 7.1). Each link breaks a global $SU(N)^2$ symmetry to the diagonal $SU(N)$. This results in the presence of Goldstone bosons. The gauge symmetry explicitly breaks the large global symmetry group. However, no single gauge coupling alone breaks enough symmetry to give the Goldstone bosons a mass.

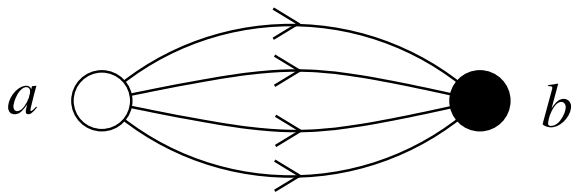


Fig. 7.1: Moose diagram for the minimal moose from Ref. [20]. The open site corresponds to an SU(3) gauge group, while the filled site corresponds to an $SU(2)\times U(1)$ gauge group.

In Fig. 7.1 we show the theory space of the 'minimal moose' [7], the most simple little Higgs of this type. The kinetic term for the link fields is given by:

$$\sum_{i=1}^{4} |D_\mu \Sigma_i|^2 \,, \tag{7.7}$$

with

$$D_\mu \Sigma_i = \partial_\mu \Sigma_i + i A_1 \Sigma_i - i \Sigma_i A_2 \quad \text{and} \quad \Sigma_i = \exp(i \pi_i^a T^a) \,, \tag{7.8}$$

where $T^a$ are the generators of SU(3). The global symmetry group is $\mathrm{SU}(3)^4_L \times \mathrm{SU}(3)^4_R$ (i.e., one copy of $\mathrm{SU}(3)_L \times \mathrm{SU}(3)_R$ for each link) broken down to the diagonal $\mathrm{SU}(3)^4_D$, resulting in $4 \times 8 = 32$ Goldstone bosons. The spontaneous breaking of the global group also breaks the $\mathrm{SU}(2)_L \times \mathrm{U}(1)_L \times \mathrm{SU}(3)_R$ gauge symmetry down to the diagonal $\mathrm{SU}(2)_L \times \mathrm{U}(1)_Y$ subgroup, which eats 8 Goldstone bosons leaving 24 pseudo-Goldstone bosons. The gauge group also explicitly breaks the global symmetry and the 24 pseudo-Goldstone bosons will get a potential generated by gauge interactions. Note that if only the SU(3) gauge coupling is nonzero, there is an exact $\mathrm{SU}(3)^4_L \times \mathrm{SU}(3)_R$ global symmetry broken to the diagonal SU(3). In this case there would be 32 Goldsone bosons, 8 of which would be eaten, leaving 24 exact Goldstone bosons. This tells us that we need the gauge couplings of both sites to generate any potential for the 24 pseudo-Goldsone bosons. The potential is in fact parametrically of the form:

$$\frac{g_1^2 g_2^2}{16\pi^2}(c_1 f^2 \phi^2 + c_2 \phi^4 + \cdots), \tag{7.9}$$

where $c_1$ and $c_2$ are coefficients of order one and $\phi$ represents the various pseudo-Goldstone bosons. As in Eq. (7.2), the minimum is either at zero or parametrically at $\phi \sim f$. To correct this situation, we need to generate a large quartic coupling for $\phi$. This can be achieved with 'plaquette' interactions of the form

$$\lambda \mathrm{Tr}\Sigma_1 \Sigma_2^\dagger \Sigma_3 \Sigma_4^\dagger. \tag{7.10}$$

These interactions also break some of the global symmetries. They do not respect the collective breaking principle for all the pseudo-Goldsones, and they therefore give mass of order $f$ to 8 of them. But still, each of these interactions respects enough global symmetries to protect the mass of the remaining 16 pseudo-Goldstones, which consist of two Higgs doublets, two triplets and two singlets. The important feature of the plaquette terms is that, at tree level, they give no mass to the Higgs doublets, but they do give them an order one quartic coupling. In the extra-dimensional picture, the plaquette term corresponds to the $F_{56}$ part of the gauge kinetic term. These plaquettes are also the reason why we need four link fields. With fewer link fields, the global symmetry structure is not large enough to allow for the desired plaquette terms.

Finally, a top Yukawa coupling can be introduced in a way very similar to Eq. (7.6):

$$\lambda Q \Sigma_1 \Sigma_2^\dagger \begin{pmatrix} 0 \\ 0 \\ t^c \end{pmatrix} + MTT^c. \tag{7.11}$$

The variety of little Higgs models that can be built from theory space is infinite provided one follows a simple set of rules [20]. Along with the minimal moose model, other interesting 'mooses' include a model with a custodial SU(2) symmetry built in [8], and a model with T-parity [9], both constructed to relax constraints from electroweak precision measurements.

Typically, the little Higgs models based on theory spaces are slightly more involved than the 'Littlest Higgs' type model that we will present in the next subsection. However, as already mentioned, they can have interesting extra dimensional interpretations, and many models of a Higgs as the extra-dimensional component of gauge fields [21–27] can be reinterpreted as theory space little Higgs models once the extra dimension is deconstructed.

### *7.1.3 Product gauge group models*

Product gauge group models [6, 10–12, 28] do not have any extra dimensional interpretations. In these models, the gauge groups are subgroups of a single global symmetry. The typical example, and the most studied little Higgs model, is the Littlest Higgs [6]. The global group structure is SU(5)/SO(5). This generates $24 - 10 = 14$ Goldstone bosons that can be parametrized by the following nonlinear sigma

model:

$$\Sigma(x) = \exp(i\Pi)\Sigma_0 \exp(i\Pi^T) \qquad \Sigma_0 = \begin{pmatrix} & & \mathbf{1} \\ & 1 & \\ \mathbf{1} & & \end{pmatrix} \tag{7.12}$$

$$\Pi = \begin{pmatrix} & h & \phi \\ h^\dagger & & h^T \\ \phi^\dagger & h^* & \end{pmatrix}, \tag{7.13}$$

where $\mathbf{1}$ is the $2 \times 2$ identity matrix, $\phi$ is an SU(2) triplet, and $h$ is an SU(2) doublet.

Two SU(2)×U(1) subgroups of SU(5) are gauged with the following generators:

$$Q_{1a} = \begin{pmatrix} \sigma_a & & \\ & & \\ & & \end{pmatrix} \qquad Q_{2a} = \begin{pmatrix} & & \\ & & \\ & & \sigma_a^* \end{pmatrix} \tag{7.14}$$

$$Y_1 = \frac{1}{10}\text{diag}(2,2,-3,-3,-3) \qquad Y_2 = \frac{1}{10}\text{diag}(3,3,3,-2,-2). \tag{7.15}$$

The diagonal subgroup belongs to SO(5) and is unbroken by the $\Sigma$ vev. The gauging explicitly breaks the SU(5) and generates a potential for the Goldstone bosons. Out of the 14 original Goldstones, 4 are eaten by the gauge bosons that become massive. There are 10 left. If only one SU(2)×U(1) gauge coupling constant is turned on, the global symmetry breaking pattern is (SU(3)×SU(2))/(SO(3)×U(1)). This leaves 7 exact Goldstones, three of which are eaten, and four of which remain massless. These massless Goldstone bosons are the Higgs bosons, whose mass is protected by collective symmetry breaking. To summarize, out of the 10 uneaten pseudo-Goldstone bosons, 6, forming an electroweak triplet, do not have their mass protected by collective symmetry breaking and get a mass of order $f$ (and possibly a vev $v'$ of order $v^2/f$), while 4, corresponding to an electroweak doublet, get a lower mass of order the electroweak scale.

An interesting feature of the littlest Higgs model is that gauge boson loops generate the following operators:

$$f^4 \left( c_1 g_1^2 \text{Tr}\Sigma Q_{1a} \Sigma^* Q_{1a}^* + c_2 g_2^2 \text{Tr}\Sigma Q_{2a} \Sigma^* Q_{2a}^* \right) . \tag{7.16}$$

These operators give a mass of order $f$ for the electroweak triplet $\phi$, and generate a quartic coupling of order one for the Higgs. Therefore we do not need to add a plaquette term 'by hand'. It is naturally there, generated by gauge interactions.

Similarly, a top quark Yukawa coupling can be written down in a way analogous to Eq. (7.6) (see Section 7.1.8 for details):

$$\mathcal{L}_Y = \frac{i}{2}\lambda_1 f \epsilon_{ijk}\epsilon_{xy}\chi_i \Sigma_{jx}\Sigma_{ky} u_3'^c + \lambda_2 f \tilde{t}\tilde{t}'^c + \text{h.c.} \tag{7.17}$$

From these couplings, one finds that the heavy vector-like SU(2)-singlet quark $T$ is heavier than $\sqrt{2}f$.

There are many possible variations on the Littlest Higgs theme. The simplest one is the SU(6)/Sp(6) model [10]. This model trades the electroweak triplet scalar of the Littlest Higgs model for an electroweak singlet and an extra light Higgs doublet. To relax constrains from electroweak precision measurements it is also possible to build in a custodial SU(2) symmetry in the gauge sector of the Littlest Higgs model by having an SO(9)/(SO(5)×SO(4)) coset space [11]. Finally one can build a Littlest Higgs model with T-parity [12, 28], which we will discuss further in Section 7.1.5; the phenomenology of models with T-parity will be reviewed in more detail in Section 7.5.

### *7.1.4 Simple gauge group models*

In the previous models we could obtain the desired low energy gauge couplings in a way that respects the collective symmetry breaking by using a product of gauge groups. When one gauge coupling of the product was set to zero, the Higgs was exactly massless and that is how collective symmetry breaking was achieved. One can also use a simple gauge group and get the collective symmetry breaking by having two nonlinear sigma fields that get a vacuum expectation value [13–15]. Each field alone 'thinks' that it is the one breaking the symmetry and getting absorbed by the massive gauge bosons, and the couplings of both fields are needed to generate a potential for the uneaten pseudo-Goldstone bosons. The simplest model [14] of this type is an SU(3)×U(1) gauge theory broken down to SU(2)×U(1) by the vev of two different SU(3) fundamentals:

$$\langle \phi_1 \rangle = \begin{pmatrix} 0 \\ 0 \\ f_1 \end{pmatrix}, \qquad \langle \phi_2 \rangle = \begin{pmatrix} 0 \\ 0 \\ f_2 \end{pmatrix}. \tag{7.18}$$

The global symmetry in this case is an $(\mathrm{SU(3)}\times\mathrm{U(1)})^2/(\mathrm{SU(2)}\times\mathrm{U(1)})^2$ that rotates the two fields independently. The pseudo-Goldstone bosons can be parameterized by fluctuations about the vacuum:

$$\phi_1(x) = \exp(iT^a\pi_1^a/f_1) \begin{pmatrix} 0 \\ 0 \\ f_1 \end{pmatrix}, \qquad \phi_2(x) = \exp(iT^a\pi_2^a/f_2) \begin{pmatrix} 0 \\ 0 \\ f_2 \end{pmatrix}. \tag{7.19}$$

Once again, the gauge couplings explicitly break the global symmetry, but couplings to both $\phi_1$ and $\phi_2$ are needed to generate a potential for the pseudo-Goldstone bosons. The Higgs mass is then suppressed relative to the $f$ scale; however, the Higgs quartic coupling is also small. An extra 'plaquette' operator that breaks the $(\mathrm{SU(3)}\times\mathrm{U(1)})^2$ global symmetry must be added to give a large enough quartic coupling [14]. Alternately, a large quartic can be produced if the theory is enlarged to an SU(4) gauge theory with four fundamentals breaking it to SU(2) [13]. Another model, consisting of a SU(9)/SU(8) global symmetry with SU(3)×U(1) gauged, contains two light Higgs doublets and also generates a large enough quartic [15].

The field content of simple group models is slightly different than in the other models. Instead of an electroweak triplet of vector bosons at the scale $f$, there are the broken SU(3) or SU(4) generators: one or two $Z'$ bosons and an extra electroweak doublet of vector bosons. Also, the spectrum of fermions is enlarged. Before we only needed an extra fermion in the top sector to cancel the one loop quadratic divergence of the Standard Model top quark. Here, because of the extended gauge group, extra fermions for all generations of the Standard Model are needed. Finally, because of the two vevs $f_1$, $f_2$, there is no simple relationship between the mass of the heavy vector bosons and the mass of the heavy top. As we will see next, this helps in avoiding constraints from electroweak precision measurements.

### *7.1.5 Constraints from electroweak precision measurements*

Even if the extra states of little Higgs models are predicted to be out of reach of LEP II and the Tevatron, precision electroweak tests provide stringent constraints on the properties of these particles. This is sometimes referred to as the LEP paradox [29, 30]: we need new states at about 1 TeV to stabilize the Higgs mass, however LEP precision data have probed physics at the TeV scale via its influence on radiative corrections and do not see anything new. Little Higgs models suffer from this paradox; the new TeV scale states that are responsible for the cancellation of the Higgs quadratic divergences can be exchanged at tree level, and this can result in a significant departure from the LEP I and LEP II data. There are many studies on the subject [31–39], and a more detailed review will be presented in Section 7.2. In the Littlest Higgs model for example, exchange of the $B'$ and $W', Z'$ gauge bosons, as well as a vev for the heavy triplet, can all cause trouble. In product group models and theory space models, the couplings of

the new gauge bosons can be written solely in terms of Standard Model currents [40], and the deviation from the Standard Model can be parametrized by the oblique parameters $S, T, Y$ and $W$ [37, 40]. In general, none of the dangerous couplings that give large contributions to these parameters are tied to the couplings that ensure the cancellation of the Higgs mass quadratic divergences. Therefore it is in general possible to find regions of parameter space where the constraints are satisfied with reasonable fine tuning in the Higgs mass ($\sim 10\%$). However, the allowed region is in general quite small. One reason is that, in both the product group models and the theory space models, to avoid contrains from exchange of heavy gauge bosons one needs a largish $f$. However, in these models the mass of the heavy top partner, responsible for the cancellation of the top quark quadratic divergence, is tied to the scale $f$. Since the top loop quadratic divergence is the largest, the heavy top quark partner cannot be too heavy without reintroducing fine-tuning, and this tends to push the models into a small corner of parameter space. In simple gauge group models, the relationship between the heavy gauge boson and the heavy top partner masses is not as direct. Therefore, one gains a little bit. In particular, in simple gauge group models the electroweak precision measurements typically give strong constraints on $\sqrt{f_1^2 + f_2^2}$, while the heavy top quark partner mass is not directly tied to this combination, and can be made relatively light.

Several models have been built with the specific intention of reducing the constraints of electroweak precision measurements. One straightforward option to improve the Littlest Higgs model is to gauge only the diagonal $\mathrm{U}(1)_Y$ instead of a $\mathrm{U}(1)^2$ [32, 34, 41]. This eliminates the constraints coming from the exchange of the $B'$, which is removed from the spectrum, at the expense of not cancelling the quadratic divergence due to the hypercharge gauge boson. This is not a serious problem since with a cutoff of 10 TeV, the quadratic divergence due to the hypercharge gauge boson is not very big. There are also models with a custodial SU(2) symmetry built in to eliminate the worst contributions to the $T$ parameter; these models are typically more complicated but slightly less constrained [8, 11].

The most interesting direction in trying to avoid electroweak precision measurements is probably the idea of T-parity [9, 12, 28, 42, 43]. Just as in the MSSM where R-parity forbids the coupling of one superpartner with two Standard Model particles, T-parity tries to avoid tree-level exchange of the heavy states by making them odd under a new parity, while all the Standard Model particles are even. This has the additional advantage of ensuring the presence of a stable heavy particle which could play the role of dark matter [44]. The main drawback of this approach is that it requires the addition of one new TeV scale fermion for each of the fermions of the Standard Model [12]. This in turns raises flavor questions similar to those in the MSSM. T-parity has been introduced in theory space models, where the parity has a nice geometric interpretation, and in product group models, but not in simple group models. The phenomenology of models with T-parity will be discussed in more detail in Section 7.5.

### *7.1.6 Theoretical constraints*

In addition to the electroweak precision constraints, there are additional constraints on little Higgs models from unitarity and from considering the log-divergent terms in the Higgs potential. We also discuss here the prospects for little Higgs models to incorporate dark matter, neutrino masses, and the baryon asymmetry of the universe.

One can analyze the scattering of all possible pairs of Goldstone bosons in little Higgs models to find where unitarity is violated. The violation of unitarity at some scale indicates that the theory is not valid above that scale, or that perturbation theory has broken down. Due to the large number of Goldstones in little Higgs models, this unitarity analysis generically predicts an upper cutoff $\Lambda \simeq (3-4) f$ depending on the model, which is somewhat less than the $4\pi f \sim$ 10–30 TeV usually quoted using Naive Dimensional Analysis [45].

There are also constraints on the scale $f$. The Naive Dimensional Analysis used to predict that $f \simeq 1$ TeV neglects the contributions to the potential that go like

$$\mathrm{Tr} M^4(\Sigma) \log \frac{M^2(\Sigma)}{\Lambda^2}. \tag{7.20}$$

Including these terms, it is found that a light Higgs can only be achieved with $f$ somewhat smaller than 1 TeV. For large $f \gg 1$ TeV, the Higgs mass is pulled up toward the scale $f$, destroying the desired hierarchy [46]. Therefore the desired hierarchy $v \ll f \ll \Lambda$ can be preserved, but the separation between each of these scales may only be a factor of 3–5 instead of $4\pi$. While worsening the electroweak precision constraints, these observations significantly improve the possibility of finding not only the $f$-scale particles at the LHC, but also the $\Lambda$-scale particles as well.

Because little Higgs models have a cutoff at a relatively low scale $\Lambda \sim 10$ TeV, the issues of dark matter, neutrino masses, and the baryon asymmetry of the universe can be deferred to energy scales above the cutoff. However, there have been some attempts to incorporate this physics within little Higgs models themselves.

Dark matter appears naturally as the lightest T-odd particle in little Higgs models with T-parity [44]. Even without T-parity, theory space models often contain discrete symmetries, some part of which can remain unbroken even after electroweak symmetry breaking; the dark matter could then consist of a nonlinear sigma model field made stable by this accidental exact global symmetry [47].

There have been two main approaches to neutrino mass generation in little Higgs models. First, some models (such as the Littlest Higgs) contain a scalar triplet with a nonzero vev. This triplet can be used to generate neutrino Majorana masses through a lepton number violating coupling to two left-handed SM neutrinos [35, 48–50]. Second, simple group models naturally contain a pair of extra SM gauge singlets $N, N^c$ at the $f$ scale due to the expansion of the lepton doublets into fundamentals of the enlarged gauge group. If lepton number is broken at a small scale $M \sim$ keV, generating a small Majorana mass for $N^c$, then the SM neutrinos can get a radiatively generated Majorana mass [51] of the correct size through their mixing with $N$, without requiring extremely tiny Yukawa couplings.

Electroweak baryogenesis relies on the restoration of electroweak symmetry at high temperature. This happens as a result of an effective positive mass squared term $m_{\text{eff}}^2 \sim T^2$ acquired by the Higgs from interactions with the ambient thermal plasma. However, this effective mass is generated precisely by the Higgs self-energy diagrams that are quadratically divergent at $T = 0$ [52], i.e., those that are canceled by the little Higgs mechanism. A similar cancellation happens in the MSSM, in which the quadratically divergent contributions cancel between bosonic and fermionic degrees of freedom; at finite temperature, these contributions enter the thermal mass with different coefficients due to the different statistics of the relevant particles in the thermal bath, and thus no longer cancel. In little Higgs models, however, the quadratic divergences cancel between particles *of the same statistics*, so that the thermal mass is also canceled [52]. A detailed study [52] of the Littlest Higgs model with SU(2)$^2\times$U(1) gauged shows an initial symmetry restoration as in the Standard Model as $T$ is increased, followed by a rebreaking at $T \sim f$ to a new global minimum.

The baryon asymmetry of the universe could also arise through leptogenesis, with an initial lepton asymmetry transmitted to the baryon sector through electroweak sphalerons. Leptogenesis generates the initial CP asymmetry through out-of-equilibrium decay of heavy right-handed neutrinos. To generate a large enough asymmetry, the right-handed neutrinos must have large enough CP-violating couplings to the light neutrinos and the SM Higgs. Normally this forces the right-handed neutrino scale to be near the GUT scale ($\sim 10^{16}$ GeV) so that the SM neutrinos will be kept light enough by the see-saw mechanism. Such a scenario cannot be fit into a little Higgs model because the cutoff is much lower, $\Lambda \sim 10$ TeV.

However, recently it was shown [53] how to implement TeV-scale leptogenesis in little Higgs models, both in simple group models and in Littlest Higgs-type models. In simple group models the SM neutrino masses can be radiatively generated as discussed above [51], so that the CP-violating couplings relevant for leptogenesis can still be large without generating too large a neutrino mass. In Littlest Higgs-type models with the SM neutrino masses generated through couplings to a scalar triplet, leptogenesis can be implemented by adding a moderately heavy fourth neutrino family which carries the large CP-violating coupling.

### *7.1.7 New gauge bosons*

Little Higgs models extend the electroweak gauge group at the TeV scale. The structure of the extended electroweak gauge group determines crucial properties of the model, which can be revealed by studying the new gauge bosons at the TeV scale. Experimental studies for the LHC will be presented in Sections 7.6 and 7.7; prospects for ILC measurements will be discussed in Section 7.8. In the Littlest Higgs model [6], the heavy gauge bosons consist of an SU(2)$_L$ triplet $Z_H, W_H^\pm$ from the breaking of SU(2)×SU(2) down to the electroweak SU(2)$_L$. A similar structure arises in many of the product group and theory space models. In the SU(3)×U(1) simple group model [13, 14], the heavy gauge bosons consist of an SU(2)$_L$ doublet $(Y^0, X^-)$ corresponding to the broken off-diagonal generators of SU(3), and a $Z'$ gauge boson corresponding to the broken linear combination of the $T^8$ generator of SU(3) and the U(1). Again, a similar pattern arises in other simple group models.

The extra gauge bosons get their masses from the $f$ condensate, which breaks the extended gauge symmetry. For example, in the Littlest Higgs and the SU(3) simple group models, the gauge boson masses are given in terms of the model parameters by

$$\left.\begin{array}{l} M_{W_H} = M_{Z_H} = gf/2sc = 0.65f/\sin 2\theta \\ M_{A_H} = gs_W f/2\sqrt{5}c_W s'c' = 0.16f/\sin 2\theta' \end{array}\right\} \text{in the Littlest Higgs model,}$$

$$\left.\begin{array}{l} M_{Z'} = \sqrt{2}gf/\sqrt{3-t_W^2} = 0.56f \\ M_X = M_Y = gf/\sqrt{2} = 0.46f = 0.82M_{Z'} \end{array}\right\} \text{in the SU(3) simple group model.} \quad (7.21)$$

In the SU(3) simple group model the heavy gauge boson masses are determined by only one free parameter, the scale $f = \sqrt{f_1^2 + f_2^2}$. The Littlest Higgs model has two additional gauge sector parameters, $\tan\theta = s/c = g_2/g_1$ [in the SU(2)$^2$ →SU(2) breaking sector] and $\tan\theta' = s'/c' = g_2'/g_1'$ [in the U(1)$^2$ →U(1) breaking sector]. If only one copy of U(1) is gauged [32], the $A_H$ state is not present and the gauge sector of the Littlest Higgs model is controlled by only two free parameters, $f$ and $\tan\theta$.

The gauge couplings of the Higgs doublet take the general form [54]

$$\mathcal{L} = \left\{ \begin{array}{l} \left[G_{HHVV}VV + G_{HHV'V'}V'V' + G_{HHVV'}VV'\right] H^2 \\ \left[G_{HHV^+V^-}V^+V^- + G_{HHV'^+V'^-}V'^+V'^- + G_{HHV^+V'^-}(V^+V'^- + V^-V'^+)\right] H^2, \end{array} \right. \quad (7.22)$$

where the top line is for $V$ neutral and the bottom line is for $V$ charged. Here $V$ and $V'$ stand for the SM and heavy gauge bosons, respectively. This Lagrangian leads to two quadratically divergent diagrams contributing to the Higgs mass: one involving a loop of $V$, proportional to $G_{HHVV}$, and the other involving a loop of $V'$, proportional to $G_{HHV'V'}$. The divergence cancellation in the gauge sector can thus be written as

$$\sum_i G_{HHV_iV_i} = 0, \quad (7.23)$$

where the sum runs over all gauge bosons in the model. The couplings in the Littlest Higgs and SU(3) simple group models are given, e.g., in Table 3 of Ref. [54]. In the SU(3) simple group model, the quadratic divergence cancels between the $Z$ and $Z'$ loops and between the $W$ and $X$ loops. In the Littlest Higgs model, the quadratic divergence cancels between the $W$ and $W_H$ loops and there is a partial cancellation between the $Z$ and $Z_H$ loops. Including the $A_H$ loop leads to a complete cancellation of the quadratic divergence from the $Z$ loop. The key test of the little Higgs mechanism in the gauge sector is the experimental verification of Eq. (7.23).

After EWSB, the couplings of $H^2$ to one heavy and one SM gauge boson induce mixing between the heavy and SM gauge bosons:

$$V' = V_0' - \delta_V V_0, \qquad \delta_V = -v^2 G_{HHVV'}/M_{V'}^2, \quad (7.24)$$

where $V_0'$, $V_0$ stand for the states before EWSB. This mixing gives rise to triple gauge couplings between one heavy and two SM gauge bosons.

In the Littlest Higgs model, the couplings of the heavy gauge bosons to the SU(2)$_L$ fermion currents take the form

$$Z_H^\mu \overline{f} f: \quad ig\cot\theta\, T_f^3 \gamma^\mu P_L, \qquad\qquad W_H^{+\mu}\overline{u}d: \quad -\frac{ig}{\sqrt{2}}\cot\theta\,\gamma^\mu P_L, \tag{7.25}$$

where $T_f^3 = 1/2\ (-1/2)$ for up (down) type fermions. Below the TeV scale, exchange of $W_H$ and $Z_H$ gives rise to four-fermi operators, which are constrained by the electroweak precision data. The experimental constraints are loosened by going to small values of $\cot\theta$, for which the couplings of the heavy gauge bosons are suppressed. In the SU(3) simple group model, the $Z'$ couples to SM fermions with gauge strength, while the $X, Y$ gauge bosons couple only via the mixing between SM fermions and their TeV-scale partners. The $Z'$ couplings are fixed by the charges of the SM fermions under SU(3)×U(1)$_X$, and cannot be written in terms of the usual SM currents. The electroweak precision constraints in this case cannot be parameterized solely in terms of the oblique parameters [37, 40].

### *7.1.8 New fermions and the top partner*

The new heavy quark sector in the Littlest Higgs model [6] consists of a pair of vectorlike SU(2)-singlet quarks that couple to the top sector. The Lagrangian is [54]

$$\mathcal{L}_Y = \frac{i}{2}\lambda_1 f \epsilon_{ijk}\epsilon_{xy}\chi_i \Sigma_{jx}\Sigma_{ky} u_3'^c + \lambda_2 f \tilde{t}\tilde{t}'^c + \text{h.c.}, \tag{7.26}$$

where $\chi_i = (b_3, t_3, i\tilde{t})$ and the factors of $i$ in Eq. (7.26) and $\chi_i$ are inserted to make the masses and mixing angles real. The summation indices are $i, j, k = 1, 2, 3$ and $x, y = 4, 5$, and $\epsilon_{ijk}$, $\epsilon_{xy}$ are antisymmetric tensors. The vacuum expectation value $\langle\Sigma\rangle \equiv \Sigma_0$ marries $\tilde{t}$ to a linear combination of $u_3'^c$ and $\tilde{t}'^c$, giving it a mass of order $f \sim$ TeV. The resulting new charge 2/3 quark $T$ is an isospin singlet up to its small mixing with the SM top quark (generated after EWSB). The orthogonal linear combination of $u_3'^c$ and $\tilde{t}'^c$ becomes the right-handed top quark and marries $t_3$.

In the SU(3)×U(1) simple group model [13, 14], the top quark mass is generated by the Lagrangian [54]

$$\mathcal{L}_Y = i\lambda_1^t u_1^c \Phi_1^\dagger Q_3 + i\lambda_2^t u_2^c \Phi_2^\dagger Q_3, \tag{7.27}$$

where $Q_3^T = (t, b, iT)$ and the factors of $i$ in Eq. (7.27) and $Q_3$ are again inserted to make the masses and mixing angles real. The $\Phi$ vevs marry $T$ to a linear combination of $u_1^c$ and $u_2^c$, giving it a mass of order $f \sim$ TeV. The new charge 2/3 quark $T$ is a singlet under SU(2)$_L$ up to its small mixing with the SM top quark (generated after EWSB). The orthogonal linear combination of $u_1^c$ and $u_2^c$ becomes the right-handed top quark. For the rest of the quarks, the scalar interactions depend on the choice of their embedding into SU(3). The most straightforward choice is to embed all three generations in a universal way, $Q_m^T = (u, d, iU)_m$, so that each quark generation contains a new heavy charge 2/3 quark. This embedding leaves the SU(3) and U(1)$_X$ gauge groups anomalous; the anomalies can be canceled by adding new spectator fermions at the cutoff scale $\Lambda \sim 4\pi f$. An alternate, anomaly-free embedding [55, 56] puts the quarks of the first two generations into antifundamentals of SU(3), $Q_m^T = (d, -u, iD)_m$, with $m = 1, 2$, so that the first two quark generations each contain a new heavy charge $-1/3$ quark. Interestingly, an anomaly-free embedding of the SM fermions into SU(3)$_c$×SU(3)×U(1)$_X$ is only possible if the number of generations is a multiple of three [55–58].[1]

The masses of the top quark $t$ and its heavy partner $T$ are given in terms of the model parameters

[1] This rule can be violated in models containing fermion generations with non-SM quantum numbers, e.g., mirror families [59].

by

$$m_t = \lambda_t v = \begin{cases} \dfrac{\lambda_1\lambda_2}{\sqrt{\lambda_1^2+\lambda_2^2}}v & \text{in the Littlest Higgs model,} \\ \dfrac{\lambda_1\lambda_2}{\sqrt{2}\sqrt{\lambda_1^2 c_\beta^2+\lambda_2^2 s_\beta^2}}v & \text{in the SU(3) simple group model;} \end{cases}$$

$$M_T = \begin{cases} \sqrt{\lambda_1^2+\lambda_2^2}\, f = (x_\lambda + x_\lambda^{-1})\dfrac{m_t}{v} f & \text{in the Littlest Higgs model,} \\ \sqrt{\lambda_1^2 c_\beta^2+\lambda_2^2 s_\beta^2} f = \sqrt{2}\,\dfrac{t_\beta^2+x_\lambda^2}{(1+t_\beta^2)x_\lambda}\dfrac{m_t}{v}\, f & \text{in the SU(3) simple group model.} \end{cases}$$

Fixing the top quark mass $m_t$ leaves two free parameters in the Littlest Higgs model, which can be chosen to be $f$ and $x_\lambda \equiv \lambda_1/\lambda_2$. We see that the SU(3) simple group model contains one additional parameter, $t_\beta \equiv \tan\beta = f_2/f_1$. In the SU(3) simple group model, we define $f \equiv \sqrt{f_1^2+f_2^2}$.

To reduce fine-tuning in the Higgs mass, the top-partner $T$ should be as light as possible. The lower bound on $M_T$ is obtained for certain parameter choices:

$$M_T \geq \begin{cases} 2\dfrac{m_t}{v} f \approx \sqrt{2} f & \text{for } x_\lambda = 1 \text{ in the Littlest Higgs model,} \\ 2\sqrt{2} s_\beta c_\beta \dfrac{m_t}{v} f \approx f \sin 2\beta & \text{for } x_\lambda = t_\beta \text{ in the SU(3) simple group model,} \end{cases}$$

where in the last step we used $m_t/v \approx 1/\sqrt{2}$. The $T$ mass can be lowered in the SU(3) model for fixed $f$ by choosing $t_\beta \neq 1$, thereby introducing a mild hierarchy between $f_1$ and $f_2$.

The couplings of the Higgs doublet to the $t$ and $T$ mass eigenstates can be written in terms of an effective Lagrangian [54],

$$\mathcal{L}_Y \supset \lambda_t H t^c t + \lambda_T H T^c t + \frac{\lambda_T'}{2M_T} H H T^c T + \text{h.c.}, \tag{7.28}$$

where the four-point coupling arises from the expansion of the nonlinear sigma model field. This effective Lagrangian leads to three diagrams contributing to the Higgs mass corrections at one-loop level, shown in Fig. 7.2: (a) the SM top quark diagram, which depends on the well-known SM top Yukawa coupling $\lambda_t$; (b) the diagram involving a top quark and a top-partner $T$, which depends on the $HTt$ coupling $\lambda_T$; and (c) the diagram involving a $T$ loop coupled to the Higgs doublet via the dimension-five $HHTT$ coupling. The couplings in the three diagrams of Fig. 7.2 must satisfy the following relation [60] in order for the quadratic divergences to cancel:

$$\lambda_T' = \lambda_t^2 + \lambda_T^2. \tag{7.29}$$

This equation embodies the cancellation of the Higgs mass quadratic divergence in any little Higgs theory. The couplings in the Littlest Higgs and SU(3) simple group models are given, e.g., in Table 1 of Ref. [54]. If the little Higgs mechanism is realized in nature, it will be of fundamental importance to establish the relation in Eq. (7.29) experimentally.

After EWSB, the coupling $\lambda_T$ induces a small mixing of electroweak doublet into $T$,

$$T = T_0 - \delta_T t_0, \quad \delta_T = \lambda_T \frac{v}{M_T}, \tag{7.30}$$

where $T_0, t_0$ stand for the electroweak eigenstates before the mass diagonalization at the order of $v/f$. This mixing gives rise to the couplings of $T$ to the SM states $bW$ and $tZ$ with the same form as the corresponding SM couplings of the top quark except suppressed by the mixing factor $\delta_T$.

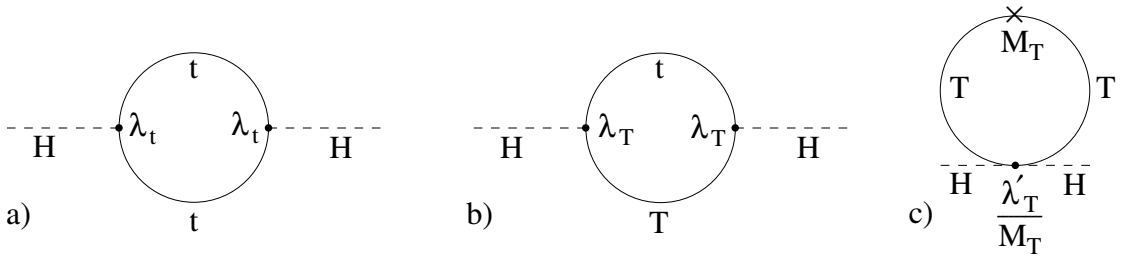


Fig. 7.2: Quadratically divergent one-loop contributions to the Higgs boson mass-squared from the top sector in little Higgs models. From Ref. [54].

Table 7.2: Particle content of the scalar sectors of little Higgs models. SU(2) doublets, triplets, complex singlets, and singlet pseudoscalars are denoted by $h$, $\phi$, $\sigma$, and $\eta$, respectively. SU(2) multiplets are complex unless specified otherwise; the real triplet and singlet are denoted by $\phi^r$ and $\sigma^r$, respectively. In the minimal moose with SU(2)$_C$, the $\sigma^\pm$, $\sigma^r$ fields form a triplet under the custodial SU(2) symmetry but are SU(2)$_L$ singlets.

| Model | EW-scale scalars | TeV-scale scalars |
|---|---|---|
| Minimal moose [7] | $h_1$, $h_2$, $\phi$, $\sigma$ | (none) |
| Minimal moose with SU(2)$_C$ [8] | $h_1$, $h_2$ | $\phi^r$, $\sigma^\pm$, $\sigma^r$ |
| Moose with T-parity [9] | $h_1$, $h_2$ | $h_{3,4,5}$, $\phi^r_{1,2,3}$, $\sigma_{1,2,3,4,5}$, $\eta_{1,2,3}$ |
| Littlest Higgs [6] | $h$ | $\phi$ |
| SU(6)/Sp(6) model [10] | $h_1$, $h_2$ | $\sigma$ |
| Littlest Higgs with SU(2)$_C$ [11] | $h$ | $\phi$, $\phi^r$, $\eta$ |
| Littlest Higgs with T-parity [12] | $h$ | $\phi$ |
| SU(3) simple group [13, 14] | $h$, $\eta$ | (none) |
| SU(4) simple group [13] | $h_1$, $h_2$, $\eta_1$, $\eta_2$ | $\sigma_1$, $\sigma_2$, $\sigma_3$ |
| SU(9)/SU(8) simple group [15] | $h_1$, $h_2$ | $\sigma_1$, $\sigma_2$ |

### *7.1.9 The scalar sector*

The scalar sectors of little Higgs models are very model dependent, because they correspond to the coset space of the broken global symmetries minus those exact Goldstone bosons that are eaten by the broken gauge generators. The phenomenology of the scalar sector thus provides a very important experimental handle on the global symmetry of the model and the symmetry breaking pattern.

The states in the scalar sector are characterized by their SU(2)$_L$×U(1) and CP quantum numbers. The scalar sector must contain at least one SU(2)-doublet Higgs field with mass near the electroweak scale to reproduce SM electroweak symmetry breaking. The scalar content of various little Higgs models is summarized in Table 7.2. We denote SU(2) doublets as $h$, SU(2) triplets as $\phi$, complex SU(2) singlets as $\sigma$, and SU(2) singlet pseudoscalars as $\eta$.

Some models, including the Littlest Higgs [6], its extensions with custodial SU(2)$_C$ symmetry [11] and with T-parity [12], and the SU(3) simple group model [13, 14], contain a single SU(2) doublet Higgs field at the electroweak scale. The physical Higgs boson in these models has couplings that are identical to those of the SM Higgs up to corrections suppressed by the ratio of scales $v/f$; the corrections to the Higgs production cross sections and decay partial widths are then proportional to $(v/f)^2 \sim$ few percent [61–63]. These corrections come from the mixing between SM and TeV-scale states, from the higher-order terms in the expansion of the nonlinear sigma model, and from corrections to the SM input parameters such as $G_F$. In such models, high-precision Higgs coupling measurements will be a useful test of the model structure, and could shed light on strongly-coupled new physics at the UV-completion scale around 10 TeV. This will be reviewed in more detail in Section 7.3.

Other models give rise to two Higgs doublets at the electroweak scale. The Higgs phenomenology below the TeV scale is then that of a two Higgs doublet model, typically with a constrained form of the scalar potential that can give rise to characteristic relations between the Higgs masses and mixing angles.

Little Higgs models often contain at least one additional U(1) global symmetry that is broken by the $f$ vev. This gives rise to an additional physical pseudoscalar mode, $\eta$, typically with mass near the electroweak scale, which can have significant effects on the phenomenology [64]. This occurs in, e.g., the SU(3) simple group model [13, 14]. A pseudoscalar also arises in the Littlest Higgs model [6] when only $\mathrm{SU}(2)^2\times\mathrm{U}(1)$ is gauged, instead of the usual $[\mathrm{SU}(2)\times\mathrm{U}(1)]^2$. The origin and phenomenology of these pseudoscalars will be reviewed in more detail in Section 7.4.

Finally, some models contain Higgs triplets at the TeV scale, or even at the electroweak scale. These triplets can give rise to potentially dangerous contributions to electroweak precision observables through their nonzero vevs $v'$. They can also yield interesting phenomenology such as decays of the doubly-charged member of the triplet into pairs of like-sign $W$ bosons or, in versions of the models with lepton number violation [35, 48–50], into like-sign dileptons.

## 7.2 Impact of electroweak precision data on the little Higgs models

*Aldo Deandrea*

The electroweak sector of the SM has been tested to a very high accuracy and an important test of the validity of little Higgs models is therefore through comparison with precision data (for reviews treating this subject see [65, 66]). The strategy to compute limits from the electroweak precision data is not unique and indeed different methods are discussed in the literature. It is possible to compute directly quantities which are constrained by the experimental data and fit the whole set in order to get constraints on the model. One can also rely on the computation of a restricted set of relevant quantities. Finally one can integrate out the heavy fields and study the effective low energy lagrangian. The originally proposed models are tightly constrained while more recent ones, such as the Littlest Higgs model with T-parity, satisfy the electroweak constraints in a larger region of the parameter space.

A special feature of the SM with one Higgs doublet is the validity of the tree level relation

$$\rho = 1 = \frac{M_W^2}{M_Z^2 c_\theta^2} \tag{7.31}$$

due to the tree level custodial symmetry. In many little Higgs models the custodial symmetry is no longer a good symmetry of the model, *i.e.* $\rho \neq 1$ already at the tree level. Another source of constraints from the electroweak precision data are $\mathrm{SU}(2)_L$ triplet Higgs, as a trilinear coupling between the doublet and the triplet Higgs, $H^T\Phi^\dagger H$, is allowed by the gauge symmetry $\mathrm{SU}(2)_L\times\mathrm{U}(1)_Y$. Unless a discrete symmetry is imposed to forbid such a trilinear interaction, the vev of the triplet is non-zero and leads to a new input parameter in the gauge sector, and many predictions of the Standard Model are changed by the presence of such a term.

### *7.2.1 Littlest Higgs*

Many studies in the literature concern the little Higgs model and its extensions [31–33, 35, 37–39, 60, 67, 68]. As an example we show in Fig. 7.3 the limits obtained in the $\mathrm{SU}(5)/\mathrm{SO}(5)$ Littlest Higgs in [32]. The leading corrections are given by the tree-level exchanges of heavy gauge bosons and the effects of the non-zero triplet scalar vev. Weak isospin violating contributions arise at tree level due to the absence of a custodial SU(2) symmetry. The main component of the corrections come from heavy gauge boson exchanges, while a smaller contribution is due to the triplet vev $v'$.

The input parameters in the analysis of the electroweak data can be chosen to be the Fermi constant $G_F$, the mass of the $Z$ vector boson $m_Z$ and the fine–structure coupling $\alpha(m_Z)$. One can first look at the

modification to $G_F$. We have two types of modifications: one directly from the mixing of the heavy $W_H$ bosons to the coupling of the charged current and the second one from the contribution of the charged current to the equations of motion of the heavy gauge bosons. In terms of the model parameters:

$$\frac{G_F}{\sqrt{2}} = \frac{\alpha\pi(g^2+g'^2)}{2g^2g'^2m_Z^2}\left(1 - c^2(c^2-s^2)\frac{v^2}{f^2} + 2c^4\frac{v^2}{f^2} - \frac{5}{4}(c'^2-s'^2)^2\frac{v^2}{f^2}\right) . \tag{7.32}$$

where $s, c, s'$, and $c'$ denote the sines and cosines of two mixing angles, respectively. They can be expressed with the help of the coupling constants:

$$\begin{aligned} c' &= g'/g'_2 \qquad s' = g'/g'_1 \\ c &= g/g_2 \qquad s = g/g_1 \ , \end{aligned} \tag{7.33}$$

with the usual SM couplings $g, g'$, related to $g_1$, $g_2$, $g'_1$ and $g'_2$ by

$$\frac{1}{g^2} = \frac{1}{g_1^2} + \frac{1}{g_2^2}, \qquad \frac{1}{g'^2} = \frac{1}{{g'_1}^2} + \frac{1}{{g'_2}^2} \ . \tag{7.34}$$

The Weinberg angle is defined through

$$\frac{G_F}{\sqrt{2}} = \frac{\alpha\pi}{2s_\theta^2c_\theta^2m_Z^2} \ . \tag{7.35}$$

In terms of the model parameters the mass of the $Z$-boson is given by

$$m_Z^2 = (g^2+g'^2)\frac{v^2}{4}\left[1 - \frac{v^2}{f^2}\left(\frac{1}{6} + \frac{(c^2-s^2)^2}{4} + \frac{5}{4}(c'^2-s'^2)\right) + 8\frac{v'^2}{v^2}\right] , \tag{7.36}$$

whereas the $W$-mass is

$$m_W^2 = \frac{g^2v^2}{4}\left[1 - \frac{v^2}{f^2}\left(\frac{1}{6} + \frac{(c^2-s^2)^2}{4}\right) + 4\frac{v'^2}{v^2}\right] . \tag{7.37}$$

The expression for the $Z$-mass can be used to determine the value of $v$ for a given ratio $v/f$. One can also compute from the previous results the correction to the $\rho$ parameter.

By doing a complete analysis one can establish that the symmetry breaking scale is generically bounded by $f > 4$ TeV at 95% C.L. with more stringent bounds for particular choices of the couplings. Modifying the way in which the gauged U(1) generators are embedded, the fermion $U(1)$ charges, or gauging a single U(1), gives the possibility of relaxing the constraints on the scale $f$ [32]. For example one can modify the U(1) charges of the first two generations in the form $RY_F$ under the first U(1) and $(1-R)Y_F$ under the second U(1), where $Y_F$ is the SM hypercharge of the fermion. By requiring the invariance of the Yukawa couplings under the U(1)'s (for details see [32]) one can show that $R$ can take only values which are integer multiples of $1/5$. Results depend also on an additional parameter $a$ expected to be $\mathcal{O}(1)$ in the Coleman-Weinberg potential of the Littlest Higgs. This parameter affects the size of the triplet vev $v'$.

### *7.2.2 Other little Higgs models*

Little Higgs models implementing custodial symmetry were discussed in [8, 11]. Precision electroweak constraints were considered in the previous papers and also in [38, 69]. The breaking scale $f$ can be as low as 700 GeV without contradiction with the precision electroweak data.

A different approach to reduce the impact of electroweak constraints is based on a discrete parity called T-parity [9, 12, 28] in analogy with R-parity in supersymmetric models. T-parity forbids tree-level contributions from the heavy gauge bosons to observables involving only standard model particles as

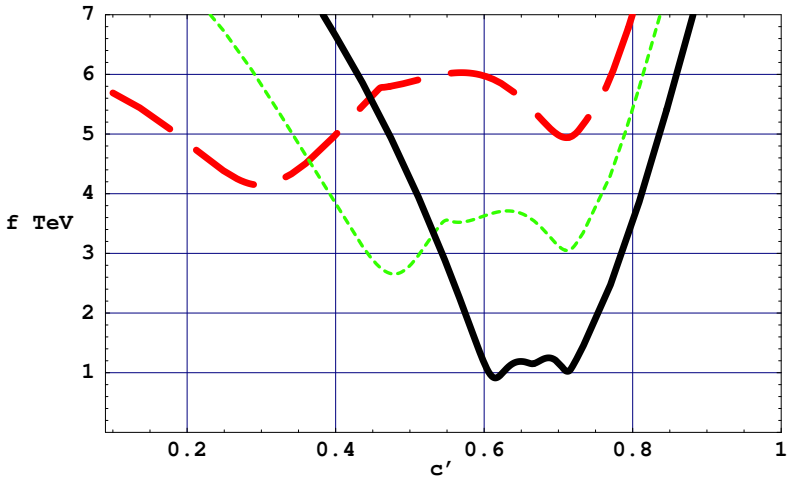


Fig. 7.3: 95% confidence level bound on $f$ for $a = 1$ and $R = 1$ (dashed), $R = 4/5$ (dotted), and $R = 3/5$ (solid). The bounds for $R = 2/5, 1/5$ and 0 can be obtained by reflection around $c'^2 = 1/2$ due to the $R \to 1 - R$, $c'^2 \to 1 - c'^2$ symmetry of the expressions for the electroweak corrections. From [32].

external states. In the case of the Littlest Higgs model, it also forbids the interactions that induce the triplet vev. Corrections to precision electroweak observables are therefore loop level effects. Analysis of the electroweak precision data allows the scale $f$ to be as low as 500 GeV in these models [43]. However one should keep in mind that T-parity introduces new mirror fermions and their presence leads to tree level flavour changing currents which must be kept under control by an appropriate choice of the mirror fermions mass spectrum and mixing parameters [70].

### *7.2.3 Low energy precision data*

Precision experiments at low energy allow a determination of the $g-2$ of the muon and of the weak charge of cesium atoms. These data can be used to put constraints on little Higgs models [38]. Concerning the $g - 2$ of the muon, the contributions of the additional heavy particles are completely negligible and the dominant contributions arise from the corrections to the light $Z$ and $W$ couplings. On the contrary the measure of the weak charge of cesium atoms, gives constraints on the little Higgs models, even if weaker that those at LEP energies. Parity violation in atoms is due to the electron-quark effective Lagrangian

$$\mathcal{L}_{\mathit{eff}} = \frac{G_F}{\sqrt{2}}(\bar{e}\gamma_\mu\gamma_5 e)(C_{1u}\bar{u}\gamma^\mu u + C_{1d}\bar{d}\gamma^\mu d) \; . \tag{7.38}$$

The experimentally measured quantity is the so-called "weak charge" defined as

$$Q_W = -2\left(C_{1u}(2Z + N) + C_{1d}(Z + 2N)\right) \; , \tag{7.39}$$

where $Z$ and $N$ are the number of protons and neutrons of the atom, respectively. The value of the scale $f$ should be in the range of few TeV in order to obtain the measured deviation. The allowed scale is slightly lower in the custodial model with respect to the non-custodial one as the custodial model is closer to the standard model in its predictions. When the scale $f$ is too large the new physics effects become negligible. The scale $f$ in the few TeV range is consistent with what is expected on the model-building side and from the LEP data for little Higgs model. Obviously this result should be taken only as a first indication as the error on $\delta Q_W(Cs)$ is large.

## 7.3 Couplings of the Littlest Higgs boson

*Heather E. Logan*

A light Higgs boson is the central feature of the little Higgs models. In general, the couplings of the light Higgs boson to Standard Model particles receive corrections due to the structure of the Higgs sector and the presence of new TeV-scale particles [35, 38, 54, 61–63, 67]. In models containing only one light Higgs doublet, such as the Littlest Higgs model [6], the SO(9)/SO(5)×SO(4) model of Ref. [11], the SU(3) simple group model [13, 14], and the "Littlest Higgs" model with T-parity [12], these corrections are suppressed by the square of the ratio of the electroweak scale to the TeV scale, $v^2/f^2$, and are thus parametrically at the level of a few percent. In this contribution we give a convenient parameterization for these corrections, discuss their sources, and summarize their generic features, focusing on the Littlest Higgs model. We also discuss the outstanding issue of tree-level heavy particle exchange in Higgs production and decay, and sketch the generalization to other little Higgs models.

### *7.3.1 Higgs couplings*

In general, all masses that originate with the Standard Model Higgs mechanism and all couplings of SM particles to the Higgs boson $H$ are modified in the Littlest Higgs model at order $v^2/f^2$. We parameterize the modifications by the factors $y_i$, which are the couplings of $H$ to SM particle $i$ normalized according to [71, 72]

$$\mathcal{L} = -\frac{m_t}{v} y_t \bar{t}tH - \frac{m_f}{v} y_f \bar{f}fH + 2\frac{M_W^2}{v} y_W W^+W^-H + \frac{M_Z^2}{v} y_Z ZZH. \tag{7.40}$$

The coupling factors $y_i$ in Eq. (7.40) are of order $1+\mathcal{O}(v^2/f^2)$ and are given for the Littlest Higgs model in Table 7.3. The Higgs coupling to the top quark gets a different correction than the couplings to the light fermions due to the mixing between $t$ and $T$ in the Littlest Higgs model, which can be parameterized by $c_t \equiv \lambda_1/\sqrt{\lambda_1^2+\lambda_2^2}$ (with $0 < c_t < 1$). The remaining corrections arise from (i) the mixing between $H$ and the neutral CP-even component of the scalar triplet, controlled by $x \equiv 4fv'/v^2$ (with $0 \le x < 1$), where $v'$ is the triplet vev; (ii) mixing between $W^\pm$ and $W_H^\pm$ (parameterized by $c$) and between $Z$ and $Z_H, A_H$ (parameterized by $c, c'$), which affects both the Higgs couplings and the physical $W$ and $Z$ masses; and (iii) the difference in the contribution to masses and couplings of genuine dimension-six terms arising from the expansion of the nonlinear sigma model in powers of the Higgs field.

In any theory of new physics, corrections to observables must be calculated relative to the SM predictions for a given set of electroweak inputs. These electroweak inputs are usually taken to be the Fermi constant $G_F$ defined in muon decay, the $Z$ mass $M_Z$, and the electromagnetic fine structure constant $\alpha$. Thus, a calculation of corrections to the Higgs couplings due to new physics must necessarily involve a calculation of the corrections to the SM electroweak input parameters due to the same new physics. In the Littlest Higgs model, it is most straightforward to calculate corrections to the Higgs couplings with the SM Higgs vev $v \simeq 246$ GeV as an input, as in Eq. (7.40). To obtain useful predictions for the couplings, however, this must be related to the Fermi constant in the Littlest Higgs model according to $v^{-2} = \sqrt{2}G_F y_{G_F}^2$, where $y_{G_F}^2 = 1 + \mathcal{O}(v^2/f^2)$ (given in Table 7.3) is the correction factor to the relation between the Higgs vev $v$ and $G_F$ as measured in muon decay.

The partial widths of the Higgs boson into $Z$ boson pairs ($\Gamma_Z$), top quark pairs ($\Gamma_t$), and pairs of other fermions ($\Gamma_f$) normalized to their SM values are given by [35, 62]

$$\Gamma_Z/\Gamma_Z^{\rm SM} = y_{G_F}^2 y_Z^2, \qquad \Gamma_t/\Gamma_t^{\rm SM} = y_{G_F}^2 y_t^2, \qquad \Gamma_f/\Gamma_f^{\rm SM} = y_{G_F}^2 y_f^2. \tag{7.41}$$

The calculation of the partial width for the Higgs decay to $W$ bosons is a little subtle when $G_F$, $M_Z$ and $\alpha$ are used as inputs because the relation between these inputs and the physical $W$ boson mass receives corrections from the Littlest Higgs model. The partial width of $H \to WW^{(*)}$ depends on the $W$ mass in the kinematics, especially in the intermediate Higgs mass range, $115\ {\rm GeV} \lesssim M_H \lesssim 2M_W$. To deal with

Table 7.3: Coupling factors $y_i$ in the Littlest Higgs model, in terms of the inputs $f, c_t, x, c$, and $c'$.

| | |
|---|---|
| $y_t$ | $1 + \frac{v^2}{f^2}\left[-\frac{2}{3} + \frac{1}{2}x - \frac{1}{4}x^2 + c_t^2 s_t^2\right]$ |
| $y_f$ | $1 + \frac{v^2}{f^2}\left[-\frac{2}{3} + \frac{1}{2}x - \frac{1}{4}x^2\right]$ |
| $y_W$ | $1 + \frac{v^2}{f^2}\left[-\frac{1}{6} - \frac{1}{4}(c^2 - s^2)^2\right]$ |
| $y_Z$ | $1 + \frac{v^2}{f^2}\left[-\frac{1}{6} - \frac{1}{4}(c^2 - s^2)^2 - \frac{5}{4}(c'^2 - s'^2)^2 + \frac{1}{4}x^2\right]$ |
| $y_{G_F}^2$ | $1 + \frac{v^2}{f^2}\left[-\frac{5}{12} + \frac{1}{4}x^2\right]$ |
| $y_{M_Z}^2$ | $1 + \frac{v^2}{f^2}\left[-\frac{1}{6} - \frac{1}{4}(c^2 - s^2)^2 - \frac{5}{4}(c'^2 - s'^2)^2 + \frac{1}{2}x^2\right]$ |
| $y_{M_W}^2$ | $1 + \frac{v^2}{f^2}\left[-\frac{1}{6} - \frac{1}{4}(c^2 - s^2)^2 + \frac{1}{4}x^2\right]$ |
| $y_{c_W}^2$ | $1 + \frac{v^2}{f^2}\frac{s_W^2}{c_W^2 - s_W^2}\left[-\frac{1}{4} + \frac{1}{4}(c^2 - s^2)^2 + \frac{5}{4}(c'^2 - s'^2)^2 - \frac{1}{4}x^2\right]$ |
| $y_T$ | $-c_t^2 s_t^2 \frac{v^2}{f^2}$ |
| $y_{W_H}$ | $-s^2 c^2 \frac{v^2}{f^2}$ |
| $y_{\Phi^+}$ | $\frac{v^2}{f^2}\left[-\frac{1}{3} + \frac{1}{4}x^2\right]$ |
| $y_{\Phi^{++}}$ | $\mathcal{O}(v^4/f^4)$ |

this, one can follow the approach taken by the program HDECAY [73] for the Minimal Supersymmetric Standard Model (MSSM), which is to define the $H \to WW^{(*)}$ partial width in the MSSM in terms of the SM partial width simply by scaling by the ratio of the $WWH$ couplings-squared in the two models, ignoring the shift in the kinematic $W$ mass. Calculating only the correction to the coupling-squared in the Littlest Higgs model and ignoring the shift due to the $W$ mass correction in the kinematics, one finds [35, 62]

$$\Gamma_W/\Gamma_W^{\rm SM} = y_{G_F}^2 y_W^2 \frac{y_{M_W}^4}{y_{M_Z}^4} y_{c_W}^4. \tag{7.42}$$

The additional correction factors $y_{M_W}^2$, $y_{M_Z}^2$, and $y_{c_W}^2$ are of order $1 + \mathcal{O}(v^2/f^2)$ and are listed in Table 7.3. An alternative approach [63] uses the $W$ mass directly as an input; in this case one has

$$\Gamma_W/\Gamma_W^{\rm SM} = y_{G_F}^2 y_W^2. \tag{7.43}$$

In order to calculate the contributions to the loop induced Higgs couplings to $gg$, $\gamma\gamma$, and $\gamma Z$, the couplings of the Higgs to the colored and/or charged TeV-scale particles are also needed. In the Littlest Higgs model, these are,

$$\mathcal{L} = -\frac{M_T}{v} y_T \bar{T} T H + 2\frac{M_{W_H}^2}{v} y_{W_H} W_H^+ W_H^- H - 2\frac{M_\Phi^2}{v} y_{\Phi^+} \Phi^+ \Phi^- H - 2\frac{M_\Phi^2}{v} y_{\Phi^{++}} \Phi^{++} \Phi^{--} H. \tag{7.44}$$

(For this calculation it is sufficient to use a common mass $M_\Phi$ for the components $\Phi^+$, $\Phi^{++}$ of the TeV-scale scalar triplet.) Because the masses of the TeV-scale particles do not arise from their couplings to the Higgs boson, the coupling factors $y_i$ for these particles are generically of order $v^2/f^2$. They are listed in Table 7.3.

The partial width of the Higgs boson into two photons, normalized to its SM value, is given in the Littlest Higgs model by [61]

$$\Gamma_\gamma/\Gamma_\gamma^{\rm SM} = y_{G_F}^2 \frac{\left|\sum_{i,\rm LH} y_i N_{ci} Q_i^2 F_i(\tau_i)\right|^2}{\left|\sum_{i,\rm SM} N_{ci} Q_i^2 F_i(\tau_i)\right|^2}, \tag{7.45}$$

where $N_{ci}$ is the color factor ($= 1$ or 3), $Q_i$ is the electric charge, $\tau_i = 4m_i^2/m_H^2$, and $m_i$ is the mass, respectively, for each particle $i$ running in the loop: $t$, $T$, $W$, $W_H$, and $\Phi^+$ in the Littlest Higgs (LH) case (the $\Phi^{++}$ loop can be neglected at order $v^2/f^2$ [61]; see Table 7.3); and $t$ and $W$ in the SM case. The standard dimensionless loop factors $F_i$ for particles of spin 1, 1/2, and 0 can be found in Ref. [71]. Likewise, the partial width of the Higgs boson into two gluons, normalized to its SM value, is given in the Littlest Higgs model by [61]

$$\Gamma_g/\Gamma_g^{\rm SM} = y_{G_F}^2 \frac{\left|\sum_{i,\rm LH} y_i F_{1/2}(\tau_i)\right|^2}{\left|\sum_{i,\rm SM} F_{1/2}(\tau_i)\right|^2}, \tag{7.46}$$

where $i$ runs over the fermions in the loop: $t$ and $T$ in the Littlest Higgs case, and $t$ in the SM case.

The partial width of the Higgs boson into $\gamma Z$, normalized to its SM value, is given in the Littlest Higgs model by [63]

$$\Gamma_{\gamma Z}/\Gamma_{\gamma Z}^{\rm SM} = y_{G_F}^2 \frac{\left|\sum_{i,\rm LH} A_i^{\rm LH}\right|^2}{\left|\sum_{i,\rm SM} A_i^{\rm SM}\right|^2}, \tag{7.47}$$

where the amplitude factors $A_i^{\rm LH}$ are given in Ref. [63] and contain the appropriate scaling factors $y_i$. In this process the corrections to the $Z$ couplings to the particles in the loop must also be taken into account [63].

### *7.3.2 Generic features*

The Higgs decay branching ratio to a final state $X$, $\mathrm{BR}(H \to X) = \Gamma_X/\Gamma_{\rm tot}$, is computed in terms of the SM branching ratio as

$$\frac{\mathrm{BR}(H \to X)}{\mathrm{BR}(H \to X)^{\rm SM}} = \frac{\Gamma_X/\Gamma_X^{\rm SM}}{\Gamma_{\rm tot}/\Gamma_{\rm tot}^{\rm SM}}. \tag{7.48}$$

The numerator can be read off from the partial width ratios given above. The denominator requires a calculation of the Higgs total width in both the SM and the little Higgs model. This can be computed using, e.g., HDECAY [73] to calculate the SM Higgs partial width into each final state for a given Higgs mass; the SM total width $\Gamma_{\rm tot}^{\rm SM}$ is of course the sum of these partial widths, while the total width in the Littlest Higgs model is found by scaling each partial width in the sum by the appropriate ratio.

A quick examination of the corrections to the Higgs partial widths given above reveals that the corrections are all parametrically of order $v^2/f^2$. In particular, no coupling receives especially large corrections. This is in contrast to the MSSM, in which the corrections to the couplings of the light SM-like Higgs boson to fermions are parametrically larger than those to $W$ and $Z$ bosons (the deviations in the down-type fermion sector are also enhanced by $\tan\beta$); this coupling structure is due to the two-Higgs-doublet nature of the MSSM Higgs sector [74]. Thus in the Littlest Higgs model there is no "golden channel" in which one expects to see especially large deviations from the SM Higgs couplings. We therefore expect the experimentally best-measured channel to give the highest sensitivity to TeV-scale effects. For example, with $f = 1$ TeV and $M_H = 115$ GeV, the rate for $\gamma\gamma \to H \to b\bar{b}$ in the Littlest Higgs model is reduced by about 6–7% compared to that in the SM [62]. The shifts in the other Higgs branching fractions are of a comparable magnitude.

### *7.3.3 Heavy particle exchange in Higgs production and decay*

The partial width ratios given above can immediately be used to find the corrections to the Higgs boson production cross sections in gluon fusion and in two-photon fusion, since the production cross section is simply proportional to the corresponding Higgs partial width (detailed results were given in Ref. [61]). For other Higgs boson production channels, the cross section corrections are more complicated because

in addition to the corrections to the Higgs couplings to SM particles, tree-level exchange of the TeV-scale particles in the production diagrams must also be taken into account. This has been studied in the Littlest Higgs model for Higgs production at an $e^+e^-$ linear collider via $ZH$ associated production [75, 76], $W$ boson fusion [77], and associated $t\bar{t}H$ production [78].

The process $e^+e^- \to ZH$ receives a correction in little Higgs models from s-channel exchange of the neutral TeV-scale gauge bosons [75, 76]. If the $e^+e^-$ center-of-mass energy $\sqrt{s}$ is well below the mass scale of the heavy gauge bosons, their exchange is propagator-suppressed and the dominant effect comes from the interference term between the SM process and the new diagrams. This correction is parametrically of order $v^2/f^2$, i.e., the same size as the corrections to the Higgs couplings. In this case the corrections to the SM $e^+e^- \to ZH$ amplitude due to the modifications of the $ZZH$ and $e^+e^-Z$ couplings at order $v^2/f^2$ must also be taken into account. In general, however, the effect of the TeV-scale gauge boson exchange varies with $\sqrt{s}$, providing a valuable additional handle on the model parameters, and dramatic resonance effects appear when $\sqrt{s}$ is close to the mass of one of the heavy gauge bosons. This process can be used to probe the crucial $ZZ_HH$ coupling with high precision [76].

Similarly, the $WW$ fusion process $e^+e^- \to \nu\bar{\nu}H$ receives corrections in little Higgs models from substitution of one or both of the t-channel $W$ bosons with their TeV-scale counterparts [77]. Again, for relatively low $\sqrt{s}$, propagator suppression ensures that the dominant effect comes from the interference term between the SM process and diagrams in which one of the two $W$ bosons is replaced with a $W_H$. This correction is parametrically of order $v^2/f^2$, again the same size as the corrections to the Higgs couplings. For this reason, the corrections to the SM $WW$ fusion amplitude due to modifications of the $WWH$ and $We\nu$ couplings at order $v^2/f^2$ must also be taken into account. As in $ZH$ production, the correction due to tree-level $W_H$ exchange will depend on $\sqrt{s}$. The new diagrams can also potentially modify the final-state kinematic distributions, leading to additional observables; these have not yet been studied.

The process $e^+e^- \to t\bar{t}H$ receives corrections in little Higgs models from the substitution of the internal top quark line with the heavy top-partner and from the substitution of the s-channel $Z$ or $\gamma$ with a TeV-scale gauge boson [78]. Diagrams in which the Higgs is radiated off the s-channel gauge boson also contribute. As before, for relatively low $\sqrt{s}$, propagator suppression ensures that the dominant effect comes from the interference term between the SM process and diagrams containing one TeV-scale particle, leading to corrections of order $v^2/f^2$. Again, corrections due to order $v^2/f^2$ modifications of the SM couplings must be included. The corrections will depend on $\sqrt{s}$, with resonances appearing when $\sqrt{s}$ is close to the mass of one of the heavy neutral gauge bosons. Final-state kinematic distributions can provide additional observables; these have likewise not yet been studied.

Tree-level exchange of the TeV-scale particles can also appear in off-shell contributions to Higgs decays. We expect their largest effect to appear in decays in which the SM exchange is also off shell, e.g., $H \to W^{(*)}W^*, Z^{(*)}Z^*$ for $M_H$ below the $WW$ or $ZZ$ threshold, respectively. In this case the decay products of the off-shell $W$ or $Z$ boson(s) have a broad invariant mass distribution, allowing a potentially non-negligible correction from interference of $H \to W^{(*)}W_H^*, Z^{(*)}Z_H^*$ with the SM amplitude. Propagator suppression ensures that the corrections are again of order $v^2/f^2$. These effects can modify the invariant mass distribution of the relevant final-state fermion pair, leading to an additional observable and introducing a potential dependence of the measured decay branching fraction on details of the experimental selection. These contributions to $H \to WW^*, ZZ^*$ have not been studied at all.

Finally, we note that in little Higgs models with T-parity, the TeV-scale gauge bosons are T-parity odd and therefore cannot contribute at tree-level to Higgs production or decay. However, models with T-parity typically contain a T-parity even top-partner which can contribute at tree level to $t\bar{t}H$ production.

### *7.3.4 Generalization to other models*

In the preceding we have discussed the modifications of the light Higgs boson couplings in the Littlest Higgs model [6]. The other little Higgs models that contain only one light Higgs doublet [11, 13, 14] can be fit into the same structure and exhibit the same generic corrections of order $v^2/f^2$. A partial list of coupling correction factors as in Table 7.3 has been worked out [54] only for the SU(3) simple group model [13, 14]. The Higgs coupling corrections in this model differ in their details from those in the Littlest Higgs model. In particular, (i) the model contains no scalar triplet, so there is no correction from Higgs mixing with the triplet; (ii) there is no mixing between $W^\pm$ and the charged TeV-scale gauge bosons; and (iii) corrections to $G_F$ come from the mixing of neutrinos with their TeV-scale partners while the contribution from tree-level exchange of the TeV-scale charged gauge boson is negligible.

Higgs production and decay in the "Littlest Higgs" model with T-parity was studied in detail in Ref. [79]. Because almost all of the new TeV-scale particles in this model are odd under T-parity (the exception being a single T-even top-partner), there are no corrections to tree-level Higgs couplings (aside from $Ht\bar{t}$) due to mixing or exchange of the TeV-scale particles; the only corrections to these couplings come at order $v^2/f^2$ from the genuine dimension-six terms arising from the expansion of the nonlinear sigma model in powers of the Higgs field. The $Ht\bar{t}$ coupling receives additional corrections from the mixing of the top quark with its heavy T-even partner. Finally, the loop-induced Higgs couplings to photon or gluon pairs receive corrections from loops of the new TeV-scale particles, including the T-odd states. All the corrections to Higgs couplings are parametrically of order $v^2/f^2$. However, because electroweak precision constraints on the mass scale $f$ of the heavy particles are much weaker in models with T-parity [9, 12, 28, 43], the spectrum of new particles can be significantly lighter resulting in much larger modifications of Higgs couplings than in models without T-parity.

Many little Higgs models contain two light Higgs doublets [7, 8, 10, 13, 15]. In such models, the dominant corrections to the couplings of the lightest CP-even Higgs boson typically come from the two-doublet mixing effects, rather than the genuine $v^2/f^2$-suppressed effects of the TeV-scale states. In this case the Higgs phenomenology will look more like that of the MSSM Higgs sector. If the dimensionless couplings in the Higgs potential are not large, the Higgs sector exhibits a *decoupling limit* (for a review see Ref. [80]) in which one doublet becomes heavy, leaving a single light SM-like Higgs boson. The corrections to the couplings will then follow a pattern similar to a general two Higgs doublet model, with the parametrically largest deviations expected in the couplings of the Higgs to fermions. Beyond the couplings of the lightest Higgs, the Higgs potential in these two-doublet models exhibits interesting restrictions due to the global symmetry structure; further study in this direction would be interesting.

Finally, we note here that corrections to the Higgs couplings can also be induced by the UV completion at $\sim 10$ TeV. For example, the loop-induced Higgs coupling to photon pairs receives corrections from the dimension-six operator $(c/\Lambda^2)h^\dagger h F^{\mu\nu}F_{\mu\nu}$ suppressed by the UV completion scale $\Lambda$ [62, 81]; this can be thought of as arising from the particles of the UV completion running in the loop. If the UV completion is weakly coupled, these corrections should naively be suppressed by the square of the ratio of the electroweak scale to the 10 TeV scale, $v^2/\Lambda^2$, and thus be too small to detect; in particular, the corrections to the Higgs couplings will then be accurately predicted by the TeV-scale theory alone. However, if the UV completion is strongly coupled, the strong-coupling enhancement can counteract the suppression from the high mass scale, leading to corrections naively of the same order as those from the TeV scale physics.

### 7.4 Pseudo-axions in Little Higgs models

*Wolfgang Kilian, David Rainwater and Jürgen Reuter*

Little Higgs models have an extended structure of global symmetries, broken both spontaneously and explicitly. Among these global symmetries there can appear U(1) factors, which lead to the presence of light pseudoscalar particles, Goldstone bosons associated with this U(1) group, in the spectrum of little Higgs models [64]. These global U(1) factors arise from two different mechanisms.

In the first case, in the Littlest Higgs type models, there is a $[\mathrm{SU}(2)\times\mathrm{U}(1)]^2$ product structure, where U(1) groups happen to be quasi arbitrary additional factors (we do not discuss possible embeddings into larger symmetry groups here). The doubled gauge group $[\mathrm{SU}(2)]^2$ of weak interactions is broken to the diagonal SU(2) of the Standard Model. Analogously, both U(1) factors can be gauged and be broken down to the diagonal U(1) of hypercharge. In many models, especially those without a built-in custodial symmetry or T-parity, the second U(1) gauge boson is tightly constrained from direct searches (Tevatron) and electroweak precision observables. So considering the second U(1) factor ungauged as a removal of the constraints, leaves one with a global U(1) symmetry.

Secondly, in simple group models the breaking of the global symmetries can be understood as a breaking from e.g. in the SU(3) simple group model [14] U(3) to U(2) instead of SU(3) to SU(2) with an additional U(1) symmetry left unbroken at this stage. If this symmetry were exact, the corresponding Goldstone boson, parameterized by

$$\xi = \exp[i\eta/f], \tag{7.49}$$

would be exactly massless and would have only derivative interactions. But in these models, there is always an explicit breaking of the global symmetries, necessary to give a large enough quartic coupling to the Higgs boson. This explicit breaking generates a mass for the pseudoscalar particle. The U(1) quantum numbers of the pseudoscalar in this second case are predicted by the model because the U(1) symmetry is embedded in a larger symmetry whose structure is known. In contrast, in the Littlest Higgs type models, where the global U(1) is an additional factor not connected to non-Abelian group structure there is no prediction for the quantum numbers. Note that anomaly cancellation is not an issue, since the global U(1) symmetry may well be anomalous. This second type of pseudoscalars resembles the breaking of chiral symmetries in QCD, with the $\eta$ meson playing the role of the pseudoscalar here.

Since these U(1)-Pseudo-Goldstone bosons are pseudoscalars and electroweak singlets, they do not have couplings to the Standard Model gauge bosons. All their couplings to Standard Model fermions are suppressed by the ratio $v/f$ of the electroweak scale over the TeV scale. In Littlest Higgs type models, the mass of the pseudoaxions is not predicted , while in simple group models it is connected to the masses of the Higgs bosons by the Coleman-Weinberg potential. In order not to reintroduce fine tuning and to destabilize the so called little hierarchy between the electroweak and the TeV scale, the pseudoaxion mass should be approximately bounded by $v$, $m_\eta \lesssim 250$ GeV. In principle, the pseudoaxions can become quite light, of the order of a few GeV or less, but for masses in that range there exist constraints from rare $\Upsilon$ decays and other flavour processes [82, 83]. Even in simple group models, the pseudoscalar mass – like the Higgs mass – cannot be fixed, because there are too many free parameters, e.g. the mass parameter $\mu$ and a mixing angle $t_\beta \equiv \tan\beta = f_2/f_1$ [54, 64] similar to the Minimal Supersymmetric Standard Model. As an example we show the connection of the pseudoscalar and Higgs masses as functions of the $\mu$ parameter in the SU(3) simple group model on the left of Fig. 7.4.

From the structure of the couplings above a quite generic pattern of branching ratios can be deduced. All decays to electroweak vector bosons (even off-shell) are absent. The dominant decay modes are into the heaviest available Standard Model fermions, i.e. $b\bar{b}$, $c\bar{c}$ and $\tau^+\tau^-$. Compared to the Higgs branching ratios, the decays to two gluons or two photons are more important for the pseudoaxions due to two reasons: Firstly, the absence of the $WW$ and $ZZ$ decays and the $v^2/f^2$ suppression for the fermionic decays enhance these final states. Secondly, the triangle anomaly graphs responsible for the $gg$ and $\gamma\gamma$

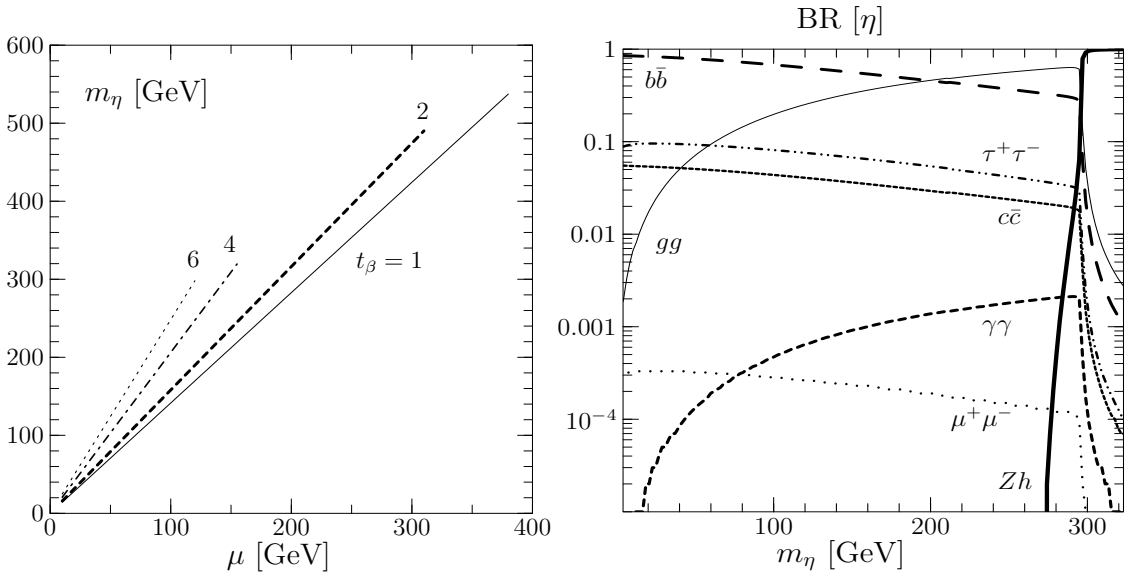


Fig. 7.4: On the left: Typical masses of the pseudoaxion in the SU(3) simple group model as a function of the $\mu$ mass parameter. The four lines correspond to different values of $\tan\beta$. On the right: Branching ratios for the pseudoaxion in the SU(3) simple group model as a function of its mass.

decays are enhanced by the additional heavy top state and possibly further heavy fermionic states present in the simple group Models (this second point partly also applies to the Higgs boson). A typical set of branching ratios as a function of the pseudoscalar's mass is shown on the right in Fig. 7.4. The decay to $Zh$ is special for simple group Models, and does not appear in Littlest Higgs type models.

The couplings of the pseudoaxion to two gluons or two photons generated by the triangle anomalies offer the best search possibility for these particles at the LHC. There the pseudoaxions can be produced in analogy to the Higgs boson in gluon fusion, while the decay to two photons gives the cleanest decay signature as a peak in the diphoton spectrum. Fig. 7.5 shows the cross section for this process as a function of the invariant diphoton mass and hence the pseudoaxion mass, for the Littlest Higgs and the SU(3) simple group model. In principle, the associated production $t\bar{t}\eta$ can also be used, but is plagued by huge backgrounds at the LHC (note again the $v/f$ suppression of this coupling). At a future ILC, this would be the dominant search mode, by looking for narrow peaks in the invariant mass of pairs of $b$ jets in the final state $b\bar{b}b\bar{b}$ and missing energy. As was shown in [64], this is in fact the only viable search possibility for 50 GeV $< m_\eta <$ 85 GeV. A search for an $s$-channel resonance at the photon collider is the best search option for masses of the pseudoaxion well above the $Z$ threshold and allows for precision measurements of such a state; however, the photon spectrum deteriorates dramatically for energies as low as the $Z$ mass.

Introducing T-parity into little Higgs models, one finds that generically the pseudoaxion becomes T-odd. This means, if it is the lightest T-odd particle (LTP), it can be a Cold Dark Matter candidate. As was discussed in [44], in the Littlest Higgs model with T-parity the heavy partner of the hypercharge boson, called $A_H$, becomes the LTP. Note that an ungauging of the additional U(1) is unnecessary from the point of view of the electroweak precision observables, since T-parity already forbids tree-level contributions to gauge-boson self energies. Nevertheless, if this second U(1) *is* ungauged, its gauge boson $A_H$ is traded for the pseudo-Goldstone boson $\eta$, which takes over the role of the LTP. The consequences for the dark matter content in [44] remains the same, since it is mainly the Goldstone boson couplings in the $A_H$ which are responsible for the dominant annihilation channel to Higgs or longitudinal electroweak gauge bosons.

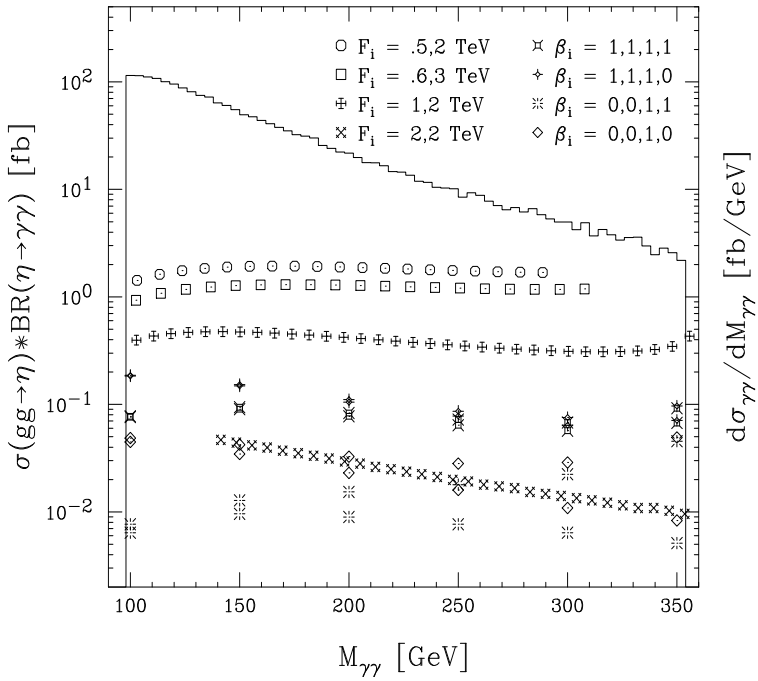


Fig. 7.5: Cross section times branching ratio for the gluon fusion production of the pseudoaxion in the Littlest and the SU(3) simple group model and subsequent decay into two photons. The symbols on the left correspond to the SU(3) simple group model, showing different scales (which can also be expressed as $f$ and $\tan\beta$). On the right, the Littlest Higgs, where the $\beta$'s are different assignments of $U(1)_\eta$ quantum numbers. For more details see [64].

## 7.5 Little Higgs with T-parity

*Jay Hubisz*

The earliest implementations of the little Higgs structure suffered from electroweak precision (EWP) constraints [31–33]. After electroweak symmetry breaking, mixing is generally induced between the standard model gauge bosons and their TeV scale partners. This mixing can lead to, for example, violations of custodial SU(2). This leads to a tree level shift in the $\rho$ parameter, a relation between the $W$ and $Z$ mass which is tightly constrained. In addition, SM fermions couple to the heavy gauge bosons, leading to large four-fermion operators which must be suppressed.

T-parity is a postulated discrete symmetry under which the SM particles are neutral, while most new heavy states are odd [9, 12, 28]. This is in analogy with R-parity (or matter parity) where the supersymmetric partners of the SM fields are odd. This discrete symmetry, if unbroken, then forbids mixing of the SM particles with the new states. Contributions to EWP observables and four-fermion operators are then not generated at tree level, but at the one-loop level.

T-parity is a symmetry that is inherited from an automorphism of the gauge group algebra of little Higgs models. In the Littlest Higgs model T-parity exchanges the two copies of $\mathrm{SU}(2) \times \mathrm{U}(1)$ gauge bosons. In the moose models with T-parity, this symmetry has a geometrical interpretation as a parity symmetry of the moose diagram. Implementing T-parity as a symmetry of the theory requires that the gauge couplings for the two $\mathrm{SU}(2) \times \mathrm{U}(1)$ gauge groups be equal. In this way, the diagonal subgroup (the standard model gauge group) is even under T-parity, while the other combinations of gauge bosons, which receive $f$ scale masses, are odd. In addition, if one wishes to implement this symmetry consistently throughout the entire model, the matter sector of the model must also be symmetric under this interchange. For every multiplet that transforms under $[SU(2) \times U(1)]_1$, there must be a partner

multiplet that transforms under $[SU(2) \times U(1)]_2$ [12]. This opens up a new flavor structure in the low energy effective theory, which is constrained by studies of neutral meson mixing and rare decays [70]. This discrete symmetry, while it eliminates the tree level shifts in standard model observables, drastically changes the phenomenology of little Higgs models [44].

If the discrete symmetry is made exact, the lightest T-odd particle is stabilized, and is a potential dark matter candidate. In collider phenomenology, this lightest particle becomes a missing energy signal, making observation of this new physics more complicated. In particular, it is likely that this type of model will look very much like supersymmetry. This is similar to studies of universal extra dimensions, where the signals are also similar to those of supersymmetry [84, 85]. In the Littlest Higgs model with T-parity, the heavy partner of the hypercharge gauge boson, the $A_H$, is the dark matter candidate, and can account for the WMAP observed relic density [44, 86].

### *7.5.1 New features in models with T-parity*

In the Littlest Higgs model, the action of T-parity on the gauge bosons and scalars is as follows:

$$\begin{aligned} T &: A_1 \to A_2 \\ T &: \Pi \to -\Omega \Pi \Omega, \end{aligned} \tag{7.50}$$

where $\Omega = \mathrm{diag}(1, 1, -1, 1, 1)$. It is easily verified that the Higgs doublet is neutral under this transformation, whereas the scalar triplet is odd under T-parity. This assignment forbids a vev for the triplet which would break custodial SU(2).

Implementing T-parity fixes the gauge couplings such that the angles defined in the introduction are set equal: $s = s' = 1/\sqrt{2}$. Thus T-parity imposes restrictions on the mass spectrum that are not present in models without T-parity. To match onto the standard model, the gauge couplings are given by

$$\begin{aligned} g_1 &= g_2 = \sqrt{2} g \\ g_1' &= g_2' = \sqrt{2} g', \end{aligned} \tag{7.51}$$

where $g$ and $g'$ are the $\mathrm{SU}(2)_L$ and hypercharge gauge couplings, respectively.

In the Littlest Higgs with T-parity, this implies that the masses of the new T-odd gauge bosons with respect to the overall breaking scale $f$ are

$$M_{W_H^\pm} = M_{Z_H} = gf, \qquad M_{A_H} = \frac{g' f}{\sqrt{5}}. \tag{7.52}$$

In models with T-parity, the standard model fermion doublet spectrum needs to be doubled. This is to ensure that there is equal matter content charged under each copy of SU(2).[2] For each lepton/quark doublet, two fermion doublets $\psi_1 \in (\mathbf{2}, \mathbf{1})$ and $\psi_2 \in (\mathbf{1}, \mathbf{2})$ are introduced. (The quantum numbers refer to representations under the $\mathrm{SU}(2)_1 \times \mathrm{SU}(2)_2$ gauge symmetry.) These can be embedded in incomplete representations $\Psi_1, \Psi_2$ of the global SU(5) symmetry. An additional set of fermions forming an SO(5) multiplet $\Psi^c$, which transforms nonlinearly under the full SU(5), is introduced to give mass to the extra fermions; the field content can be expressed as follows:

$$\Psi_1 = \begin{pmatrix} \psi_1 \\ 0 \\ 0 \end{pmatrix}, \quad \Psi_2 = \begin{pmatrix} 0 \\ 0 \\ \psi_2 \end{pmatrix}, \quad \Psi^c = \begin{pmatrix} \tilde{\psi}^c \\ \chi^c \\ \psi^c \end{pmatrix}. \tag{7.53}$$

[2] In principle, the standard model fermions could transform non-linearly under the full SU(5), and thus only under the $\mathrm{SU}(2)_L$ unbroken gauge symmetry [9]. In this case, the T-odd fermions are not present. However, this leads to large contributions to four fermion operators which are constrained primarily by studies at LEP, CDF, and D0. These constraints are referred to as compositeness bounds on quarks and leptons.

These fields transform under the SU(5) global symmetry as follows:

$$\Psi_1 \to V^* \Psi_1 \,, \quad \Psi_2 \to V \Psi_2 \,, \quad \Psi^c \to U \Psi^c, \tag{7.54}$$

where $U$ is the nonlinear transformation matrix defined in Refs. [12, 28, 44]. The action of T-parity on the multiplets takes

$$\Psi_1 \leftrightarrow \Sigma_0 \Psi_2, \quad \Psi^c \to -\Psi^c. \tag{7.55}$$

These assignments allow a term in the Lagrangian of the form

$$\kappa f (\bar{\Psi}_2 \xi \Psi^c - \bar{\Psi}_1 \Sigma_0 \Omega \xi^\dagger \Omega \Psi^c), \tag{7.56}$$

where $\xi = \exp(i\Pi/f)$. $\xi$ transforms linearly on the left, and non-linearly on the right, rendering Eq. (7.56) invariant under SU(5) transformations. Eq. (7.56) gives a Dirac mass $M_- = \sqrt{2}\kappa f$ to the T-odd linear combination of $\psi_1$ and $\psi_2$, $\psi_- = (\psi_1 - \psi_2)/\sqrt{2}$, together with $\tilde{\psi}^c$; the T-even linear combination, $\psi_+ = (\psi_1 + \psi_2)/\sqrt{2}$, remains massless and is identified with the standard model lepton or quark doublet. To give Dirac masses to the remaining T-odd states $\chi^c$ and $\psi^c$, a spinor multiplet of $SO(5)$ can be introduced, along with an additional singlet.[3]

To complete the discussion of the fermion sector, we introduce the usual SM set of the $\mathrm{SU}(2)_L$-singlet leptons and quarks, which are T-even and can participate in the SM Yukawa interactions with $\psi_+$. The Yukawa interactions induce a one-loop quadratic divergence in the Higgs mass; however, the effect is numerically small except for the third generation of quarks. The Yukawa couplings of the third generation must be modified to incorporate the collective symmetry breaking pattern.

In order to avoid large one-loop quadratic divergences from the top sector, the $\Psi_1$ and $\Psi_2$ multiplets for the third generation must be completed to representations of the $\mathrm{SU}(3)_1$ and $\mathrm{SU}(3)_2$ subgroups of SU(5). We write these as

$$\chi_1 = \begin{pmatrix} q_1 \\ U_{L1} \\ 0 \end{pmatrix}, \quad \chi_2 = \begin{pmatrix} 0 \\ U_{L2} \\ q_2 \end{pmatrix}. \tag{7.57}$$

These obey the same transformation laws under T-parity and the SU(5) symmetry as do $\Psi_1$ and $\Psi_2$. The quark doublets are embedded such that

$$q_i = -\sigma_2 \begin{pmatrix} u_{Li} \\ b_{Li} \end{pmatrix}. \tag{7.58}$$

In addition to the SM right-handed top quark field $u_R$, which is assumed to be T-even, the model contains two $\mathrm{SU}(2)_L$-singlet fermions $U_{R1}$ and $U_{R2}$ of hypercharge 2/3, which transform under T-parity as

$$U_{R1} \leftrightarrow U_{R2}. \tag{7.59}$$

The top Yukawa couplings arise from the Lagrangian of the form

$$\begin{aligned} \mathcal{L}_t \;=\; & \frac{1}{2\sqrt{2}} \lambda_1 f \epsilon_{ijk} \epsilon_{xy} \big[ (\bar{\chi}_1)_i \Sigma_{jx} \Sigma_{ky} + (\bar{\chi}_2 \Sigma_0)_i \tilde{\Sigma}_{jx} \tilde{\Sigma}_{ky} \big] u_R \\ & + \lambda_2 f (\bar{U}_{L1} U_{R1} + \bar{U}_{L2} U_{R2}) + \mathrm{h.c.} \end{aligned} \tag{7.60}$$

where $\tilde{\Sigma} = \Sigma_0 \Omega \Sigma^\dagger \Omega \Sigma_0$ is the image of the $\Sigma$ field under T-parity. The indices $i, j, k$ run from 1 to 3 whereas $x, y = 4, 5$. The T-parity eigenstates are given by

$$q_\pm = \frac{1}{\sqrt{2}}(q_1 \pm q_2), \quad U_{L\pm} = \frac{1}{\sqrt{2}}(U_{L1} \pm U_{L2}), \quad U_{R\pm} = \frac{1}{\sqrt{2}}(U_{R1} \pm U_{R2}). \tag{7.61}$$

[3] In other extensions of the Littlest Higgs model with T-parity which contain more sigma model fields and an enlarged gauge symmetry (such as the $\mathrm{SU}(5)^2/\mathrm{SO}(5)$ model of [12]), the non-linearly transforming multiplet can be avoided altogether. We choose here to focus on the most compact phenomenologically consistent model with T-parity.

The T-odd states $U_{L-}$ and $U_{R-}$ combine to form a Dirac fermion $T_-$, with mass $m_{T_-} = \lambda_2 f$. The remaining T-odd states $q_-$ receive a Dirac mass from the interaction in Eq. (7.56).

To leading order in $v/f$, after diagonalizing to the mass eigenbasis, the T-even states have masses given by

$$m_t = \frac{\lambda_1 \lambda_2 v}{\sqrt{\lambda_1^2 + \lambda_2^2}}, \quad m_T = \sqrt{\lambda_1^2 + \lambda_2^2}\, f, \tag{7.62}$$

identical to the Littlest Higgs without T-parity. It is interesting to note that in this model, the T-odd states do not participate in the cancellation of quadratic divergences in the top sector: the cancellation only involves loops of $t$ and $T_+$.[4]

### *7.5.2 Electroweak precision constraints*

As mentioned above, there are no tree level contributions to electroweak precision observables in the Littlest Higgs model with T-parity. Contributions enter at the one loop level, however, and these restrict the available parameter space in the model. A global fit analysis has been performed in [43]. The one loop constraints arising from the SU(2)$_L$ triplet, the T-odd gauge bosons, the T-even partner of the top-quark, and the T-odd fermion doublets are all taken into account.

An interesting feature of this fit is that the contributions to $\Delta\rho$ from the T-even singlet partner of the top quark come in with the correct sign to allow for a larger Higgs mass. It is shown in [43] that the Higgs mass can be increased up to the unitarity bound for certain choices of the free parameters of the theory. As we will discuss below, larger Higgs masses are preferred for dark matter as well. In Fig. 7.6, the 95, 99, and 99.9 confidence level contours are shown for $x_\lambda = 2$, and $\Lambda = 4\pi f$.

There are certain contributions to EWP that are in fact log divergent [28, 43], and thus sensitive to the UV completion of the model. In particular, SM gauge boson self energy diagrams receive divergent contributions from loops where the T-odd gauge bosons run in the loop. This is not a sign of a sickness of the theory, but is rather a consequence of working in the context of a non-linear sigma model. Just as the Higgs mass enters into electroweak precision constraints through loop diagrams, the physics of the UV completion will provide the scale which cuts off these logarithmic divergences.

The dominant contribution to EWP comes from the $T$ parameter, which is directly related to $\Delta\rho$. We summarize here the contributions to the $T$-parameter; expressions for the remaining oblique and non-oblique corrections needed for a full global fit appear in [43]. The expressions for the one loop little Higgs contributions to the T-parameter are

$$\begin{aligned}
T_{T_+} &= \frac{3}{8\pi}\frac{1}{s_w^2 c_w^2} x_\lambda^2 \frac{m_t^4}{m_{T_+}^2 m_Z^2}\left[\log\frac{m_{T_+}^2}{m_t^2} - 1 + \frac{1}{2}x_\lambda^2\right] \\
T_{\text{gauge}} &= -\frac{9g^2}{128\pi c_w^2 s_w^2 m_Z^2}\frac{v^4}{f^2}\log\frac{\Lambda^2}{m_{W_H}^2} \\
T_{\Psi_-} &= -\sum_i \frac{\kappa_i^2}{192\pi^2\alpha}\frac{v^2}{f^2},
\end{aligned} \tag{7.63}$$

where the $\kappa_i$ are the T-odd fermion Yukawa couplings. The presence of the logarithmic divergence in $T_{\text{gauge}}$ signifies that a counterterm is necessary [28]. In Fig. 7.6, it is assumed that this counterterm is zero, and $\Lambda = 4\pi f$. The contribution from the T-odd fermions includes a sum over all T-odd fermion doublets. This does not take into account color factors, and so each T-odd quark doublet gets an additional factor of 3. Of interest is the fact that the contributions of the T-odd fermion doublets do not decouple with increasing $\kappa$. This reason for this is similar to non-decoupling of the top quark in the SM. The

[4] It has been recently discovered that it is possible to realize the cancellation of the top quark divergence with a T-odd partner of the top quark [42]. In these models, there are additional T-even fields, however these are allowed to be rather heavy, as they do not participate in the quadratic divergence cancellation.

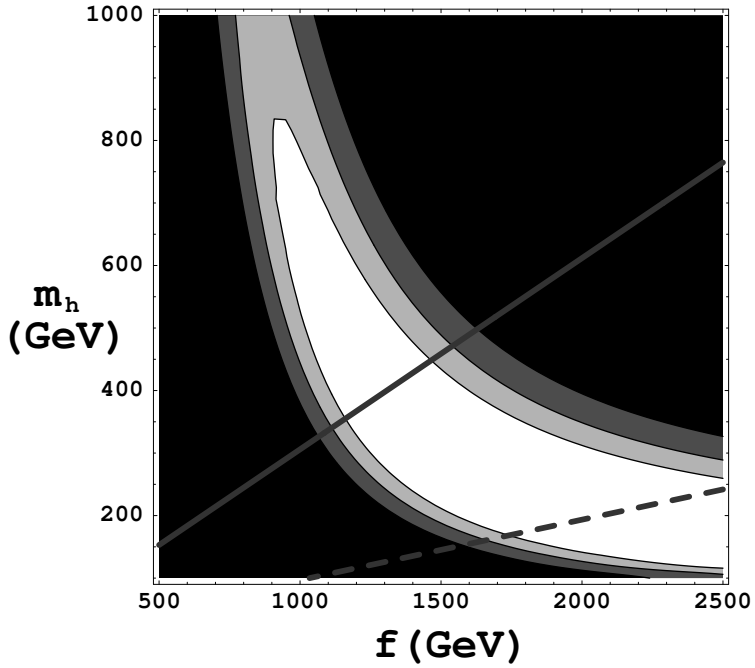


Fig. 7.6: Exclusion contours in terms of the Higgs mass $m_h$ and the symmetry breaking scale $f$. From lightest to darkest, the contours correspond to the 95, 99, and 99.9 confidence level exclusion. The white region is consistent with EWP measurements. Contours of constant values of an estimate of fine-tuning are also shown; the solid and dashed lines correspond to $10\%$ and $1\%$ fine tuning, respectively.

coupling constants $\kappa$ are proportional to the masses, and so the propagator suppression is compensated for by the coupling constant. The deeper reason is that these fermions are tied into gauge invariance of the low energy effective theory, and that there are scattering amplitudes that become non-unitary as these fermion masses approach the cutoff, $\Lambda = 4\pi f$.

### *7.5.3 Flavor constraints*

In addition to electroweak precision, there are also constraints from neutral meson mixing and rare decays. In the Littlest Higgs without T-parity, these are due to the mixing of the $T_3 = 1/2$ eigenstate, and the singlet which is responsible for canceling the top quark quadratic divergence.

With the addition of T-parity, and the consequential necessity of introducing the mirror fermions, there are new and potentially very large contributions to flavor observables. These arise from one loop box diagrams where the T-odd mirror fermions and T-odd gauge bosons run in the loop.

The origin of these interactions can be understood as follows. In terms of T-parity eigenstates, the fermion kinetic terms can schematically be expanded in the following way:

$$\bar{\Psi}_1 i\not{D}_1 \Psi_1 + \bar{\Psi}_2 i\not{D}_1 \Psi_2 = \bar{\Psi}_{\rm SM} i\not{D}_{\rm SM} \Psi_{\rm SM} + \bar{\Psi}_- i\not{D}_{\rm SM} \Psi_- + ig\bar{\Psi}_- \not{A}_- \Psi_{\rm SM} + ig\bar{\Psi}_{\rm SM} \not{A}_- \Psi_- \quad (7.64)$$

The T-odd fermion mass term in Eq. (7.56) can be extended to include generational mixing. After rewriting Eq. (7.64) in the mass eigenbasis, the last two terms generically involve flavor changing T-odd neutral and charged currents between a standard model fermion and T-odd fermion.

In [70], the contributions to neutral meson mixing observables are computed for arbitrary values of the free parameters associated with the mirror fermions. Is is found that in some regions of parameter space, the T-odd fermion spectrum must be degenerate to within a few percent to satisfy these flavor constraints. This degeneracy can be relaxed with particular choices of mass textures. However, either

the degeneracy, or these tuned values of the mixing matrices must be explained by any UV completion of this low energy effective theory.

In addition, there are in principle contributions from physics above the cutoff scale, $\Lambda = 4\pi f$, however these are sensitive to the UV completion, and thus model dependent. Flavor analyses of little Higgs models usually take these contributions to be zero, assuming that the UV completion gives no new contributions to flavor physics.

As in the flavor problem associated with supersymmetry, it is the the $\epsilon_K$ observable (associated with CP violation in the K-meson system) that gives the strongest bounds. Constraints on the fermion mass spectrum are greatly reduced if the CP violating phase which gives contributions to $\epsilon_K$ is set to zero in the new mixing matrices.

In addition, it is found that there are allowed regions of parameter space where one finds enhancements in the $B_s$ mass splitting relative to the standard model prediction. The mass splitting can be as much as a factor of 10 or more larger than in the standard model.

### *7.5.4 The dark matter candidate*

We calculate the relic density of the lightest T-odd particle assuming that T-parity is an exact symmetry, and that the T-odd fermions are heavy. The mass spectrum is sufficiently non-degenerate that coannihilation effects are unimportant, and only direct annihilation channels need be considered. The dominant channels are those involving s-channel Higgs exchange with $W^{\pm}$, $Z$, Higgs, or top quarks in the final state. As a result, the annihilation cross section is primarily a function of the Higgs mass, and the mass of the dark matter candidate. Imposing the constraints given by the WMAP collaboration [87] leads to Fig. 7.7. We see that there is a strong correlation between the scale $f$ and the Higgs mass if the dark matter is to come purely from little Higgs physics. This is due to the s-channel pole present when $m_{A_H} = m_H/2$. Notably, for larger values of $f$, larger Higgs masses than the standard model best fit value are preferred.

We consider regions as ruled out where the relic density exceeds the 95% confidence limits imposed by the WMAP bound. In Fig. 7.7, these regions are shown in black. In regions where the relic density of the $A_H$ is below the WMAP 95% confidence band, there is the possibility that there is another form of dark matter, such as axions, which could make up the difference. These are the lighter contours in Fig. 7.7. Finally, the second darkest region is where the relic density of $A_H$ lies within the 95% confidence bounds given by WMAP.

The narrow region where $f$ is below 600 GeV is where $M_{A_H}$ drops below the $W$ boson mass, and can only annihilate to SM fermions. Because the s-channel Higgs exchange is the only contribution, and the coupling of the Higgs to the accessible fermions is small, it is required that the annihilation happen very close to the Higgs resonance to enhance the cross section enough to get the correct relic density. For values of $f$ below 600 GeV then, the Higgs mass must be very close to $M_{A_H}/2$ in order to get the right abundance of dark matter.

A study of the one loop electroweak precision corrections in this model reveals that certain contributions to $\Delta\rho$ from one-loop diagrams arise with the opposite sign as the terms which are logarithmic in the Higgs mass [43]. This effect is due to the contributions from singlet-doublet quark mass mixing in the third generation Yukawa. Consequentially, the Higgs mass can be raised far above its standard electroweak precision bound while remaining consistent with LEP. Thus, for certain ranges of the parameters in the top-quark Yukawa sector, both dark matter and EWP bounds may be satisfied simultaneously.

We note that the T-odd fermion doublets may in principle be quite light, such that they play a significant role in the relic abundance calculation through coannihilation channels. This has been considered in detail in [86]. In addition, this paper also discusses the potential for direct and indirect detection of the relic $A_H$. Currently, the best way to search for this type of dark matter is with the upcoming GLAST gamma ray telescope. The nucleon scattering cross section turns out to be quite small, as the amplitude

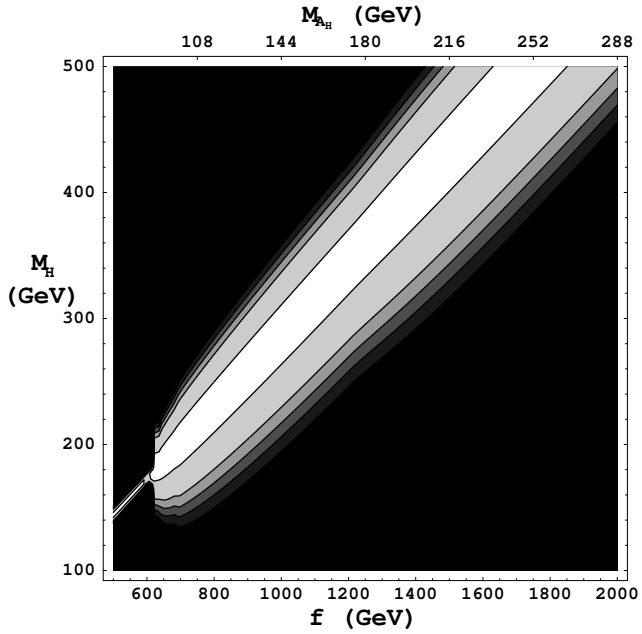


Fig. 7.7: This plot depicts the variation of the relic density with respect to the Higgs mass and the symmetry breaking scale, $f$. In order from lightest to darkest regions, the $A_H$ makes up ($0-10\%$, $10-50\%$, $50-70\%$, $70-100\%$, $100\%$, $>100\%$) of the observed relic abundance of dark matter. The second darkest region is the preferred region, where the $A_H$ dark matter candidate relic density lies within the 95% confidence level bounds determined by the WMAP collaboration. The black region is excluded at the 95% confidence level.

is dominated by T-channel Higgs exchange, which couples to the nucleon through the $hgg$ vertex. The ultimate projected sensitivity of CDMS will begin probing the parameter space relevant to dark matter in the Littlest Higgs model, however the current experimental precision is orders of magnitude away from being able to discover the $A_H$.

### *7.5.5 Collider phenomenology*

Nearly all of the phenomenology of T-parity models is distinct from little Higgs models without T-parity. Because almost all of the new particles are odd under T-parity, they must be pair produced, which reduces the production cross sections due to the additional energy cost. Also, the new T-odd particles will not appear as resonances in detectable particles, as all T-odd particles cascade decay to the lightest T-odd particle, the $A_H$. This makes identification of the little Higgs mechanism nearly impossible at the LHC. The exception is the $T_+$, which is a new T-even state. The production mechanisms and cross section for the $T_+$ are precisely the same as in the original Littlest Higgs. This has been well studied in [67]. The potential for discovery and parameter extraction in the Littlest Higgs without T-parity at Atlas and CMS respectively are discussed in Sections 7.6 and 7.7. However, the decay modes are modified as the $T_+$ now has the channel $T_+ \to T_- A_H \to t A_H A_H$ open to it. This means that the $T_+$ has a sizable portion of its width which cannot be reconstructed. This further complicates attempts to identify the little Higgs mechanism at the LHC.

The pattern of cascade decays in models with T-parity resembles the decay chains of supersymmetry, meaning that it could potentially be quite easy to mistake one for the other at the LHC. There is a

phenomenology dictionary between the Littlest Higgs model with T-parity and supersymmetry:

$$\begin{aligned} \text{electroweak gauginos} &\leftrightarrow \text{T} - \text{odd gauge bosons} \\ \text{sfermions} &\leftrightarrow \text{T} - \text{odd fermion doublets} \\ \text{second Higgs doublet} &\leftrightarrow \text{scalar triplet} \\ \text{higgsinos} &\leftrightarrow \text{NONE} \\ \text{gluinos} &\leftrightarrow \text{NONE} \\ \text{NONE} &\leftrightarrow \text{T} - \text{even partner of top} \end{aligned} \tag{7.65}$$

For a certain choice of spectra, a cascade decay in the Littlest Higgs with T-parity can be duplicated in supersymmetry using this dictionary. Clearly there are distinguishing features of the two, such that not all regions of MSSM parameter space could be confused with a corresponding region of parameter space in this particular little Higgs model. For example, there is no analog of the gluino in little Higgs models. Similarly, there is no translation for the $T_+$ in supersymmetry. However, modifications and extensions can be made on both sides. The Littlest Higgs model is only the most compact way to extend the SM to include collective symmetry breaking (just as the MSSM is the most compact way to extend the SM to include supersymmetry).

To date, only the T-odd gauge bosons, scalars, and singlet fermions ($T_+$ and $T_-$) have been studied in detail, in the limit that the T-odd fermion doublets are taken to be heavy. The phenomenology of the T-odd fermion doublets is potentially quite rich, especially as EWP, flavor physics, and compositeness bounds all favor them being light with respect to the breaking scale, $f$. There are numerous studies currently underway which will study the phenomenology of these states.

## 7.6 Little Higgs studies with ATLAS

*Eduardo Ros and David Rousseau*

Observability of new particles predicted by little Higgs models at the LHC has been studied using a simulation of the ATLAS detector. We discuss first the channels available for the discovery of the new heavy quark $T$, then for new gauge bosons $A_H$, $Z_H$ and $W_H$, and finally for the doubly charged Higgs boson $\phi^{++}$. Most of the results presented here are extracted from [88], with more recent studies in [90–92], where further details can be found. The Monte Carlo program `PYTHIA` 6.203 [93] with suitably normalised rates was used to generate signal events. The Higgs boson branching ratios were taken to be as in the standard model. These events were passed through the ATLAS fast simulation which provides a parametrised response of the ATLAS detector to jets, electrons, muons, isolated photons and missing transverse energy. This fast simulation has been validated using a large number of studies [94] where it was adjusted to agree with the results of a full, `GEANT` based, simulation. Jets are reconstructed using a cone algorithm with a size of $\Delta R = 0.4$. Performance for the high luminosity ($10^{34}$ cm$^{-2}$ sec$^{-1}$) is assumed. Results will be in general quoted for 300 fb$^{-1}$, which correspond approximately to the amount of data collected during three years running at high luminosity. It is assumed that the Higgs boson will have been found and its mass measured. The event selections are based on the characteristics of the signal being searched for, and are such that they will pass the ATLAS trigger criteria. The most important triggers arise from the isolated leptons, jets or photons present in the signal. `PYTHIA` was also used for simulation of the backgrounds. Other event generators were used if backgrounds were needed in regions of phase space where `PYTHIA` is not reliable.

### *7.6.1 Search for the heavy quark T*

The $T$ quark can be produced at the LHC via two mechanisms: QCD production via the processes $gg \rightarrow T\overline{T}$ and $q\overline{q} \rightarrow T\overline{T}$ which depend only on the mass of $T$; and production via $W$ exchange

$qb \to q'T$ which leads to a single $T$ in the final state and therefore falls off much more slowly as $M_T$ increases. This latter process depends on the model parameters and, in particular, upon the mixing of the $T$ with the conventional top quark. The Yukawa couplings of the new $T$ are given by two constants $\lambda_1$ and $\lambda_2$ (following the notation from [67]). The physical top quark mass eigenstate is a mixture of $t$ and $T$, and the various couplings contain three parameters $\lambda_1$, $\lambda_2$ and $f$ that determine the masses of $T$ and the top quark as well as their mixings. Two of the parameters can be reinterpreted as the top mass and the $T$ mass. The third can then be taken to be $\lambda_1/\lambda_2$. This determines the mixings and hence the coupling strength $TbW$ which controls the production rate via the $qb \to q'T$ process. The production rates have been calculated in [67]. It is found that single production dominates for masses above 700 GeV. As we expect that we are sensitive to masses larger than this, we consider only the single production process in what follows. We assume a cross-section of $\sigma = 200$ fb for $M_T = 1.0$ TeV and $\lambda_1/\lambda_2 = 1$. Events generated using PYTHIA were normalised to these values. The decay rates of $T$ are as follows

$$\Gamma(T \to tZ) = \Gamma(T \to tH) = \frac{1}{2}\Gamma(T \to bW) = \frac{\kappa^2}{32\pi}M_T \tag{7.66}$$

with $\kappa = \lambda_1^2/\sqrt{\lambda_1^2 + \lambda_2^2}$ implying that $T$ is a narrow resonance. The last of these decays would be expected for a charged 2/3 $4^{th}$ generation quark; the first two are special to the "little Higgs Model". We now discuss the reconstruction of these channels.

#### 7.6.1.1 Study of the decay $T \to Zt$

This channel can be observed via the final state $Zt \to \ell^+\ell^-\ell\nu b$, which implies that the events contain three isolated leptons, a pair of which reconstructs to the $Z$ mass, one $b-$jet and missing transverse energy. The background is dominated by $WZ$, $ZZ$ and $tbZ$. Events were selected as follows.

- Three isolated leptons (either $e$ or $\mu$) with $p_T > 40$ GeV and $|\eta| < 2.5$. One of these is required to have $p_T > 100$ GeV.
- No other leptons with $p_T > 15$ GeV.
- $E_T^{miss} > 100$ GeV.
- At least one tagged $b-$jet with $p_T > 30$ GeV.

The presence of the leptons ensures that the events are triggered. A pair of leptons of same flavour and opposite sign is required to have an invariant mass within 10 GeV of $Z$ mass. The third lepton is then assumed to arise from a $W$ and the $W$'s momentum reconstructed using it and the measured $E_T^{miss}$. The selection efficiency is 3.3% for $M_T = 1$ TeV. The invariant mass of the $Zt$ system can then be reconstructed by including the $b-$jet. This is shown in Fig. 7.8 for $M_T = 1$ TeV where a clear peak is visible above the background. Following the cuts, the background is dominated by $tbZ$ which is more than 10 times greater than all the others combined. Using this analysis, the discovery potential in this channel can be estimated. The signal to background ratio is excellent as can be seen from Fig. 7.8. Requiring a peak of at least $5\sigma$ significance containing at least 10 reconstructed events implies that for $\lambda_1/\lambda_2 = 1(2)$ and 300 fb$^{-1}$ the quark of mass $M_T < 1050(1400)$ GeV is observable. At these values, the single $T$ production process dominates, justifying *a posteriori* the neglect of $T\overline{T}$ production in this simulation.

#### 7.6.1.2 Study of the decay $T \to Wb$

This channel can be reconstructed via the final state $\ell\nu b$. The following event selection was applied.

- At least one charged lepton with $p_T >$100 GeV.
- One $b$-jet with $p_T > 200$ GeV.
- No more than 2 jets with $p_T > 30$ GeV.
- Mass of the pair of jets with the highest $p_T$ is greater than 200 GeV.

– $E_T^{miss}$ >100 GeV.

The lepton provides a trigger. The backgrounds arise from $t\bar{t}$, single top production and QCD production of $Wb\bar{b}$. The requirement of only one tagged $b-$jet and the high $p_T$ lepton are effective against all of these backgrounds. The requirement of only two energetic jets is powerful against the dangerous $t\bar{t}$ source where the candidate $b-$jet arises from the $t$ and the lepton from the $\bar{t}$. The selection efficiency is 14% for $M_T = 1$ TeV. The signal to background ratio in the case of $T$ with 1 TeV mass is somewhat worse than in the previous case primarily due to the $t\bar{t}$ contribution. From this analysis, the discovery potential in this channel can be estimated. For $\lambda_1/\lambda_2 = 1(2)$ and 300 fb$^{-1}$, $M_T < 2000(2500)$ GeV has at least a $5\sigma$ significance.

#### 7.6.1.3 Study of the decay $T \to Ht$

In this final state, the event topology depends on the Higgs mass. For a Higgs mass of 120 GeV the decay to $b\bar{b}$ dominates. The semileptonic top decay $t \to Wb \to \ell\nu b$ produces a lepton that can provide a trigger. The final state containing an isolated lepton and several jets then needs to be identified. The initial event selection is as follows.

– One isolated $e$ or $\mu$ with $p_T > 100$ GeV and $|\eta| < 2.5$.
– Three jets with $p_T > 130$ GeV.
– At least one jet tagged as a $b-$jet.

Events were further selected by requiring that at least one di-jet combination have a mass in the range 110 to 130 GeV. If there is a pair of jets with invariant mass in the range 70 to 90 GeV, the event is rejected in order to reduce the $t\bar{t}$ background. The measured missing transverse energy and the lepton are then combined using the assumption that they arise from a $W \to \ell\nu$ decay. Events that are consistent with this hypothesis are retained and the $W$ momentum inferred. The selection efficiency is 2.3% for $M_T = 1$ TeV. The invariant mass of the reconstructed $W$, $H$ and one more jet is formed and the result is shown in Fig. 7.8. The width of the reconstructed $T$ resonance is dominated by experimental resolution. This analysis assumes that $\lambda_1/\lambda_2 = 1$. The background is dominated by $t\bar{t}$ events. The significance is lower than the previous channels, about $4\sigma$ for $M_T = 1$ TeV, down to $3\sigma$ for $M_T = 700$ GeV, thus only providing a confirmation if the signal is seen in the previous channel.

### *7.6.2 Search for new gauge bosons*

The model predicts the existence of one charged $W_H$ and two neutral ($Z_H$ and $A_H$) heavy gauge bosons. $W_H$ and $Z_H$ are almost degenerate in mass and are typically heavier than $A_H$. From fine tuning arguments [95], an upper bound can be set: $M_{W_H,Z_H} < 6\ \mathrm{TeV}(m_H/200\ \mathrm{GeV})^2$, i.e. 2 TeV for $m_H = 120$ GeV and 6 TeV for $m_H = 200$ GeV. All these bosons are likely to be discovered via their decays to leptons. However, in order to distinguish these gauge bosons from those that can arise in other models, the characteristic decays $Z_H \to ZH$ and $W_H \to WH$ must be observed [96]. Two new couplings are present, in addition to those of the Standard Model. These additional parameters can be taken to be two angles $\theta$ and $\theta'$. Once the masses of the new bosons are specified, $\theta$ determines the couplings of $Z_H$ and $\theta'$ those of $A_H$. In the case of $Z_H$, the branching ratio into $e^+e^-$ and $\mu^+\mu^-$ rises with $\cot\theta$ to an asymptotic value of 4%.

#### 7.6.2.1 Discovery of $Z_H$, $A_H$ and $W_H^{\pm}$

A search for a peak in the invariant mass distribution of either $e^+e^-$ or $\mu^+\mu^-$ is sensitive to the presence of $A_H$ or $Z_H$. As an example, Fig. 7.9 shows the $e^+e^-$ mass distribution arising from a $Z_H$ of mass of 2 TeV for $\cot\theta = 1$ and $\cot\theta = 0.2$. The production cross-section for the former (latter) case is 1.2 (0.05) pb [67]. Events were required to have an isolated $e^+$ and $e^-$ of $p_T > 20$ GeV and $|\eta| < 2.5$ which provides a trigger. The Standard Model background shown on the plot arises from the Drell-Yan process. In order to establish a signal we require at least 10 events in the peak of at least $5\sigma$ significance.

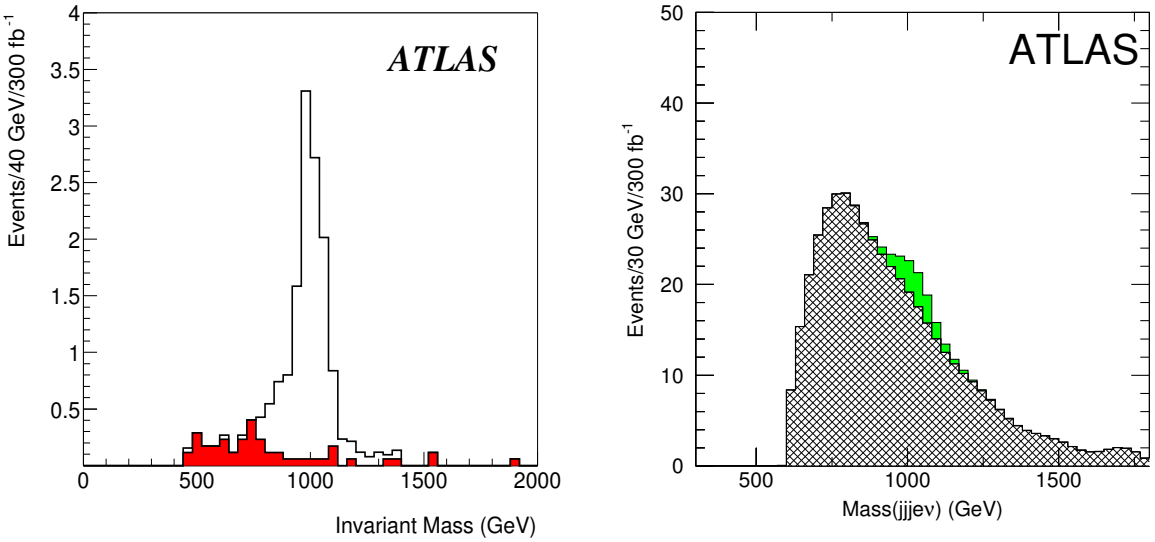


Fig. 7.8: The signal $T \to Zt$ (left) and $T \to Ht$ (right) is shown for a mass of 1 TeV. The background is dominated by $WZ$ and $tbZ$ production (left) and $t\bar{t}$ production (right).

Including the $\mu + \mu^-$ channel improves the reach slightly, given the poorer mass resolution. Fig. 7.14 top left shows the accessible region as a function of $\cot\theta$ and $M_{Z_H}$. A similar search for $A_H$ can be carried out and the accessible region as a function of $\tan\theta'$ and $M_{A_H}$ is shown in Fig. 7.14 top right. Masses greater than 3 TeV are not shown as these are not allowed in the model. There is a small region around $\tan\theta' \sim 1.3$ where the branching ratio to $\mu^+\mu^-$ and $e^+e^-$ is very small and the channel is insensitive. The decay $W_H^{\pm} \to \ell\nu$ manifests itself via events that contain an isolated charged lepton and missing transverse energy. Events were selected by requiring an isolated electron with $e^-$ or $e^+$ of $p_T > 200$ GeV, $|\eta| < 2.5$ and $E_T^{miss} > 200$ GeV. The transverse mass from $E_T^{miss}$ and the observed lepton is formed and the signal appears as a peak in this distribution. The main background arises from $\ell\nu$ production via a virtual $W$. In order to establish a signal we require at least 10 events in the signal region of at least $5\sigma$ significance. Fig. 7.14 top left shows the accessible region as a function of $\cot\theta$ and $M_{W_H}$.

#### 7.6.2.2 Observation of $Z_H \to ZH$, $A_H \to ZH$ and $W_H \to WH$ for $m_H = 120$ GeV

Observation of the cascade decays $Z_H \to ZH$, $A_H \to ZH$, and $W_H \to WH$ provides crucial evidence that an observed new gauge boson is of the type predicted in the little Higgs Models. For a Higgs mass of 120 GeV, two signatures have been searched for : the more abundant $H \to b\bar{b}$ (with a branching ratio of 68%) [90] , and the much rarer $H \to \gamma\gamma$ (with a branching ratio of 0.2%) compensated by a clearer signature [91] .

The decay $ZH \to \ell^+\ell^- b\bar{b}$ results in a final state with two $b-$jets that reconstruct to the Higgs mass and a $\ell^+\ell^-$ pair that reconstructs to the $Z$ mass. The coupling $Z_H ZH$ is proportional to $\cot 2\theta$. When combined with the coupling of $Z_H$ to quarks that controls the production cross-section, the $\cot\theta$ dependence of the rate in this channel is shown in Fig. 7.10, which shows that this decay vanishes for $\cot\theta \sim 1$. A typical value of $\cot\theta \sim 0.5$ is chosen, in the following. The signal is extracted from the $Z_H \to ZH$ state using the following event selection:

- Two leptons of opposite charge and same flavour with $p_T > 6(5)$ GeV for muons (electrons) and $|\eta| < 2.5$. One of them is required to satisfy $p_T > 25$ GeV in order to provide a trigger.
- The lepton pair has a mass between 76 and 106 GeV

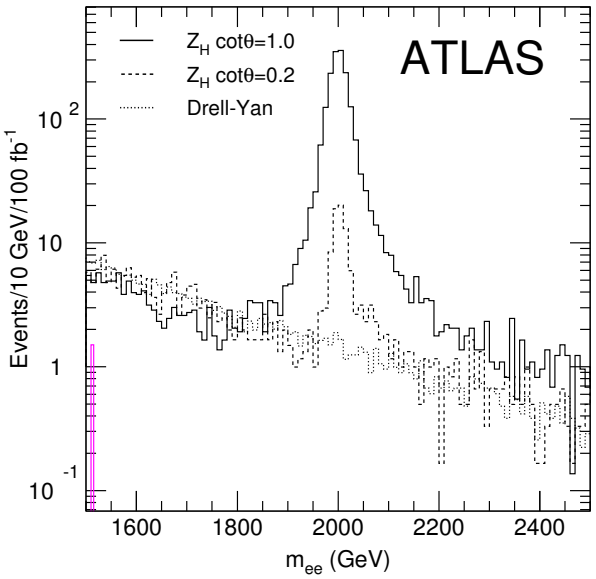


Fig. 7.9: The $e^+e^-$ mass distribution arising from a $Z_H$ of mass of 2 TeV for $\cot\theta = 1$ (upper, solid, histogram) and $\cot\theta = 0.2$ (middle, dashed, histogram). The lowest, dotted histogram shows the distribution from background only.

– Two reconstructed $b-$jets with $p_T > 25$ GeV and $|\eta| < 2.5$, which are within $\Delta R = \sqrt{(\Delta\eta)^2 + (\Delta\phi)^2} < 1.5$.
– The $b-$jet pair should have a mass between 60 and 180 GeV.

The efficiency for $M_{Z_H} = 1$ TeV is 35 %.The mass of the reconstructed $ZH$ system is shown in Fig. 7.11 for a $Z_H$ mass of 1 TeV and $\cot\theta = 0.5$. The presence of a leptonic $Z$ decay in the signal ensures that the background arises primarily from $Z + jet$ final states.

A similar method can be used to reconstruct the $W_H \to WH \to \ell\nu b\bar{b}$ decay. The $b-$jet selections were the same as above while the lepton selection is now as follows:

– One isolated $e$ or $\mu$ with $p_T > 25$ GeV and $|\eta| < 2.5$.
– $E_T^{miss} > 25$ GeV.

The missing transverse energy is assumed to arise only from the neutrino in the leptonic $W$ decay, and the $W$ momentum is then reconstructed. The efficiency for $M_{W_H} = 1$ TeV is 38 %. The background which is dominated by $W + jets$ and $t\bar{t}$ events is larger than in the previous case, nevertheless a signal can be extracted.

The decay $H \to \gamma\gamma$ provides a very characteristic signal. A preliminary event selection requiring two isolated photons, one having $p_T > 25$ GeV and the other $p_T > 40$ GeV and both with $|\eta| < 2.5$ was made. This requirement ensures that the events are triggered. The invariant mass of the two photon system is required to be within $2\sigma$ of the Higgs mass, $\sigma$ being the measured mass resolution of the diphoton system. The reconstructed jets in the event are then combined in pairs and the pair with invariant mass closest to $M_W$ was selected. If this pair has a combined $p_T > 200$ GeV, its mass was corrected to the $W$ mass and then combined with the $\gamma\gamma$ system. The efficiency for $M_{W_H,Z_H} = 1$ TeV is 50 %. The mass distribution of the resulting system is shown in Fig. 7.11. The contributions from $W_H$ and $Z_H$ are shown separately, the former dominates due to its larger production rate. The presence of the two photons with a mass comparable to the Higgs mass ensures that the background is small. This background arises from either direct Higgs production or the QCD production of di-photons.

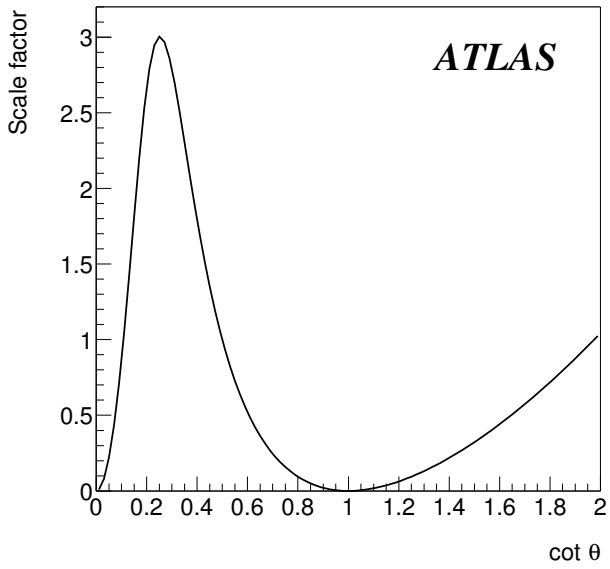


Fig. 7.10: The $\cot\theta$ dependence of the production rate times branching ratio $Z_H \to ZH$.

The analyses were redone for $M_{W_H,Z_H}$= 1, 1.5, and 2 TeV. The reach is shown in Fig. 7.14 bottom left. If $m_H = 120$ GeV, the mass of the heavy bosons is bound to be less than 2 TeV for fine-tuning considerations. A large fraction of the parameter space is hence covered, except for the region around $\cot\theta = 1$.

The search for $A_H \to ZH$ is identical to the search for $Z_H \to ZH$. However, the $A_H$ production and decay to $ZH$ depend on the mixings and so we present the sensitivity in terms of a cross-section that allows reinterpretation of these results to other models. Using the method described above, and assuming only that the $Z_H$ signal does not mask the $A_H$ signal, Fig. 7.12 shows the value of the production cross-section times branching ratio needed to obtain discovery in the channels $A_H \to ZH \to \ell\ell b\overline{b}$ and $A_H \to ZH \to$ jets $\gamma\gamma$.

#### 7.6.2.3 Observation of $Z_H \to ZH$ and $W_H \to WH$ for $m_H = 200$ GeV

For a Higgs mass of 200 GeV, the main Higgs decays are $H \to W^+W^-$ (73 %) and $H \to ZZ$ (26 %). Different $ZH$ and $WH$ final states have been selected, resulting from a compromise between cross-section and signature, as listed in Table 7.4. For the A modes [90] , all leptons are isolated, and the Higgs boson final state is purely leptonic. For the B modes [91] , the Higgs boson final state contain one hadronic $W$ or $Z$.

For the sake of brevity, only the salient points of the analyses are reported here. In all the modes, the main background is inclusive top production, $t\overline{t} \to WbWb \to \ell^-\nu\ell^+\nu bb$ where a third lepton can arise from a $b$ jet. In the A1 and A2 modes, the missing transverse momentum is used to reconstruct the Higgs momentum, with the additional hypothesis that the neutrino is collinear to the leptons, a valid approximation given the high momentum. In addition, the $W$ mass constraint is applied in the B1 and B3 modes. The A3 and A4 modes have indistinguishable final states. For all B modes, some leptons may overlap with the hadronic $W$ or $Z$ decay, given the very high momentum of the Higgs boson (above 500 GeV). Hence a special tuning of the lepton isolation was applied. The hadronic decay of the high $p_T$ $W$ or $Z$ are reconstructed by looking for two high $p_T$ jets with mass close to the $W$ or $Z$ mass, or, if it fails, by taking the jet with largest $p_T$ (assuming that in this case the $W$ or $Z$ is reconstructed as a single jet). The efficiencies for the different modes for $M_{W_H,Z_H} = 1$ TeV are as follows : A1 34%, A2 12%, A3/A4

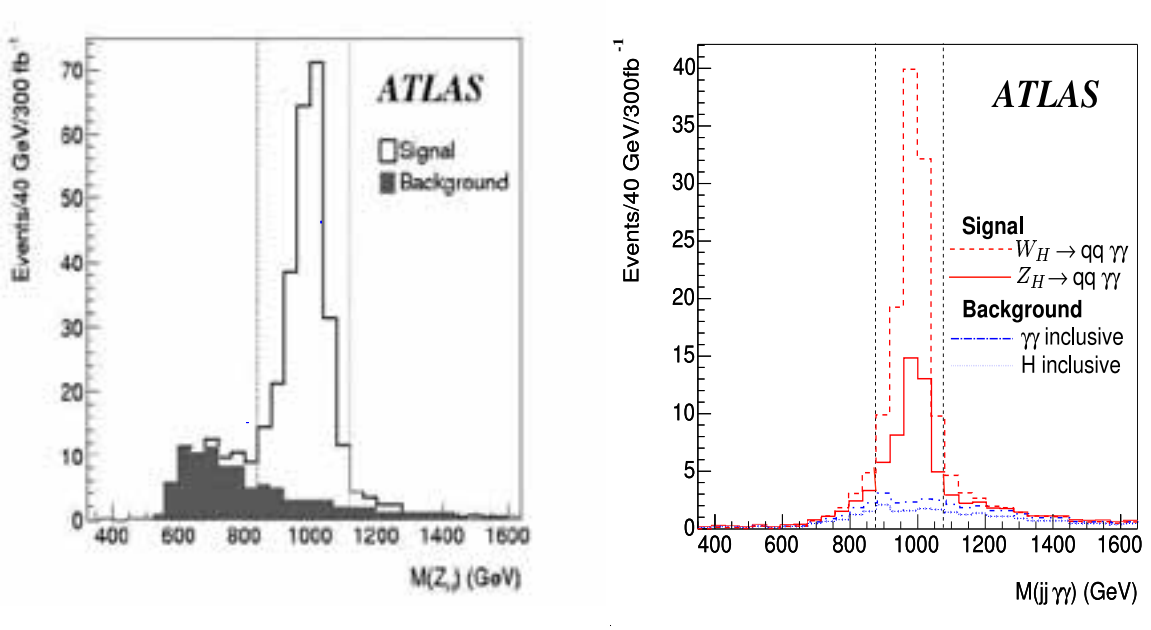


Fig. 7.11: Left : Invariant mass of the $ZH$ system reconstructed from the $\ell^+\ell^- b\bar{b}$ final state. Right : Invariant mass of the $ZH$ or $WH$ system reconstructed from the $jj\gamma\gamma$ final state. The following hypotheses are made: $M_{Z_H/W_H} = 1$ TeV, $m_H = 120$ GeV and $\cot\theta = 0.5$ .

Table 7.4: $W_H$ and $Z_H$ final states being studied. The branching ratios are computed assuming $\cot\theta = 0.5$

| Mode | BR ($10^{-4}$) | decay | signature |
|---|---|---|---|
| A1: | 1.0 | $Z_H \to ZH \to \ell^+\ell^- W^+W^- \to \ell^+\ell^-\ \ell^+\nu\ell^-\nu$ | 4 leptons + $E_T^{miss}$ |
| A2: | 3.0 | $W_H \to WH \to \ell\nu W^+W^- \to \ell\nu\ \ell^+\nu\ell^-\nu$ | 3 leptons + $E_T^{miss}$ |
| A3: | 0.4 | $Z_H \to ZH \to jjZZ \to jj\ \ell^+\ell^-\ell^+\ell^-$ | 4 leptons + jets |
| A4: | 0.4 | $W_H \to WH \to jjZZ \to jj\ \ell^+\ell^-\ell^+\ell^-$ | 4 leptons + jets |
| B1: | 6.8 | $Z_H \to ZH \to \ell^+\ell^- W^+W^- \to \ell^+\ell^-\ jj\ell\nu$ | 3 leptons + jets + $E_T^{miss}$ |
| B2: | 0.8 | $Z_H \to ZH \to \ell^+\ell^- ZZ \to \ell^+\ell^-\ jj\ell^+\ell^-$ | 4 leptons + jets |
| B3: | 2.4 | $W_H \to WH \to \ell\nu ZZ \to \ell\nu\ jj\ell^+\ell^-$ | 4 leptons + jets |

26%, B1 22%, B2 17%, B3 15%. For $M_{W_H,Z_H} = 2$ TeV, the efficiencies decrease by at most a factor of two, due to a more severe overlap of the Higgs boson decay products. An example of the expected reconstructed mass for the B1 modes is shown in Fig. 7.13.

The reach of the analyses are combined separately for A modes and B modes and are summarised in Fig. 7.14 bottom right. The reach is very similar to the $m_H = 120$ GeV case, except that now the mass of the heavy bosons is only bound to be less than 6 TeV, hence a much smaller fraction of the parameter space is covered.

#### 7.6.2.4 Search for hadronic $Z_H$ and $W_H$ decay

While the leptonic decays of $Z_H$ and $W_H$ allow the quicker discovery of the heavy bosons, a test of the little Higgs model necessitates the measurements of other decay modes, like $WH$ or $ZH$ as described in the previous sections but also the hadronic decay modes [92]. In particular, for $\cot\theta \sim 1$, $BR(W_H \to WH)$ and $BR(Z_H \to ZH)$ vanish, and the branching ratios to heavy quarks are [67] :

$$BR(Z_H \to b\bar{b}) = BR(Z_H \to t\bar{t}) = 1/8 = 12.5\% \tag{7.67}$$

$$BR(W_H \to tb) = 1/4 = 25\% \tag{7.68}$$

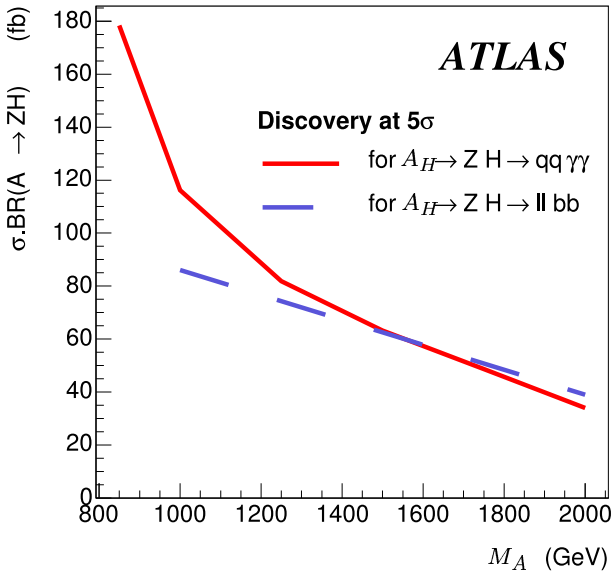


Fig. 7.12: Minimum value of the production cross-section times branching ratio needed to obtain discovery in the channels $A_H \to ZH \to \ell\ell b\overline{b}$ and $A_H \to ZH \to jets\gamma\gamma$ as a function of the $A_H$ mass, for a luminosity of 300 fb$^{-1}$.

The observability of these three final states has been assessed using fast simulation, with parameters tuned on full simulation, and with special care for $b$-tagging at very high jet $p_T$ (up to 1 TeV). While no convincing signal can be seen in the $Z_H$ case, the $W_H \to tb$ appears indeed to be visible and is now described in a few lines. The top is reconstructed in the $W(\ell\nu)b$ final state. One isolated high $p_T$ lepton is searched for, and two $b$-jets tagged, one close to the lepton, one recoiling against the lepton. The neutrino 3-momentum is estimated from the reconstructed missing transverse momentum and assuming it is parallel to the lepton momentum. The final state can be reconstructed with typical efficiency of 25% and mass resolution 110 GeV for $M_{W_H} = 1$ TeV. The background is mainly inclusive top production (irreducible) as well as $W + jets$ (reducible).

The reconstructed mass plot is shown in Fig. 7.13: the signal is clearly visible. The reach shown in Fig. 7.14 top left demonstrates that the $\cot\theta = 1$ region which was missing in the $W_H(Z_H) \to W(Z)H$ analyses is well covered up to $M_{W_H} = 2.5$ TeV.

### *7.6.3 Search for $\phi^{++}$*

The doubly-charged Higgs boson could be produced in pairs and decay into leptonic final states via $q\overline{q} \to \phi^{++}\phi^{--} \to 4\ell$. While this would provide a very clean signature, it will not be considered here since the mass reach in this channel is poor due to the small cross-section. The coupling of $\phi^{++}$ to $W^+W^+$ allows it to be produced singly via $WW$ fusion processes of the type $dd \to uu\phi^{++} \to uuW^+W^+$. This can lead to events containing two leptons of the same charge, and missing energy from the decays of the $W$'s. The $\phi WW$ coupling is determined by $v'$, the vacuum expectation value (vev) of the neutral member of the triplet. This cannot be too large as its presence causes a violation of custodial SU(2) which is constrained by measurements of the $W$ and $Z$ masses. We have examined the sensitivity of searches at the LHC in terms of $v'$ and the mass of $\phi^{++}$. For $v' = 25$ GeV and a mass of 1 TeV, the rate for production of $\phi^{++}$ followed by the decay to $WW$ is 4.9 fb if the $W$'s have $|\eta| < 3$ and $p_T > 200$ GeV [67]. As in the case of Standard Model Higgs searches using the $WW$ fusion process [94], the presence of jets at large rapidity must be used to suppress backgrounds. The event selection closely follows that used in searches for a heavy Standard Model Higgs via the $WW$ fusion process and is as follows [88, 89].

– Two reconstructed positively charged isolated leptons (electrons or muons) with $|\eta| < 2.5$.

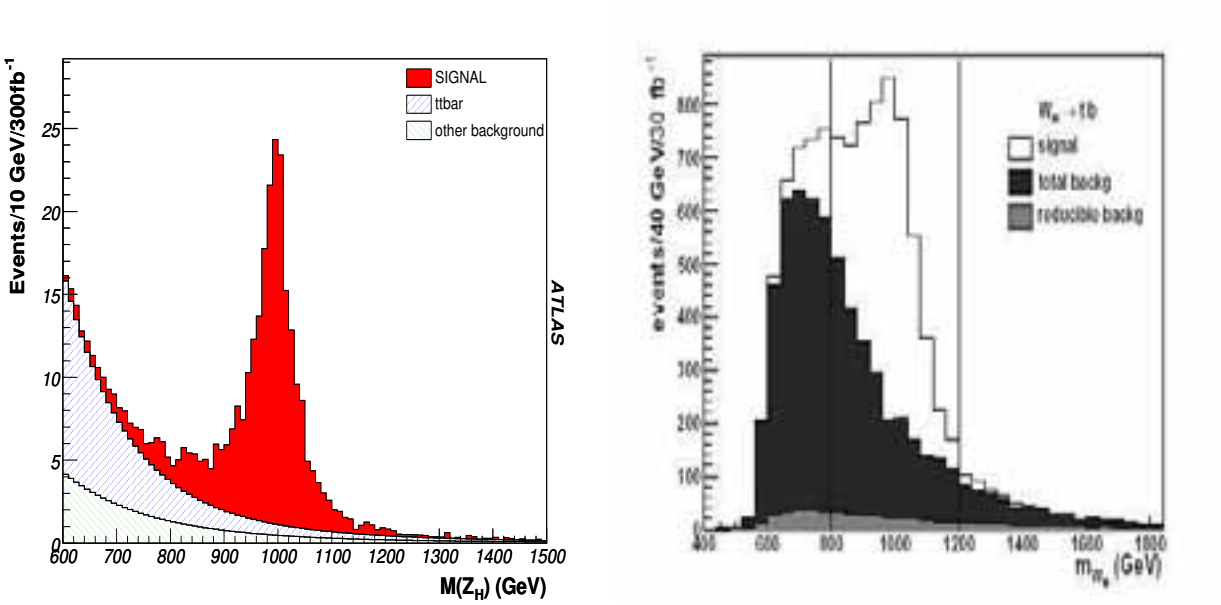


Fig. 7.13: Left : reconstructed mass of $ZH \to \ell^+\ell^- jj\ell\nu$ (B1 mode) system, for $M_{Z_H} = 1$ TeV, $m_H = 120$ GeV and $\cot\theta = 0.5$. Right: reconstructed $tb$ mass for $M_{W_H} = 1$ TeV and $\cot\theta = 1$.

- One of the leptons was required to have $p_T > 150$ GeV and the other $p_T > 20$ GeV.
- The leptons are not balanced in transverse momentum: $|p_{T1} - p_{T2}| > 200$ GeV.
- The difference in pseudorapidity of the two leptons should be $|\eta_1 - \eta_2| < 2$.
- $E_T^{miss} > 50$ GeV.
- Two jets each with $p_T > 15$ GeV, with rapidities of opposite sign, separated in rapidity $|\eta_1 - \eta_2| > 5$; one jet has $E > 200$ GeV and the other $E > 100$ GeV.

The presence of the leptons ensures that the events are triggered. The invariant mass of the $WW$ system cannot be reconstructed, but the signal can be observed using a mass variable $m_{trans}$ made from the observed leptons momenta ($\mathbf{p_1}$ and $\mathbf{p_2}$) and the missing transverse momentum $\mathbf{p_T^{miss}}$ as follows:

$$m_{trans}^2 = (E_1 + E_2 + \left|E_T^{miss}\right|)^2 - (\mathbf{p_1} + \mathbf{p_2} + \mathbf{p_T^{miss}})^2 \tag{7.69}$$

The reconstructed mass distribution is shown in Fig. 7.15 for a mass of 1 TeV. Standard Model backgrounds are shown separately on the figure. Note that the rate shown in this figure is small and the signal does not appear as a clear peak. The process is very demanding of luminosity, the ability to detect forward jets at relatively small $p_T$, and the ability to control backgrounds. These issues cannot be fully addressed until actual data is available. At this stage, we can only estimate our sensitivity using our current, best estimates, of these issues. Since the cross-section for a $\phi^{++}$ of a fixed mass is proportional to $(v')^2$, the simulation can be used to determine the sensitivity. Requiring at least 10 events with $m_{trans} > 700(1000)$ GeV for $M_\phi = 1000(1500)$ GeV and a value of $S/\sqrt{B} > 5$ implies that discovery is possible if $v' > 29(54)$ GeV. Such values are larger than the constraint of $v' < 25$ GeV from electro-weak fits [67].

### *7.6.4 Model constraints and conclusions*

We have shown, using a series of examples, how measurements using the ATLAS detector at the LHC can be used to reveal various particles predicted by little Higgs models. The $T$ quark is observable up to masses of approximately 2.5 TeV via its decay to $Wb$. Sensitivity in $Zt$ or $Ht$ is lower but it still extends over the range expected in the model provided that the Higgs mass is not too large. In the case of $Ht$

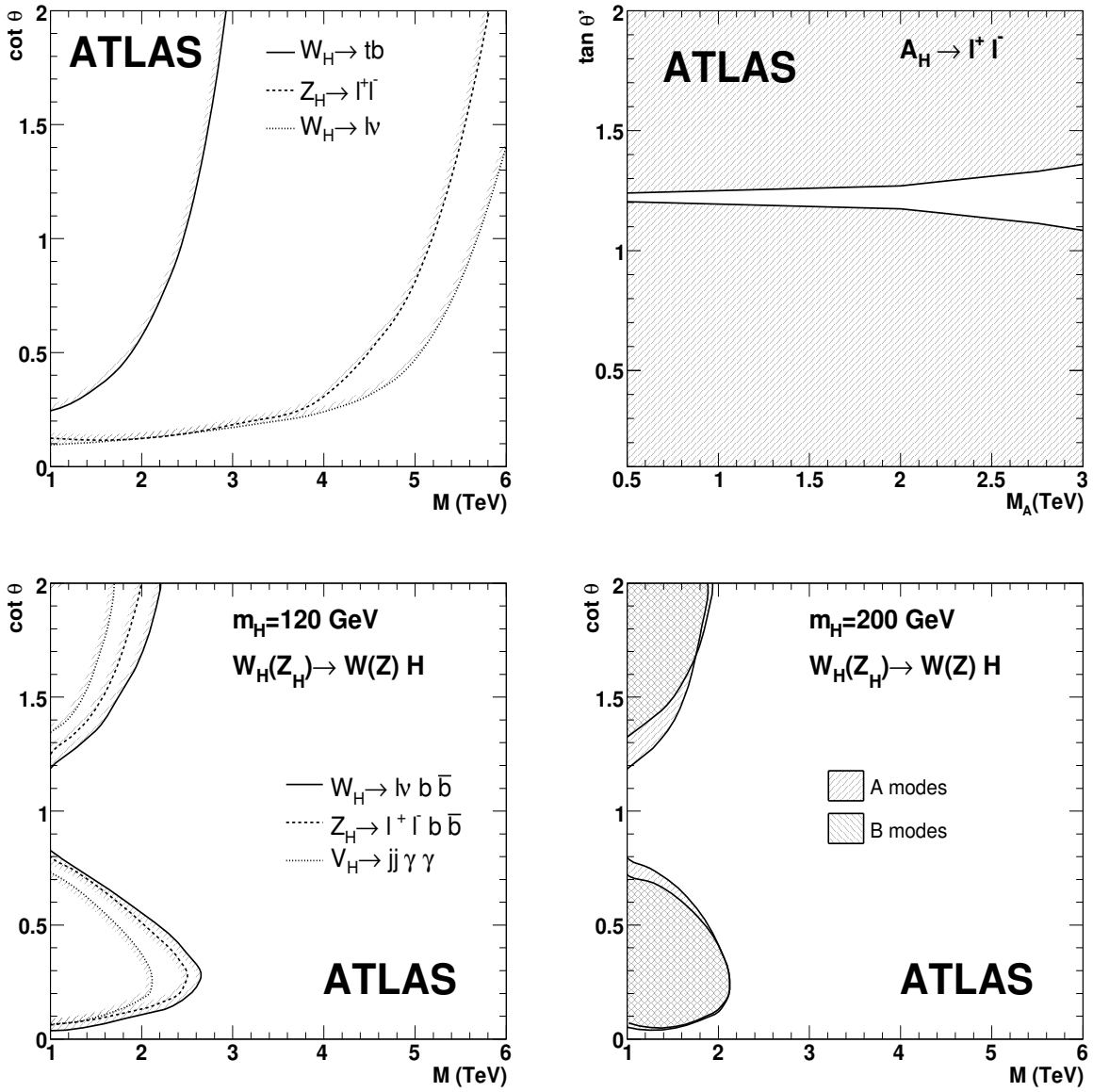


Fig. 7.14: These plots show the accessible regions for $5\sigma$ discovery of the gauge bosons $W_H$, $Z_H$ and $A_H$ as a function of their mass and $\cot\theta$ or $\tan\theta'$ for the various final states. The regions to the left of the lines are accessible with 300 fb$^{-1}$: top right for $A_H \to e^+e^-$, top left for $W_H$ or $Z_H$ leptonic and hadronic decays, bottom left for decays with a Higgs in the final state with $m_H = 120$ GeV, bottom right for decays with a Higgs in the final state with $m_H = 200$ GeV (see text for details).

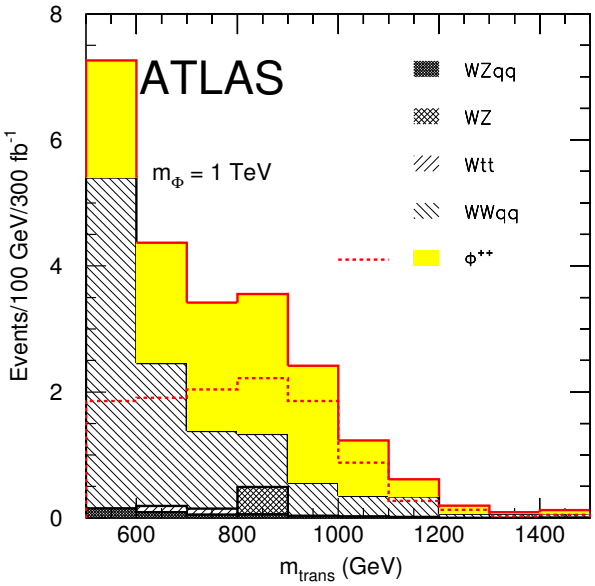


Fig. 7.15: The mass distribution $m_{trans}$, see text, for a $\phi^{++}$ of mass 1 TeV and $v' = 25$ GeV. The dashed histogram shows the signal alone and the solid shows the sum of signal and backgrounds. The components of the background are also shown separately.

the sensitivity will depend on the Higgs mass. The $H \to b\bar{b}$ channel is effective until the Higgs mass exceeds 150 GeV. In this case ATLAS will be able to detect $T$ in its three decay channels and provide a test of the model.

In the case of the new gauge bosons, the situation is summarised in Fig. 7.14, that shows the accessible regions via leptonic final states of $Z_H$ and $W_H$ as a function of the mixing angle. However observation of such a gauge boson will not prove that it is of the type predicted in the little Higgs Models. In order to do this, the decays to the Standard Model bosons must be observed. Fig. 7.14 also shows the sensitive regions for decays of $Z_H$ and $W_H$ into various final states as a function of $\cot\theta$ and the masses. It can be seen that several decay modes are only observable for smaller masses over a restricted range of $\cot\theta$ where the characteristic decays $Z_H \to ZH$ and $W_H \to WH$ can be detected. The region of $\cot\theta \sim 1$ is covered searching for $W_H \to tb$ There is a small region at very small values of $\cot\theta$ where the leptonic decays are too small, and only the decays to $W$ or $Z$ can be seen.

In the case of $\phi^{++}$ the situation is not so promising. The Higgs sector is the least constrained by fine tuning arguments and this particle's mass can extend up to 10 TeV. We are only sensitive to masses up to 2 TeV or so provided that $v'$ is large enough. Other "little Higgs" models have a different Higgs structure that is similar to models with more than one Higgs doublet. Work is needed to evaluate the sensitivity of the LHC to these models.

### 7.7 Search for new heavy quark $T$ in CMS

*Aristotelis Kyriakis and Kajari Mazumdar*

Most extensions of the Standard Model contain an extended gauge sector and/or an extended Higgs sector but they are severely constrained by precision electroweak data. The little Higgs models [5,7,97] give an alternative solution to the fine-tuning problem present in the SM and consequently invoke a new set of particles. Since the mass upper limits depend on the relative importance of the contribution to the Higgs

Table 7.5: Major background processes with their cross-sections folded with leptonic branching ratios, the expected number of events at integrated luminosity $\mathcal{L}$ = 30 fb$^{-1}$ and the number of events analyzed.

| Background | $\sigma\times$ BR (pb) | $N_{\rm expected}$ ($\mathcal{L}$=30 fb$^{-1}$) | $N_{\rm analyzed}$ |
|---|---|---|---|
| $t\bar{t} \rightarrow$ leptons | 85 | 2550K | 908K |
| inclusive $ZW \rightarrow$ leptons | 2.6 | 78K | 49K |
| inclusive $ZZ \rightarrow$ leptons | 0.16 | 4.8K | 93K |
| inclusive $WW \rightarrow$ leptons | 19.8 | 549K | 93K |
| $Zb\bar{b}$ | 116 | 3480 K | 220K |
| $Z(\rightarrow$ leptons)+jets | 161.7 | 4851K | 142K |

boson mass, we have a new singlet heavy quark, $T$ which is the least massive ($< 2$ TeV) among all the new particles predicted and hence likely to be more easily produced at the LHC.

In this contribution, the potential of the CMS experiment at the LHC to discover $T$ is investigated for the production channel $q\ b \rightarrow q'\ T$ where the heavy quark is produced singly in the $t$-channel fusion process $Wb \rightarrow T$. This process is model dependent, being governed by the ratio of the Yukawa coupling constants involved in the model. The pair production of $T\bar{T}$ via gluon-gluon fusion is model independent and falls off more rapidly at higher values of $T$-mass [67]. The details of the CMS study can be found in [98].

The study is performed for the decay channel $T \rightarrow t\ Z$, which has a branching fraction of 25%. The cleanest signal is expected for the leptonic ($e,\ \mu$) decay modes of $Z$ and $W$ (from top decay), though the event rate is low. We have not considered their tau-decay modes. The complete process with the final state considered is $q\ b \rightarrow q'\ T,\ T \rightarrow Zt,\ Z \rightarrow \ell^+\ell^-,\ t \rightarrow bW,\ \ W \rightarrow \ell\nu$. Hence there are three isolated, charged leptons, one $b$ jet, and genuine missing transverse energy in the central part and one forward going, light-quark jet in the event.

### *7.7.1 Event simulation and reconstruction*

The major background types with their cross-section folded with the leptonic branching ratios, the expected number of events for an integrated luminosity of 30 fb$^{-1}$ and the number of events analyzed for the present study are shown in Table 7.5.

We have used the PYTHIA package [93] for signal and background event generation. For signal we used the subprocess corresponding to 4th-generation heavy quark production and treating it as a resonance with mass 1 TeV. We have used CTEQ5L structure function for the event generation of the channel. For $t\bar{t}$ and double vector boson productions (*i.e.,* $WW, WZ, ZZ$) the accompanying jet is not very hard in PYTHIA. We plan to use dedicated event generators, based on matrix element calculation, in future where the accompanying jets in inclusive processes are much harder. The events for the process $Zb\bar{b}$ are produced withALPGEN package [99]. We have also considered inclusive $Z$ production events, since, the production rate is very high (Z+jets, Drell-Yan $\sim$ 10 nb). The third lepton may be either from the jet or due to the initial state gluon radiation in DY events. In CMS detector the jet misidentification probability is very low ($10^{-4}$ for electron and $10^{-5}$ for muon). It is impossible to simulate the background channels for full statistics. To save on computing resources we have considered for $Z$ + jets background a specific kinematic region of ($\hat{p}_t$ =75-500 GeV) which overlaps with typical transverse momentum of $Z$ in the subprocess. We note here that the $Q^2$ scale for the signal channel is much higher than that in most of the simulated events for SM background processes. We are in the process of studying the SM events specially produced at higher $Q^2$ values.

Generated events are processed through GEANT-based CMS detector simulation package (OSCAR [10 and reconstructed subsequently using CMS-specific software (ORCA [101]). We have taken into account event pileup situation for low luminosity running phase of the LHC for an instantaneous luminosity of

Table 7.6: Efficiency of the selection criteria for the signal and various backgrounds analyzed.

| Selection | $T \to Zt(\%)$ | $t\bar{t} \to (\%)$ | $ZZ(\%)$ | $ZW(\%)$ | $WW(\%)$ | $Z$+jets (%) | $Zbb(\%)$ |
|---|---|---|---|---|---|---|---|
| Trigger | 95 | 43 | 59 | 16 | 25 | 43 | 92 |
| $Z$ | 63 | 0.240 | 4.160 | 1.130 | 0.14 | 11 | 7.4 |
| $W$ | 39 | 0.014 | 1.120 | 0.500 | 0. | 0.036 | 0.39 |
| $W + b$-jet | 13 | 0.005 | 0.020 | 0.002 | 0. | 0. | 0.09 |
| $SM$ top | 11 | 0.001 | 0.006 | 0.002 | 0. | 0. | 0.02 |
| $T$ | 9.7 | 0. | 0.001 | 0. | 0. | 0. | 0. |

$2\times10^{33}$ cm$^{-2}$ s$^{-1}$.

We have used standard reconstruction softwares of CMS. For jet reconstruction we used the iterative cone algorithm with cone radius of 0.5. A cut on jets with the minimum transverse energy 10 GeV is applied during jet reconstruction. The missing transverse energy in the event, $E_T^{\rm miss}$, is estimated from the balance of calorimeter tower energies used in jet reconstruction.

Lepton isolation is defined by choosing a cone of radius $\Delta R = \sqrt{\Delta\eta^2 + \Delta\phi^2} < 0.1$ around the candidate (electron or muon) track and searching for other tracks within the cone having $p_T > 0.9$ GeV. The sum $\Sigma\, p_T$ is required to be $< 4\%$ of the candidate track momentum for muon or transverse energy deposited in electromagnetic calorimeter for electron.

### *7.7.2 Event trigger and selection*

The reconstructed events are first checked if they pass standard CMS-trigger criteria. For 'double electron' and 'double muon' topology, the thesholds for lepton transverse momentum at higher level trigger are 17 GeV and 7 GeV respectively [102]. The combined trigger effeciency was evaluated to be 95%.

Our main selection conditions for off-line analysis are summarized below:

- The 'same flavour opposite sign dileptons:' $e^+e^-$ and $\mu^+\mu^-$ combinations should have a $p_T > 100$ GeV (Fig. 7.16) and a mass of $\pm10$ GeV around the nominal $Z$ mass (Fig. 7.17). This is referred to later as *Z criteria*.
- We further require a third lepton compatible with the leptonic decay of $W$. Hence the combination of lepton momentum and the missing transverse energy (nominally $E_t^{\rm miss} > 20$ GeV), should have a transverse momentum greater than 60 GeV and a transverse mass less than 120 GeV. This is referred to as *W criteria*.
- We allow only one jet with transverse momentum greater than 30 GeV within the tracker acceptance ($|\eta| < 2.5$) satisfying the conditions of a $b$-jet. The combination of $W$ and the $b$-jet should have a transverse momentum greater than 150 GeV , the condition referred to as *W + b-jet criteria*.
- The $(W, b)$ combination is required to have a mass in the range 110–220 GeV, referred to as *SM top criteria*.
- Finally we apply the *Heavy Top* characteristics: the combination ($Z,\ W,\ b$) should have a mass in the range 850−1150 GeV (Fig. 7.18).

In Table 7.6 we have summarized the efficiency of our selection cuts to signal and background events. The hard cuts applied during selection are quite effective in removing the backgrounds in almost all cases.

### *7.7.3 Preliminary Results*

The only SM background which survives all selections is $ZZ \to$ leptonic. The total efficiency for the signal selection is 9.7%. Taking into account the single heavy $T$ production cross-section (192 fb for equal Yukawa couplings $\lambda_1 = \lambda_2$) for heavy $T$ mass of 1 TeV and the various branching ratios we can

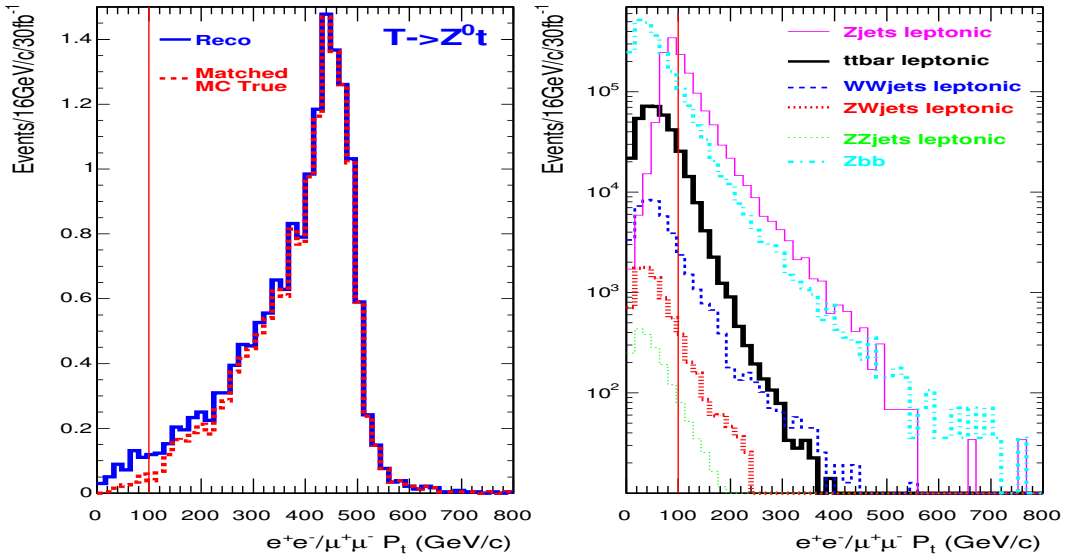


Fig. 7.16: The transverse momentum of the $e^+e^-$ and $\mu^+\mu^-$ combinations for signal (left) and background (right) events. The vertical lines show the threshold value.

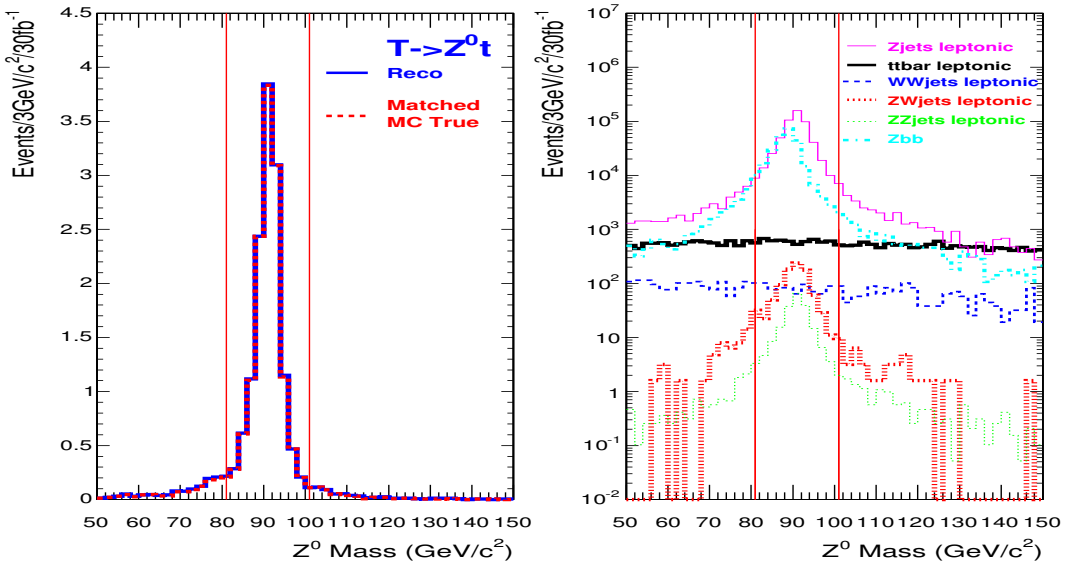


Fig. 7.17: Invariant mass of the $e^+e^-$ and $\mu^+\mu^-$ pairs for signal (left) and background (right) events (with and without $Z$ in the final state); the events within the vertical lines are accepeted combinations.

calculate that a signal sample of only $N_S = 2.1$ events are expected with an integrated luminosity of 30 fb$^{-1}$. The significance could be calculated from $S_{stat} = 2(\sqrt{N_S + N_B} - \sqrt{N_B})$, that gives: $S_{stat} = 2.5$ with a signal-to-background ratio of 41.

#### 7.7.3.1 Systematics

To study the systematic effect on the result we considered various experimental sources affecting the reconstruction of the observed leptons and jets, and estimated their impact on the selection efficiency.

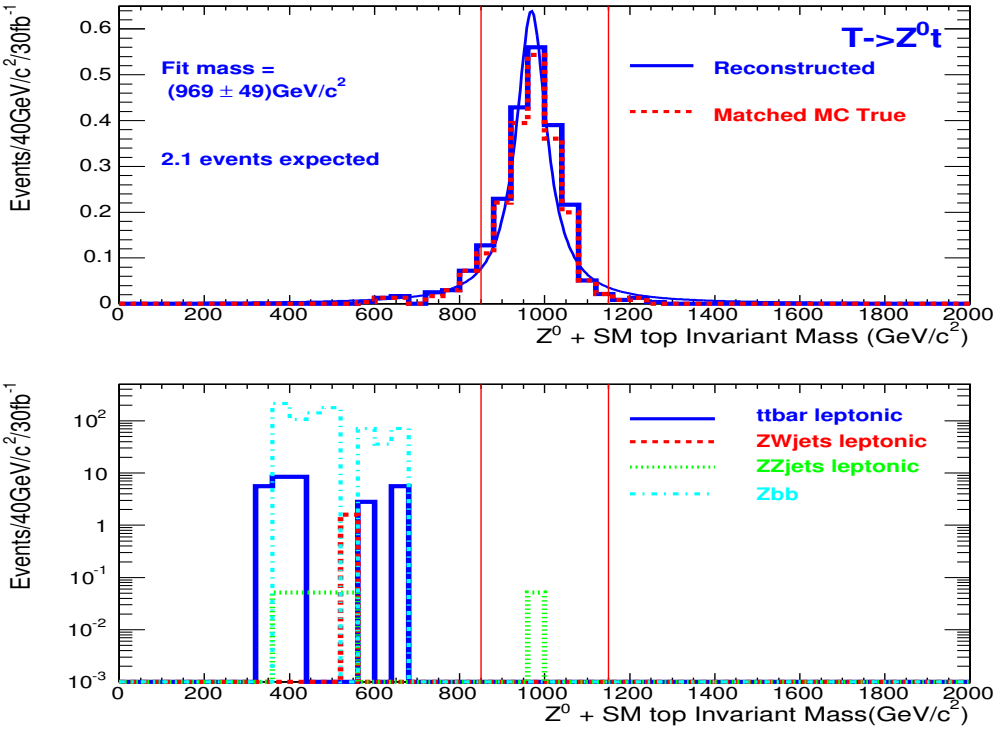


Fig. 7.18: Signal (left) and background (right) distributions for the invariant mass of the $Z$ and SM top combination for candidate heavy top with generated mass of 1 TeV.

Only the uncorrelated sources (or with negligible correlation) are included. We determined the surviving number of background events and fluctations are considered as the maximum shift for the central value without the systematic bias.

- Lepton energy scale: Due to imperfect knowledge of the detector material, the exact value of magnetic field at a given point of the detector or initial misalignments of detector units, estimates of 4-momenta of leptons have an uncertainty. This effect is accounted for by rescaling all reconstructed leptons' energy and momenta by a factor $\pm 0.005$. The error in efficiency is found to be 0.4%, whilst the background is not significantly affected.
- Jet and missing energy scale: The jet energy scale uncertainty (after 10 fb$^{-1}$ integrated luminosity) is expected to be about 5% for jets with $p_T$ =20 GeV and continuously decreasing to about 2.5% for jets with $p_T > 50$ GeV. With a $E_T^{\rm miss}$ estimated from jet energies, missing energy scale is totally correlated to the Jet Energy Scale and we considered a variation of 5%. The error in the efficiency is found to be 1% whilst the background is not significantly affected.
- $b$-tag uncertainty: The $b$-tagging of jet is important in this study and the experimental method is effective up to $|\eta| \leq 2.5$ with an efficiency of about 60% [103]. The $b$-tag uncertainty is assumed to be 4% after 10 fb$^{-1}$ integrated luminosity and it has large effect both on efficiency (5%) and on the background events ($\pm 0.15$ events).

So the significance after taking into account the systematcs is given as [104]:

$$S_{stat+syst} = S_{stat}\sqrt{\frac{N_B}{N_B + (\Delta N_B)^2}} = 2.0 \tag{7.70}$$

Thus, the significance of the channel worsens after systematic effects are taken into account. The situation can improve significantly when the signal cross-section is higher as for the choice $\lambda_1/\lambda_2 = 2$.

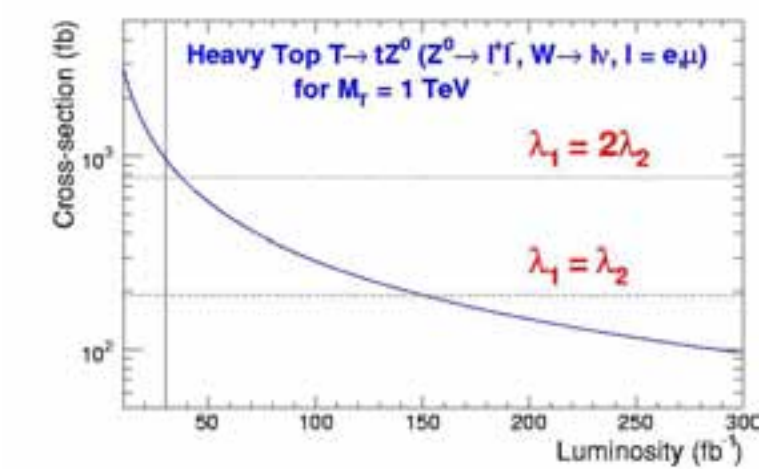


Fig. 7.19: The discovery plot. The curve represents the signal cross-section required as a function of integrated luminosity at LHC, for establishing single production of a heavy quark of mass = 1 TeV at $5\sigma$ level. The horizontal lines correspond to various choices of $\lambda_1/\lambda_2$. The vertical line corresponds to the luminosity used for this analysis *i.e.,* 30 fb $^{-1}$.

### *7.7.4 Conclusion*

The experimental signature of single **T** production with subsequent decays in $T \to Zt,\ Z \to \ell^+\ell^-$ where $W$ from top-quark decays leptonically is investigated in the context of CMS experiment. The significance of the search is determined after taking into account various systematic effects. The study demonstrates that with an integrated luminosity of 30 fb$^{-1}$, the discovery potential of the channel $T \to tZ$, with leptonic decays of $Z$ and $W$, is rather limited. Fig. 7.19 shows signal cross-section required as a function of integrated luminosity, for establishing at $5\sigma$ level, single production of a heavy quark of mass = 1 TeV. The luminosity needed for $5\sigma$ evidence is estimated to be around 150 fb$^{-1}$ and 40 fb$^{-1}$ respectively for choice of parameters $\lambda_1 = \lambda_2$ and $\lambda_1 = 2\lambda_2$.

## 7.8 Determination of Littlest Higgs model parameters at the ILC

*J.A. Conley, J.L. Hewett, and M.P. Le*

The most economical little Higgs model is the so-called "Littlest Higgs" (LH) [6]. This scenario is based on a non-linear sigma model with an SU(5) global symmetry, which is broken to the subgroup SO(5) by a vev $f$. The natural scale for $f$ is around a TeV; if $f$ is much larger, the Higgs mass must again be finely tuned and this model no longer addresses the hierarchy problem. The SU(5) contains a gauged subgroup $[\mathrm{SU}(2) \times \mathrm{U}(1)]^2$ which is broken by the vev to the SM electroweak group $[\mathrm{SU}(2)_L \times \mathrm{U}(1)_Y]$. The global SU(5) breaking leaves 14 massless Goldstone bosons, four of which are eaten by the gauge bosons of the broken gauge groups, giving these gauge bosons a mass of order $f$. These new bosons correspond to two a heavy neutral bosons, $Z_H$ and $A_H$, and two heavy charged bosons $W_H^{\pm}$.

Here, we are mainly concerned with the extended neutral gauge sector, which contains 3 new parameters: $f$ and two mixing angles. Although we focus on the Littlest Higgs model, we note that an enlarged gauge sector with generic features is present in all little Higgs scenarios. After EWSB, the mass

eigenstates are obtained via mixing

$$\begin{aligned} M^2_{A_L} &= 0, \quad M^2_{Z_L} = m^2_Z \left[1 - \frac{v^2}{f^2}\left(\frac{1}{6} + \frac{1}{4}(c^2 - s^2)^2 + \frac{5}{4}(c'^2 - s'^2)^2\right) + 8\frac{v'^2}{v^2}\right], \\ M^2_{A_H} &= m^2_Z s^2_w \left[\frac{f^2}{5s'^2c'^2v^2} - 1 + \frac{v^2}{2f^2}\left(\frac{5(c'^2 - s'^2)^2}{2s^2_w} - x_H\frac{g}{g'}\frac{c'^2s^2 + c^2s'^2}{cc'ss'}\right)\right], \\ M^2_{Z_H} &= m^2_W \left[\frac{f^2}{s^2c^2v^2} - 1 + \frac{v^2}{2f^2}\left(\frac{(c^2 - s^2)^2}{2c^2_w} + x_H\frac{g'}{g}\frac{c'^2s^2 + c^2s'^2}{cc'ss'}\right)\right], \end{aligned} \tag{7.71}$$

with $x_H$ being given in [67]. The mixing angles

$$s = \frac{g_2}{\sqrt{g_1^2 + g_2^2}} \text{ and } s' = \frac{g'_2}{\sqrt{g_1'^2 + g_2'^2}} \tag{7.72}$$

relate the coupling strengths of the two copies of $[\mathrm{SU}(2) \times \mathrm{U}(1)]$. The couplings of the neutral gauge bosons $Z_L$, $A_H$, and $Z_H$ to fermions and the light Higgs similarly depend on $s$, $s'$ and $f$:

$$\begin{aligned} g(A_L f\bar{f}) &= g_{SM}(Af\bar{f}), \quad g(Z_L f\bar{f}) = g_{SM}(Zf\bar{f})\left(1 + \frac{v^2}{f^2}a_i(s,s')\right), \\ g(A_H f\bar{f}) &= b_i\frac{g'}{2s'c'}(\frac{1}{5} - \frac{1}{2}c'^2), \\ g(Z_H f\bar{f}) &= \pm\frac{gc}{4s}, \quad g(Z_{L\mu}Z_{L\nu}H) = g_{SM}(Z_\mu Z_\nu H)\left(1 + \frac{v^2}{f^2}a(s,s')\right), \\ g(Z_{L\mu}Z_{H\nu}H) &= \frac{-i}{2}\frac{g^2}{c_W}v\frac{c^2 - s^2}{2sc}g_{\mu\nu}, \quad g(Z_{L\mu}A_{H\nu}H) = \frac{-i}{2}\frac{gg'}{c_W}v\frac{c'^2 - s'^2}{2s'c'}g_{\mu\nu}, \end{aligned} \tag{7.73}$$

where $g_{SM}$ represents the relevant coupling in the SM, and $a(b)_i$ are $\mathcal{O}(1)$ where $i$ labels the fermion species.

Equation (7.72) shows that for generic choices of $s$ and $s'$, $M_{A_H}/M_{Z_H} \simeq s_w m_Z/\sqrt{5}m_W \simeq 1/4$. This light $A_H$ is responsible for the most stringent experimental constraints on the model [31, 33]. As a result, phenomenologically viable variations of the Littlest Higgs models typically decouple the $A_H$ by modifying the gauge structure of the theory. To gain some understanding of models in which the $A_H$ decouples we take two approaches in our analysis: one is to choose a parameter value ($s' = \sqrt{3/5}$) for which the coupling of $A_H$ to fermions vanishes. Another is to artificially take $M_{A_H} \to \infty$ while letting all other quantities in the theory take on their usual, parameter-dependent values. While not theoretically consistent, this approach gives us a more general picture of the behavior of models in which the $A_H$ decouples.

We first examine the process $e^+e^- \to f\bar{f}$, where all of the LH neutral gauge bosons participate via s-channel exchange. We first study the constraints on the model from LEP II, taking as our observables the normalized, binned angular distribution and total cross section for $e^+e^- \to b\bar{b}$, $c\bar{c}$, and $\ell\bar{\ell}$, with $l = e$, $\mu$, or $\tau$. We use $\sqrt{s} = 200$ GeV and an integrated luminosity of 627 pb$^{-1}$. For the detection efficiencies, we take $\epsilon_e = 97\%$, $\epsilon_\mu = 88\%$, $\epsilon_\tau = 49\%$, $\epsilon_b = 40\%$, and $\epsilon_c = 10\%$ [105]. For the ILC, in addition to the above mentioned observables, we also include the angular binned left-right asymmetry $A_{LR}$ for each fermion pair. We use the energy $\sqrt{s} = 500$ GeV, an integrated luminosity of 500 fb$^{-1}$, and detection efficiencies of $\epsilon_e = 97\%$, $\epsilon_{\mu,\tau} = 95\%$, $\epsilon_b = 60\%$, and $\epsilon_c = 35\%$ [106].

The exclusion region at LEP II (taking $s' = s/2$) and the $5\sigma$ search reach at the ILC for various values of $s'$ are shown in Fig. 7.20. The $5\sigma$ discovery contour for the $Z_H$ at the LHC, as computed by an ATLAS based analysis [88], is included in the figure for comparison. We find that the search region at $\sqrt{s} = 1$ TeV reaches to somewhat higher values of the parameter $s$, but has essentially the same reach for $f$ as the 500 GeV results.

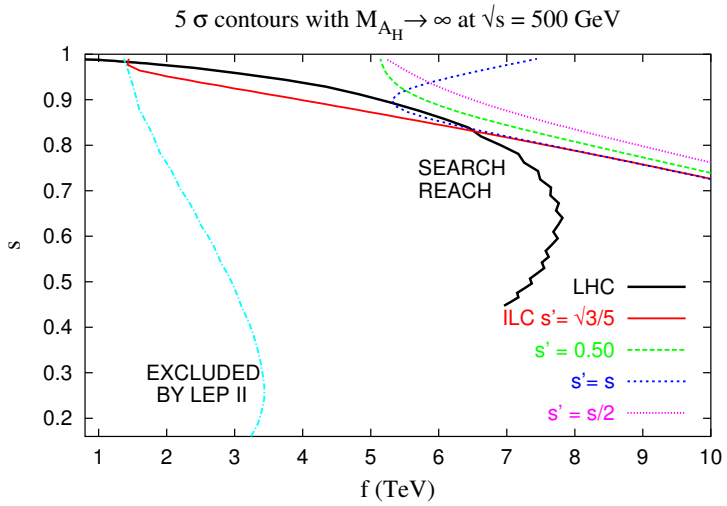


Fig. 7.20: LEP II exclusion region and ILC $5\sigma$ search reach in the $s - f$ parameter plane for various values of $s'$. The LHC result [88] is included for comparison.

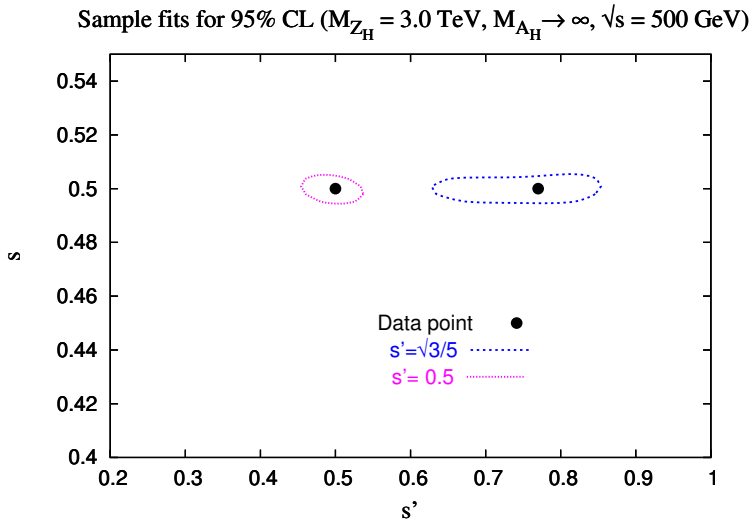


Fig. 7.21: 95% CL sample fits to the data points ($s = 0.5$, $s' = 0.5$) and ($s = 0.5$, $s' = \sqrt{3/5}$), at a 500 GeV ILC, taking $M_{Z_H} = 3.0$ TeV.

We have now determined the available parameter space accessible to the ILC and not already excluded by LEP II. It remains to ask, given the existence of an LH model with parameters in this accessible range, how accurately would the ILC be able to measure them? To answer this we perform some sample fits employing a $\chi$-square analysis. We use the same set of observables as before, and now take $M_{Z_H}$, $s$, and $s'$ as our free parameters. We choose a generic data point $(s, s', M_{Z_H})$ and use it to calculate the observables, which we then fluctuate according to statistical error. We assume that the Large Hadron Collider would have determined $M_{Z_H}$ relatively well, to the order of a few percent for $M_{Z_H} < 5 - 6$ TeV; we thus fix $M_{Z_H}$ and perform a 2-variable fit to $s$ and $s'$. Figure 7.21 shows the results of this fit for two sample data points. For both cases, the determination of $s$ is very accurate, due to the strong dependence of the $Z_H f \bar{f}$ couplings on this parameter.

In order to confirm that the LH model is the correct description of TeV-scale physics, it is important to measure the new particle couplings to the Higgs. Here we are concerned with the coupling of the $Z_H$

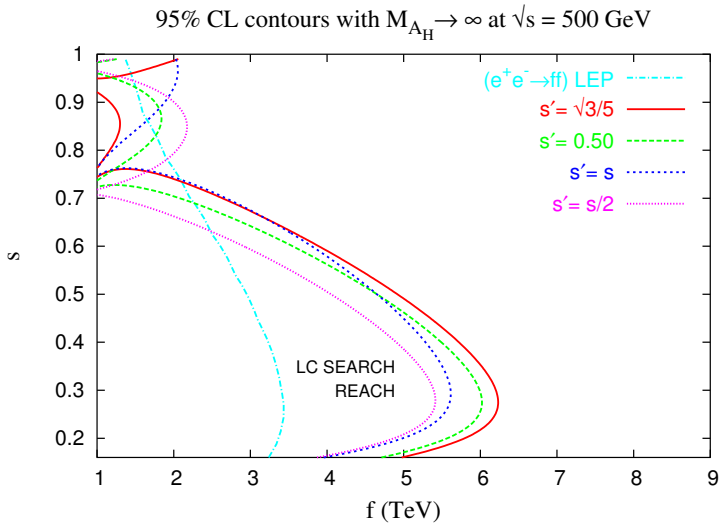


Fig. 7.22: The ILC 95% CL search reach in the $s - f$ parameter plane from the process $e^+e^- \to Z_L H$ for various values of $s'$ and $\sqrt{s} = 500$ GeV. The LEP II exclusion region from $e^+e^- \to f\bar{f}$ is shown for comparison.

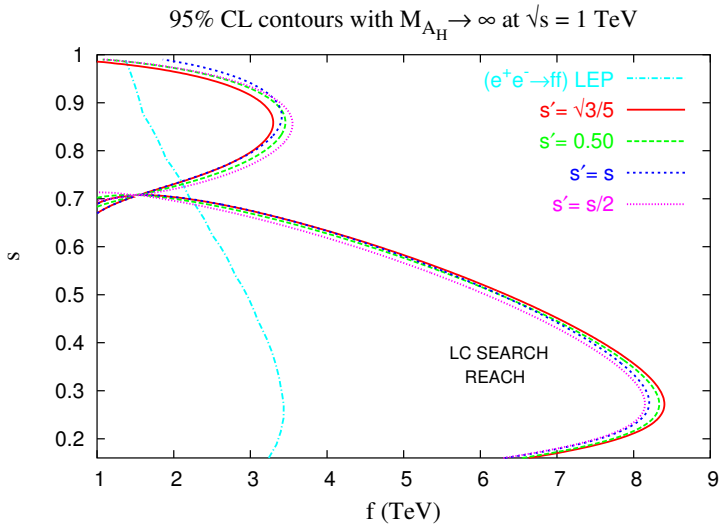


Fig. 7.23: Same as Fig. 7.22 but for $\sqrt{s} = 1$ TeV.

to the Higgs boson, which can be tested via the process $e^+e^- \to Z_L H$. In the LH model, deviations in this process from SM expectations arise from three sources: $Z_H$ and $A_H$ exchange in the s-channel and the deviation of the $Z_L Z_L H$ coupling from its SM value.

We then repeat our analysis using the process $e^+e^- \to Z_L H$ and taking the total cross section as our observable with $m_H = 120$ GeV. We assume that at a $\sqrt{s} = 500$ GeV ILC this cross section will be measured to an accuracy of 1.5% [106]. A $\chi$-squared analysis is carried out as before and our results for the ILC search reach in the LH parameter space are displayed in Figs. 7.22 and 7.23 for $\sqrt{s} = 0.5$ and 1 TeV, respectively.

In summary, we find that the reaction $e^+e^- \to f\bar{f}$ at a $\sqrt{s} = 500\ GeV$ ILC is sensitive to essentially the entire parameter region where the Littlest Higgs model is relevant to the gauge hierarchy problem. It also provides an accurate determination of the fundamental model parameters, to the precision of a few percent, provided that the LHC measures the mass of the heavy neutral gauge field. Additionally, we verified that the couplings of the extra gauge bosons to the light Higgs can be observed

from the process $e^+e^- \to ZH$ for a significant region of the parameter space. Further details of our analysis can be found in [76].

## REFERENCES


[1] D. B. Kaplan and H. Georgi, Phys. Lett. **B136**, 183 (1984).

[2] D. B. Kaplan, H. Georgi and S. Dimopoulos, Phys. Lett. **B136**, 187 (1984).

[3] M. J. Dugan, H. Georgi and D. B. Kaplan, Nucl. Phys. **B254**, 299 (1985).

[4] H. Georgi and D. B. Kaplan, Phys. Lett. **B145**, 216 (1984).

[5] N. Arkani-Hamed, A. G. Cohen and H. Georgi, Phys. Lett. **B513**, 232 (2001), [hep-ph/0105239].

[6] N. Arkani-Hamed, A. G. Cohen, E. Katz and A. E. Nelson, JHEP **07**, 034 (2002), [hep-ph/0206021].

[7] N. Arkani-Hamed *et al.*, JHEP **08**, 021 (2002), [hep-ph/0206020].

[8] S. Chang and J. G. Wacker, Phys. Rev. **D69**, 035002 (2004), [hep-ph/0303001].

[9] H.-C. Cheng and I. Low, JHEP **09**, 051 (2003), [hep-ph/0308199].

[10] I. Low, W. Skiba and D. Smith, Phys. Rev. **D66**, 072001 (2002), [hep-ph/0207243].

[11] S. Chang, JHEP **12**, 057 (2003), [hep-ph/0306034].

[12] I. Low, JHEP **10**, 067 (2004), [hep-ph/0409025].

[13] D. E. Kaplan and M. Schmaltz, JHEP **10**, 039 (2003), [hep-ph/0302049].

[14] M. Schmaltz, JHEP **08**, 056 (2004), [hep-ph/0407143].

[15] W. Skiba and J. Terning, Phys. Rev. **D68**, 075001 (2003), [hep-ph/0305302].

[16] N. Arkani-Hamed, A. G. Cohen, T. Gregoire and J. G. Wacker, JHEP **08**, 020 (2002), [hep-ph/0202089].

[17] N. Arkani-Hamed, A. G. Cohen and H. Georgi, Phys. Rev. Lett. **86**, 4757 (2001), [hep-th/0104005].

[18] C. T. Hill, S. Pokorski and J. Wang, Phys. Rev. **D64**, 105005 (2001), [hep-th/0104035].

[19] H.-C. Cheng, C. T. Hill, S. Pokorski and J. Wang, Phys. Rev. **D64**, 065007 (2001), [hep-th/0104179].

[20] T. Gregoire and J. G. Wacker, JHEP **08**, 019 (2002), [hep-ph/0206023].

[21] N. S. Manton, Nucl. Phys. **B158**, 141 (1979).

[22] D. B. Fairlie, Phys. Lett. **B82**, 97 (1979).

[23] H. Hatanaka, T. Inami and C. S. Lim, Mod. Phys. Lett. **A13**, 2601 (1998), [hep-th/9805067].

[24] G. R. Dvali, S. Randjbar-Daemi and R. Tabbash, Phys. Rev. **D65**, 064021 (2002), [hep-ph/0102307].

[25] I. Antoniadis, K. Benakli and M. Quiros, New J. Phys. **3**, 20 (2001), [hep-th/0108005].

[26] C. Csaki, C. Grojean and H. Murayama, Phys. Rev. **D67**, 085012 (2003), [hep-ph/0210133].

[27] C. A. Scrucca, M. Serone and L. Silvestrini, Nucl. Phys. **B669**, 128 (2003), [hep-ph/0304220].

[28] H.-C. Cheng and I. Low, JHEP **08**, 061 (2004), [hep-ph/0405243].

[29] R. Barbieri and A. Strumia, Phys. Lett. **B462**, 144 (1999), [hep-ph/9905281].

[30] R. Barbieri and A. Strumia, hep-ph/0007265.

[31] C. Csaki, J. Hubisz, G. D. Kribs, P. Meade and J. Terning, Phys. Rev. **D67**, 115002 (2003), [hep-ph/0211124].

[32] C. Csaki, J. Hubisz, G. D. Kribs, P. Meade and J. Terning, Phys. Rev. **D68**, 035009 (2003), [hep-ph/0303236].

[33] J. L. Hewett, F. J. Petriello and T. G. Rizzo, JHEP **10**, 062 (2003), [hep-ph/0211218].

[34] T. Gregoire, D. R. Smith and J. G. Wacker, Phys. Rev. **D69**, 115008 (2004), [hep-ph/0305275].

[35] W. Kilian and J. Reuter, Phys. Rev. **D70**, 015004 (2004), [hep-ph/0311095].

[36] C. Kilic and R. Mahbubani, JHEP **07**, 013 (2004), [hep-ph/0312053].

[37] G. Marandella, C. Schappacher and A. Strumia, Phys. Rev. **D72**, 035014 (2005), [hep-ph/0502096].

[38] R. Casalbuoni, A. Deandrea and M. Oertel, JHEP **02**, 032 (2004), [hep-ph/0311038].

[39] Z. Han and W. Skiba, Phys. Rev. **D72**, 035005 (2005), [hep-ph/0506206].

[40] R. Barbieri, A. Pomarol, R. Rattazzi and A. Strumia, Nucl. Phys. **B703**, 127 (2004), [hep-ph/0405040].

[41] E. Katz, J.-y. Lee, A. E. Nelson and D. G. E. Walker, JHEP **10**, 088 (2005), [hep-ph/0312287].

[42] H.-C. Cheng, I. Low and L.-T. Wang, hep-ph/0510225.

[43] J. Hubisz, P. Meade, A. Noble and M. Perelstein, hep-ph/0506042.

[44] J. Hubisz and P. Meade, Phys. Rev. **D71**, 035016 (2005), [hep-ph/0411264].

[45] S. Chang and H.-J. He, Phys. Lett. **B586**, 95 (2004), [hep-ph/0311177].

[46] F. Bazzocchi, M. Fabbrichesi and M. Piai, Phys. Rev. **D72**, 095019 (2005), [hep-ph/0506175].

[47] A. Birkedal-Hansen and J. G. Wacker, Phys. Rev. **D69**, 065022 (2004), [hep-ph/0306161].

[48] J. Y. Lee, JHEP **06**, 060 (2005), [hep-ph/0501118].

[49] T. Han, H. E. Logan, B. Mukhopadhyaya and R. Srikanth, Phys. Rev. **D72**, 053007 (2005), [hep-ph/0505260].

[50] S. R. Choudhury, N. Gaur and A. Goyal, Phys. Rev. **D72**, 097702 (2005), [hep-ph/0508146].

[51] F. del Aguila, M. Masip and J. L. Padilla, Phys. Lett. **B627**, 131 (2005), [hep-ph/0506063].

[52] J. R. Espinosa, M. Losada and A. Riotto, Phys. Rev. **D72**, 043520 (2005), [hep-ph/0409070].

[53] A. Abada, G. Bhattacharyya and M. Losada, hep-ph/0511275.

[54] T. Han, H. E. Logan and L.-T. Wang, hep-ph/0506313.

[55] O. C. W. Kong, hep-ph/0307250.

[56] O. C. W. Kong, J. Korean Phys. Soc. **45**, S404 (2004), [hep-ph/0312060].

[57] M. Singer, J. W. F. Valle and J. Schechter, Phys. Rev. **D22**, 738 (1980).

[58] R. Foot, H. N. Long and T. A. Tran, Phys. Rev. **D50**, 34 (1994), [hep-ph/9402243].

[59] R. A. Diaz, R. Martinez and F. Ochoa, Phys. Rev. **D72**, 035018 (2005), [hep-ph/0411263].

[60] M. Perelstein, M. E. Peskin and A. Pierce, Phys. Rev. **D69**, 075002 (2004), [hep-ph/0310039].

[61] T. Han, H. E. Logan, B. McElrath and L.-T. Wang, Phys. Lett. **B563**, 191 (2003), [hep-ph/0302188].

[62] H. E. Logan, Phys. Rev. **D70**, 115003 (2004), [hep-ph/0405072].

[63] G. A. Gonzalez-Sprinberg, R. Martinez and J.-A. Rodriguez, Phys. Rev. **D71**, 035003 (2005), [hep-ph/0406178].

[64] W. Kilian, D. Rainwater and J. Reuter, Phys. Rev. **D71**, 015008 (2005), [hep-ph/0411213].

[65] M. Perelstein, hep-ph/0512128.

[66] M.-C. Chen, hep-ph/0601126.

[67] T. Han, H. E. Logan, B. McElrath and L.-T. Wang, Phys. Rev. **D67**, 095004 (2003), [hep-ph/0301040].

[68] M.-C. Chen and S. Dawson, Phys. Rev. **D70**, 015003 (2004), [hep-ph/0311032].

[69] A. Deandrea, hep-ph/0405120.

[70] J. Hubisz, S. J. Lee and G. Paz, hep-ph/0512169.

[71] J. F. Gunion, H. E. Haber, G. L. Kane and S. Dawson, *The Higgs Hunter's Guide* (Addison-Wesley, Reading, MA, 1990), SCIPP-89/13.

[72] R. Martinez, M. A. Perez and J. J. Toscano, Phys. Rev. **D40**, 1722 (1989).

[73] A. Djouadi, J. Kalinowski and M. Spira, Comput. Phys. Commun. **108**, 56 (1998), [hep-ph/9704448].

[74] M. Carena, H. E. Haber, H. E. Logan and S. Mrenna, Phys. Rev. **D65**, 055005 (2002), [hep-ph/0106116].

[75] C.-x. Yue, S.-z. Wang and D.-q. Yu, Phys. Rev. **D68**, 115004 (2003), [hep-ph/0309113].

[76] J. A. Conley, J. Hewett and M. P. Le, Phys. Rev. **D72**, 115014 (2005), [hep-ph/0507198].

[77] C.-X. Yue, W. Wang, Z.-J. Zong and F. Zhang, Eur. Phys. J. **C42**, 331 (2005), [hep-ph/0504253].

[78] C.-X. Yue, W. Wang and F. Zhang, The littlest Higgs model and Higgs boson associated production with top quark pair at high energy linear $\mathrm{e}^+\mathrm{e}^-$ collider, hep-ph/0503260.

[79] C.-R. Chen, K. Tobe and C. P. Yuan, Higgs boson production and decay in little Higgs models with T-parity, hep-ph/0602211.

[80] J. F. Gunion and H. E. Haber, Phys. Rev. **D67**, 075019 (2003), [hep-ph/0207010].

[81] A. V. Manohar and M. B. Wise, Modifications to the properties of a light Higgs boson, hep-ph/0601212.

[82] B. A. Dobrescu and K. T. Matchev, JHEP **09**, 031 (2000), [hep-ph/0008192].

[83] G. Hiller, Phys. Rev. **D70**, 034018 (2004), [hep-ph/0404220].

[84] H.-C. Cheng, K. T. Matchev and M. Schmaltz, Phys. Rev. **D66**, 056006 (2002), [hep-ph/0205314].

[85] A. Datta, K. Kong and K. T. Matchev, Phys. Rev. **D72**, 096006 (2005), [hep-ph/0509246].

[86] A. Birkedal, A. Noble, M. Perelstein and A. Spray, hep-ph/0603077.

[87] D. N. Spergel *et al.* (WMAP Collaboration), Astrophys. J. Suppl. **148**, 175 (2003), [astro-ph/0302209].

[88] G. Azuelos *et al.*, Eur. Phys. J. **C39S2**, 13 (2005), [hep-ph/0402037].

[89] G. Azuelos, K. Benslama and G. Couture, The Little Higgs: analysis of the channel $W^+W^- \to \Phi^{++} \to W^+W^-$, 2006, ATL-PHYS-PUB-2004-002.

[90] J. E. Garcia-Navarro, *Performance of the ATLAS Silicon Tracker and Search for new Gauge Bosons in the Little Higgs Model*, Ph.D. thesis, Universidad de Valencia, 2004.

[91] M. Lechowski, *Test du modèle du Petit Higgs dans ATLAS au LHC. Simulation de la numérisation du calorimètre électromagnétique*, Ph.D. thesis, Université Paris-Sud 11, 2005.

[92] S. González de la Hoz, L. March and E. Ros, Search for hadronic decays of $Z_H$ and $W_H$ in the little Higgs model, 2006, ATL-PHYS-PUB-2006-003.

[93] T. Sjostrand, L. Lonnblad and S. Mrenna, *PYTHIA 6.2: Physics and manual*, 2001, hep-ph/0108264.

[94] ATLAS Collaboration, Physics and detector performance technical design report, 1999, LHCC 99-14/15.

[95] N. Arkani-Hamed, A. G. Cohen, E. Katz and A. E. Nelson, JHEP **07**, 034 (2002), [hep-ph/0206021].

[96] G. Burdman, M. Perelstein and A. Pierce, Phys. Rev. Lett. **90**, 241802 (2003), [hep-ph/0212228].

[97] M. Schmaltz, Nucl. Phys. Proc. Suppl. **117**, 40 (2003), [hep-ph/0210415].

[98] A. Kyriakis and K. Mazumdar, Little Higgs model and top-like heavy quark at CMS, 2006, CMS Note 2006/079.

[99] M. L. Mangano, M. Moretti, F. Piccinini, R. Pittau and A. D. Polosa, JHEP **07**, 001 (2003), [hep-ph/0206293].

[100] CMS, Object-oriented simulation for CMS analysis and reconstruction, 2006, in: CMS Physics TDR Volume 1.

[101] CMS, Object-oriented reconstruction for CMS analysis, 2006, in: CMS Physics TDR Volume 1.

[102] CMS, The data acquisition and high-level trigger project, 2002, CMS TDR 2002/6.2.

[103] G. Segneri and F. Palla, Lifetime based b-tagging with CMS, 2002, CMS Note 2002/046.

[104] S. Bityukov and N. Krasnikov, Uncertainties and discovery potential in planned experiments, 2002, CMS CR-2002/005.

[105] G. Abbiendi *et al.* (OPAL Collaboration), Eur. Phys. J. **C33**, 173 (2004), [hep-ex/0309053].

[106] J. A. Aguilar-Saavedra *et al.* (ECFA/DESY LC Physics Working Group), hep-ph/0106315.